THE UNIVERSITY OF CHICAGO

SUPPRESSION OF HOST INNATE IMMUNE RESPONSES BY THE p150 ISOFORM OF ADAR1 DURING INFLUENZA VIRUS INFECTION

A DISSERTATION SUBMITTED TO

THE FACULTY OF THE DIVISION OF THE BIOLOGICAL SCIENCES

AND THE PRITZKER SCHOOL OF MEDICINE

IN CANDIDACY FOR THE DEGREE OF

DOCTOR OF PHILOSOPHY

COMMITTEE ON MICROBIOLOGY

BY

OLIVIA ASHLEY VOGEL

CHICAGO, ILLINOIS

AUGUST 2020

TABLE OF CONTENTS

ACKNOWLEDGEMENTS

I would like to thank my mentor, Dr. Balaji Manicasammy, as well as Dr. Jasmine Perez for their excellent mentorship and encouragement throughout my PhD. I feel so grateful to have gotten to work with them and learn from them. I would also like to thank my parents and sister for their support throughout this entire process. Finally, a special thanks to all Manicassamy lab members, past and present, for their insight and friendships.

LIST OF FIGURES

LIST OF TABLES

CHAPTER I

Introduction

Some of this chapter includes text adapted from an article that is under review 'The p150 Isoform of ADAR1 Blocks Sustained RLR signaling and Apoptosis during Influenza Virus Infection'

Host Antiviral Response: Interferon Signaling

The host innate immune response to viral infection is mediated through the Pattern Recognition Receptors (PRRs) that recognize distinct molecular components of invading pathogens called pathogen-associated molecular patterns (PAMPs), which includes viral nucleic acids. Extracellular viral nucleic acids are sensed by Toll-like receptor (TLR) family of PRRs, which are transmembrane proteins expressed on the plasma membrane or in the endosomal compartments. TLR7/8 and TLR9 recognize single stranded RNA (ssRNA) and CpG DNA in the endosomal compartment, respectively; TLR3 detects viral double stranded RNA (dsRNA) (Diebold et al., 2004; Heil et al., 2004; Alexopoulou et al., 2001; Choe et al., 2005; Liu et al., 2008). Upon binding to viral nucleic acid, TLRs initiate signaling cascades that ultimately lead to the production of type I interferons (IFN) and inflammatory cytokines. In the cytoplasmic compartment, viral DNA can be sensed by AIM2-like receptors (ALRs) and cyclic GMP-AMP synthase (cGAS) (Hornung et al., 2009; Unterholzner et al., 2010; Sun et al., 2013; Wu, Sun, et al., 2013). Viral RNAs are recognized by the retinoic acid inducible gene I (RIG-I)-like receptor (RLR) family of PRRs. The RLR family includes the melanoma differentiation-associated gene 5 (MDA5), RIG-I, and Laboratory of Genetics

and physiology 2 (LGP2). RIG-I recognizes the 5'-triphosphate on short dsRNA, whereas MDA5 has been shown to sense long dsRNA (Pichlmair et al., 2006; Hornung et al., 2006; Schlee et al., 2009; Schmidt et al., 2009; Kato et al., 2008; Pichlmair et al., 2009; Peisley et al., 2012). The role of LGP2 is not completely defined yet; however, it is proposed to act as a negative regulator of other RLRs.

Three members of the RLR family share common structural features with a conserved central helicase domain, and a C-terminal domain with RNA binding activity. RIG-I and MDA5 contain tandem caspase activation and recruitment domains (CARD) in their N-termini. In the absence of viral nucleic acid, RIG-I and MDA5 are constitutively phosphorylated at specific residues on the CARD domain to prevent aberrant activation (Gack et al., 2010; Maharaj et al., 2012; Sun et al., 2011; Takashima et al., 2015; Nistal-Villan et al., 2010). Following sensing of viral RNA, RIG-I and MDA5 undergo a conformational change and are dephosphorylated (Wies et al., 2013; Kowalinski et al., 2011; Wu, Peisley, et al., 2013). Additionally, RIG-I must be ubiquitinated by the E3 ligases TRIM25 and Riplet, which add Lys63-linked ubiquitin chains to the CARD and C-terminal domains of RIG-I (Gack et al., 2007; Oshiumi et al., 2009; Gack et al., 2008). Upon activation, RIG-I and MDA5 translocate to the mitochondrial membrane using the mitochondrial trafficking proteins 14-3-3ε and 14-3-3η, respectively, to interact with mitochondrial antiviral signaling protein (MAVS) (Liu et al., 2012; Lin et al., 2019). This interaction is mediated by the CARDs of both MAVS and the RLRs, leadings to the activation of MAVS (Kawai et al., 2005; Horner et al., 2011). Activated MAVS molecules form prion-like filamentous structures to generate a signaling platform that recruits

several kinases, such as TBK1 and IKKε, to activate transcription factors IRF3, IRF7 and NF-κB (Xu et al., 2005; Seth et al., 2005; Hou et al., 2011). Activated IRF3/7 and NF-κB translocate to the nucleus and initiate the transcription of type I IFN and proinflammatory cytokines, respectively. IFN is secreted from the cells and can signal in an autocrine or paracrine manner by binding to IFN receptors on the cell surface (Schneider et al., 2014). Binding of IFN to IFN receptors leads to the activation of the janus kinase (JAK) and signal transducer and activators of transcription (STAT) signaling pathway that enables the production of a wide range of IFN-stimulated genes (ISG) (Schneider et al., 2014). These ISGs can then amplify the IFN response, generating an antiviral environment within the cell as well as alerting the neighboring cells.

Host Antiviral Response: Cell Death

In addition to transcriptional upregulation of IFN expression, PRR mediated detection of viral nucleic acids can also lead to the induction of cell death. There are 3 major types of cell death: apoptosis, necroptosis, and pyroptosis. Apoptosis is mediated by effector caspases 3 and 7 and is immunologically silent, resulting in cell shrinkage and the formation of apoptosis bodies (Elmore 2007; Lindqvist et al., 2018; White et al., 2014; Rongvaux et al., 2014). In contrast, necroptosis and pyroptosis induction require the action of gasdermin D (GSDMD) and mixed lineage kinase domain-like protein (MLKL) respectively to induce membrane damage, enabling the release of damage associated molecular patterns (DAMPs) and cytokines that can then trigger inflammatory responses in neighboring cells (Wang et al., 2017; Aglietti et al., 2016; Sborgi et al.,

2016; Liu et al., 2016; Frank et al., 2019; Wang et al., 2014; Dondelinger et al., 2014; Cai et al., 2014; Chen et al., 2014). Activation of cell death can serve as an additional method of controlling viral infection through elimination of infected cells (Maelfait et al., 2020).

Apoptosis can be categorized into two distinct pathways: extrinsic apoptosis and intrinsic apoptosis. Extrinsic apoptosis is initiated following the triggering of cell death receptors like members of the tumor necrosis factor (TNF) receptor family or Fas receptors (Elmore 2007). Activation of cell death receptors are mediated by death ligands, including TNF-α and FasL (Elmore 2007). Intrinsic apoptosis is stimulated via internal stimuli, such as DNA damage, metabolic stress, or viral infection (Elmore 2007). Activation of intrinsic apoptosis results in the destabilization of the mitochondrial membrane, leading to the release of cytochrome C (Elmore 2007). Both extrinsic and intrinsic apoptosis culminate in the activation of effector caspases 3, 6, and 7 (Slee et al., 2001). These caspases cleave a variety of substrates, ultimately resulting in the morphological characteristics associated with the induction of apoptosis (Slee et al., 2001).

While RIG-I pathway is predominantly associated with transcriptional upregulation of IFN genes, RIG-I activation can also induce intrinsic apoptosis through the RLR-induced IRF3 Mediated Pathway of Apoptosis (RIPA) (Chattopadhyay et al., 2017; Chattopadhyay et al., 2010; Chattopadhyay et al., 2011; Chattopadhyay et al., 2016). In this pathway, activated RIG-I translocates to the mitochondria and MAVS; however,

instead of RIG-I and MAVS interactions promoting IRF3 phosphorylation, the RIG-I–MAVS complex recruits the linear ubiquitin chain assembly complex (LUBAC) and stimulates the activation of IRF3 through linear polyubiquitination. Upon linear polyubiquitin modification, IRF3 interacts with the pro-apoptotic protein Bax, translocates to the mitochondria, and stimulates the release of cytochrome C, ultimately resulting in the induction of cell intrinsic apoptosis and inhibition of viral replication.

Negative Regulators of Host Antiviral Responses

While robust activation of the RLR pathway is necessary to mount effective antiviral responses, the downregulation of the RLR mediated host innate immune response is also necessary once the viral infection is cleared. Unregulated inflammatory responses can have detrimental consequences for the host including, immune-related tissue damage as well as autoimmunity. Indeed, several autoimmune diseases, such as Aicardi-Goutières syndrome (AGS), are linked to hyperactive innate immune responses.

Ubiquitination of RIG-I and MDA5 play an important role in the regulation of RLR signaling. Under steady state conditions, RIG-I and MDA5 are actively phosphorylated and prevented from aberrant activation. As mentioned previously, K63-linked polyubiquitination of RIG-I is necessary for the activation of RIG-I (Gack et al., 2007). Therefore, removal of K63-linked chains from RIG-I is important for the downregulation of RIG-I mediated signaling. The removal of K63-linked ubiquitin from RIG-I is mediated by de-ubiquitinating enzymes (DUBs), such as USP3 and USP15, which bind to RIG-I and remove K63-linked polyubiquitin chains, thereby inactivating RIG-I (Cui et al., 2014;

Zhang et al., 2015). While K63-linked polyubiquitin is necessary for RIG-I activation, K48-linked ubiquitination of RIG-I can target RIG-I for proteasomal degradation. RNF122 and RNF125 are E3 ligases that have been shown to add K48-polyubiquitin chains to RIG-I CARDs, which prevent the activation of RIG-I and target it for degradation (Wang, Jiang, et al., 2016; Arimoto et al., 2007).

Broadly, members of the suppressor of cytokine signaling (SOCS) family have been shown to inhibit IFN signaling (Trengove et al., 2013). For example, SOCS proteins have been shown to bind to JAK proteins and inhibit their tyrosine kinase activity, preventing interaction with STAT proteins (Yasukawa et al., 1999; Naka et al., 1997; Sasaki et al., 1999; Endo et al., 1997). Likewise, SOCS can inhibit IFN signaling by binding to the IFN-α receptor 1 (IFNAR1) associated kinase Tyk2 (Piganis et al., 2011). Furthermore, the box domain of SOCS proteins has also been implicated in the recruitment of factors important for the ubiquitination and degradation of proteins involved in the JAK/STAT signaling cascade (Zhang et al., 1999; Kamura et al., 2004). Taken together, RLR and IFN signaling pathways are tightly controlled through negative regulators to ensure appropriate levels of innate responses elicited against infection.

Viral Evasion of Antiviral Responses

Just as the host has developed mechanisms to downregulate innate immune responses, viruses must also develop strategies to suppress host antiviral responses for efficient viral propagation. For example, influenza A virus (IAV) encodes the multifunctional protein nonstructural protein 1 (NS1) that targets several host antiviral

processes. Notably, NS1 has been shown to inhibit TRIM25 mediated ubiquitination of RIG-I, thereby preventing the activation of the RIG-I pathway during IAV infection (Gack et al., 2009; Mibayashi et al., 2007; Rajsbaum et al., 2012). RIG-I-mediated signaling is an important aspect of the innate immune response to IAV infection, with RIG-I functioning as the predominant sensor of IAV viral RNA (vRNA) (Pichlmair et al., 2006). Similarly, Zika and Dengue viruses encode nonstructural protein 3 (NS3) that bind and sequester host protein 14-3-3ε to prevent translocation of RIG-I to the mitochondria and subsequent interaction with MAVS, ultimately suppressing the induction of IFN-β expression (Chan et al., 2016; Riedl et al., 2019). Hepatitis C virus (HCV) NS3/4a protein directly targets and cleaves the mitochondrial adaptor protein MAVS to prevent downstream signaling (Li et al., 2005; Meylan et al., 2005).

In regards to apoptosis, both proviral and antiviral roles have been attributed to the induction of apoptosis during viral infection. As a result, viruses have developed methods to either inhibit or promote apoptosis induction. For example, poxviruses encode soluble TNF decoy receptors to bind TNFα and prevent activation of cell death receptors and subsequent apoptosis induction (Reading et al., 2002). For IAV, the nonstructural protein 1 (NS1) has been shown to upregulate PI3K/AKT signaling to promote cell survival (Ehrhardt et al., 2007). In contrast, the 7a protein from SARS-CoV inhibits the anti-apoptotic protein Bcl-X_L to promote apoptosis (Tan et al., 2007).

ADAR1 as a Negative Regulator of Innate Immune Signaling

Recent studies demonstrate that the host RNA editing enzyme Adenosine Deaminase Acting on RNA (ADAR1) is a negative regulator of innate immunity. ADAR1 deaminates adenosine (A) to inosine (I) in endogenous dsRNA to destabilize dsRNA structures and prevent aberrant activation of MDA5. ADAR1 is expressed as two isoforms: a constitutively expressed p110 isoform that localizes to the nucleus, and an inducible p150 isoform that is predominantly present in the cytoplasm (George et al., 1999; Poulsen et al., 2001; Patterson and Samuel 1995; Patterson, Thomis, et al., 1995; Eckmann et al., 2001; Desterro et al., 2003). The p150 isoform is induced by viral infection as well as by IFN receptor signaling. In addition to ADAR1, there are two other ADARs, ADAR2 and ADAR3, which are expressed in a cell type specific manner. ADAR1 and ADAR2 have both been shown to exhibit RNA editing activity and are expressed ubiquitously, whereas ADAR3 lacks catalytic activity (Chen et al., 2000; Melcher, Maas, Herb, Sprengel, Higuchi, et al., 1996; Melcher, Maas, Herb, Sprengel, Seeburg, et al., 1996; Jacobs et al., 2009; Kim et al., 1994).

ADAR1 was identified in *Xenopus laevis* studies where it was initially shown to have dsRNA unwinding activity and was subsequently found to possess A-to-I editing activity (Bass et al., 1988; Rebagliati et al., 1987; Bass et al., 1987; Wagner et al., 1989; Kim et al., 1994). ADAR1 editing predominantly occurs in transcripts produced from *Alu* elements, which are transposable elements that when inserted into the genome in reverse orientation form dsRNA duplex structures. *Alu* elements are commonly found in the introns of transcribed genes and make up almost 10% of the human genome (Athanasiadis et al., 2004; Kim et al., 2004; Lander et al., 2001; Blow et al., 2004;

Levanon et al., 2004; Ramaswami et al., 2012; Bazak et al., 2014). As a result, it has been proposed that ADAR1 editing of *Alu* elements helps contribute to the diversification of the human genome (Paz-Yaacov et al., 2010). Other editing targets of ADAR1 include RNA encoding the neurotransmitter receptors, glutamate receptor (GluR-B) and serotonin receptor (5-HT2cR) (Liu, Emeson, et al., 1999; Liu and Samuel 1999). In addition to the editing of RNA transcripts, ADAR1 has also been implicated in the regulation of kidney development and intestinal homeostasis (Pestal et al., 2015).

Mutations in ADAR1 have been associated with the development of AGS, a fetal encephalopathy associated with increased type I IFN activity in the cerebrospinal fluid and serum (Lebon et al., 1988; Rice et al., 2013). In addition to mutations in ADAR1, mutations in TREX1, RNase H2 complex, SAMHD1, ADAR1 and MDA5 have been shown to cause AGS (Rice et al., 2012; Crow, Chase, Lowenstein Schmidt, et al., 2015). In a study examining ADAR1 mutations associated with AGS, a vast majority of the amino acid substitutions were found within the catalytic domain as well as a small number of substitutions occurring around the Z-DNA/RNA binding domains (Rice et al., 2012).

Genetic ablation of ADAR1 in mice results in embryonic lethality due to increased upregulation of IFN stimulated gene (ISGs) and apoptosis of hematopoietic cells (Pestal et al., 2015; Liddicoat et al., 2015; Mannion et al., 2014). Specific deletion of the p150 isoform also resulted elevated expression of ISGs as compared control embryos, suggesting that the embryonic lethality is due to the loss of p150. However, concurrent

ablation of both ADAR1 and MDA5 or p150 and MDA5 in mice led to improved survival as well as reduction in ISG expression to levels similar to control embryos, suggesting that the p150 isoform of ADAR1 prevents MDA5 from sensing endogenous dsRNA under basal conditions. Additionally, using ADAR1 editing deficient knock-in mice, it was demonstrated that the catalytic activity of ADAR1 was required to suppress MDA5 sensing of endogenous dsRNA (Liddicoat et al., 2015). In addition to preventing MDA5 sensing of endogenous dsRNA, ADAR1 has also been implicated in preventing PKR sensing of viral and endogenous RNA, thereby preventing PKR-mediated translational shutdown and IFN production (Chung et al., 2018; Wang et al., 2009; Li et al., 2012; Clerzius et al., 2009; Toth et al., 2009). As with MDA5, the catalytic activity of ADAR1 was required to suppress PKR sensing of endogenous RNA (Chung et al., 2018). Similarly, concurrent deletion of ADAR1 and RNaseL rescued the cell lethal phenotypes the authors observed in ADAR1 KO human lung adenocarcinoma (A549) cells, suggesting that ADAR1 may also inhibit the activation of the OAS/RNaseL pathway (Li et al., 2017). ADAR1 has also been implicated in the inhibition of apoptosis, with the loss of ADAR1 in mice leading to the upregulation of apoptosis in hematopoietic stem cells (Qiu et al., 2013; Hartner et al., 2009). Additionally, PARP cleavage, a byproduct of apoptosis, has been shown to increase following measles infection in ADAR1 knockdown HeLas, suggesting a role for ADAR1 in suppressing virally induced apoptosis (Toth et al., 2009). However, the molecular mechanism contributing to increased apoptosis in ADAR1 deficient cells is yet to be determined.

ADAR1 as a Viral Factor

While ADAR1 has numerous endogenous roles within the cell, ADAR1 has also been implicated in the replication of several viruses from diverse families, with ADAR1 acting as either a proviral or antiviral factor. One of the best characterized proviral role of ADAR1 is during hepatitis delta virus (HDV) replication in which p110 mediated editing of viral RNA is necessary for the production of the large HDV antigen, thereby regulating the switch from replication of the viral genome to packaging (Wong et al., 2002; Jayan et al., 2002). In terms of antiviral roles for ADAR1, knockdown of ADAR1 during hepatitis C virus (HCV) infection has been shown to increase viral RNA production, suggesting an antiviral role for ADAR1 in HCV replication (Taylor et al., 2005).

Viral genomes have also been shown to be targets of ADAR1 hyperediting. ADAR1 hyperediting has been shown to occur during persistent measles virus infection of the central nervous system, which results in subacute sclerosing panencephalitis (SSPE). Measles RNA isolated from SSPE patients showed increased A-to-G mutations in the matrix gene, a characteristic signature of ADAR1 editing (Baczko et al., 1993; Cattaneo et al., 1988; Cattaneo et al., 1986; Suspene et al., 2008). While hyperediting of the matrix gene is hypothesized to contribute to persistent measles infection, how ADAR1 contributes to normal measles virus replication is less defined. In one study using p150 KO MEFs, measles virus replication was shown to be increased compared to control cells, suggesting an antiviral role for ADAR1 in measles infection (Ward et al., 2011). In contrast, several other studies suggest that ADAR1 may promote measles infection via inhibition of PKR. Indeed, loss of ADAR1 expression during measles infection led to

increased cell death, IFN-β expression, and stress granule formation (Toth et al., 2009; Okonski et al., 2013; Li et al., 2012). This increase in cell death and IFN-β expression was associated with increased activation of PKR, suggesting that ADAR1 inhibits PKR mediated signaling during measles infection. Interestingly, cDNA complementation studies in HeLa cells deficient in ADAR1 expression demonstrated that the catalytic activity of p150 was required for suppression of PKR (Okonski et al., 2013).

ADAR1 and Influenza A Virus

IAV is a member of the *Orthomyxoviridae* family and is a common cause of acute upper respiratory tract infections in humans, leading to significant morbidity and mortality within the population. The IAV genome, single-stranded RNA with a 5'-triphosphate, is predominantly recognized by RIG-I (Pichlmair et al., 2006). The IAV viral antagonist NS1 was found to interact with ADAR1 in yeast two-hybrid screens (de Chassey et al., 2013; Ngamurulert et al., 2009). In addition, NS1 has been shown to stimulate RNA editing functions of ADAR1 (de Chassey et al., 2013). In regards to IAV infection, the role of ADAR1 has yet to be completely understood. p150 KO mouse embryonic fibroblasts (MEFs) infected with IAV exhibited increased cytopathic effect likely due to increased viral replication as compared to control MEFs, suggesting an antiviral role for p150 in IAV infection (Ward et al., 2011). In contrast, knockdown of ADAR1 in A549s led to increased IAV replication, suggesting a proviral role for ADAR1 in IAV replication (de Chassey et al., 2013). Moreover, analysis of viral genomes from influenza vaccines showed in hyperediting by ADAR1 (Suspène et al., 2011). While the exact function of

ADAR1 in IAV replication has yet to be fully elucidated, these studies highlight the potential for ADAR1 as a host factor involved in IAV replication.

CRISPR/Cas9 Technology

To determine the contribution of the different ADAR1 isoforms to IAV replication, we utilized the CRISPR/Cas9 gene disruption strategy to abolish expression of ADAR1 and the individual isoforms of ADAR1. This gene disruption strategy was first identified as a microbial immune defense mechanism for targeting and cleaving foreign nucleic acids (Ran et al., 2013). Three types of CRISPR systems have been identified in bacterial and archaeal species (Ran et al., 2013). Each CRISPR systems is composed of CRISPR-associated (*cas*) genes, noncoding RNAs, and the CRISPR RNA (crRNA) array (Ran et al., 2013). The crRNA array is composed of repetitive elements and variable sequences derived from exogenous DNA targets called protospacers (Brouns et al., 2008; Barrangou et al., 2007). The DNA target for each CRISPR system must contain a protospacer adjacent motif (PAM), which can vary depending upon the CRISPR system (Marraffini et al., 2008, 2010; Deveau et al., 2008).

The best characterized and most commonly used CRISPR system is the type II CRISPR system. The type II CRISPR system is composed of the Cas9 nuclease and a crRNA array that encodes the guide RNA and auxiliary trans-activating crRNA (tracrRNA) (Garneau et al., 2010; Jinek et al., 2012; Gasiunas et al., 2012; Sapranauskas et al., 2011; Magadan et al., 2012). The tracrRNA is necessary for the processing of cRNA into individual crRNA units that can then form a complex with Cas9

for gene targeting (Deltcheva et al., 2011). Previous studies have demonstrated that the crRNA and tracrRNA can be fused together to form a single-guide RNA (sgRNA), which can then be utilized for targeting of the desired gene to abolish expression (Jinek et al., 2012).

The CRISPR/cas9 system can be employed in mammalian cells through the expression of Cas9 and sgRNA designed to target the gene of interest. Once expressed, the sgRNA will direct Cas9 mediated cleavage through sgRNA base paring with the target DNA upstream of the PAM (Sapranauskas et al., 2011). For the type II CRISPR system derived from *Streptococcus pyogenes* utilized in our studies, the DNA target must immediately precede a 5'-NGG PAM (Deveau et al., 2008). Cas9 nuclease activity will generate a double stranded break in the DNA that then undergoes one of two pathways for DNA repair: Non-homologous end joining (NHEJ) or homology-directed repair (HDR). The HDR pathway requires a repair template in order to repair the DNA break and can, therefore, be utilized to insert modifications within the gene of interest through the use of an exogenous template (Ran et al., 2013). In the absence of a repair template, NHEJ occurs. NHEJ is an error prone repair pathway that can result in insertion or deletion mutations within the gene, which can lead to frameshift mutations or premature stop codons that can negatively impact gene expression (Ran et al., 2013).

The CRISPR/Cas9 system derived from *Streptococcus pyogenes* has been utilized by several groups to screen for host factors necessary for efficient viral replication of

different viruses including IAV, human immunodeficiency virus (HIV), Epstein-barr virus (EBV), and flaviviruses (Park et al., 2017; Savidis et al., 2016; Ma et al., 2017; Marceau et al., 2016; Han et al., 2018; Li et al., 2020). To determine the contribution of ADAR1 during IAV replication, we employed the CRISPR/Cas9 gene disruption strategy to generate ADAR1 knockout (KO) A549s, as well as ADAR1 isoform specific KOs. The cell lines generated through the CRISPR/Cas9 mediated gene disruption strategy were crucial for examining the role of ADAR1 during IAV infection and the role of ADAR1 in suppressing antiviral signaling.

Thesis Goals

Viruses are constantly developing strategies to evade host innate immune responses in order to replicate within the host, creating an evolutionary “arms race” between the host immune response and viral immune evasion. Given the significant public health and economic burden that can be imposed upon society during viral outbreaks, it is crucial to understand how the host responds to viral infection as well as the ways in which the virus subverts these defenses. In doing so, we gain a greater understanding of the virus-host interplay, enabling the development of antiviral therapeutics and treatments against viruses.

Using IAV as a model virus, we examined the role of ADAR1 in regulating the life-cycle of IAV. Through the use of CRISPR/Cas9 technology, we revealed opposing functions for the two isoforms, with the cytoplasmic p150 isoform acting as a negative regulator of RIG-I signaling and the nuclear p110 isoform acting as an IAV restriction factor. We

show that p150 promotes IAV replication independent of its role in the suppression of MDA5 mediated sensing of endogenous dsRNA. Through concurrent deletion of p150 and RLR pathway components, we demonstrate that p150 suppresses sustained activation of the RIG-I signaling cascade, resulting in decreased levels of IFN-β expression and apoptosis. In p150 deficient cells, IAV replication was restored by inhibiting both apoptosis and IFN receptor signaling. p150 mediated suppression of RLR signaling was dependent on RNA binding functions but independent of RNA editing activity.

Our studies illustrate a broad role for p150 in preventing the hyperactivation of innate immune responses, with p150 suppressing both the MDA5 pathway under basal conditions and the RIG-I pathway during viral infection. Additionally, these results demonstrate that dampening of RIG-I mediated signaling by p150 enables efficient IAV replication, illuminating an additional mechanism utilized by IAV to subvert cell intrinsic responses. Together, these studies contribute to a deeper understanding of how the host responds to viral infection and the ways in which viruses undermine these responses to replicate within the host.

CHAPTER II

Materials and Methods

This chapter includes experimental procedures from an article that is under review 'The p150 Isoform of ADAR1 Blocks Sustained RLR signaling and Apoptosis during Influenza Virus Infection'

Cell Culture and Viruses

Human lung epithelial (A549) and human embryonic kidney (HEK293) cells were cultured in DMEM supplemented with 10% fetal bovine serum (FBS) and 1% penicillin/streptomycin (P/S). Madin-Darby canine kidney (MDCK) cells were cultured in MEM supplemented with 10% FBS and 1% P/S. Dr. Adolfo Garcia-Sastre at the Icahn School of Medicine at Mount Sinai, NY kindly provided the IAV strains A/Puerto Rico/8/1934 (H1N1), low pathogenic version of A/Vietnam/1203/2004 (H5N1), and A/Hong Kong/1/1968 (H3N2). IAV strains were grown in 10-day old specific pathogen-free eggs (Charles River) and titered by standard plaque assay on MDCK cells, using 2.4% Avicel RC-581 (a gift from FMC BioPolmer, Philadelphia, PA). Two days post infection plaques were quantified via crystal violet staining. Vesicular stomatitis virus expressing GFP (VSV) was kindly provided by Dr. Glenn Barber at the University of Miami, FL (Stojdl et al., 2003). VSV viruses were grown in Vero cells and titered by plaque assay with 1% methylcellulose (Sigma).

Generation of CRISPR KO and cDNA Complemented Cells

ADAR1 KO A549s were generated using the lentiCRISPR v2 single vector system, which has been previously described (Sanjana et al., 2014). Oligonucleotides were annealed and cloned into the lentiCRISPR v2 vector through BsmBI sites (Table II.1). A549s were transduced with lentivirus expressing specific sgRNA and selected with 2 μg/ml puromycin for 14 days. CTRL A549s were generated through the same method using the lentiCRISPR v2 vector without sgRNA. To generate clonal KO A549s, puromycin selected population were seeded at ~100-150 cells per 15cm plates and individual colonies were isolated using cloning cylinders. Subsequently, gDNA was extracted from isolated KO cells using the Blood and Cell Culture Mini kit (Qiagin) per the manufacturers specification and the targeted region was PCR amplified using EconoTaq and gene specific primers. PCR products were cloned into pGEM-T vector and approximated 12-15 individual bacterial colonies were sequenced (University of Chicago DNA sequencing facility). Sequences were analyzed by SeqMan program (LaserGene).

To generate isoform specific KO A549s, WT A549s were transduced with lentiCRISPR v2 containing sgRNA targeting a region 200-300 nucleotides upstream of transcription start site and lentiCRISPR v2-GFP containing a sgRNA downstream of the transcription start site. Cells were selected with 2 μg/ml puromycin for 14 days and then selected for GFP expression by single-cell sorting, to ensure the presence of both sgRNA. Individual

KO clones were identified by PCR analysis of targeted region and confirmed by western blot for ADAR1 expression.

To generate p150/MDA5 DKOs, clonal p150 KOs were transduced with a lentiCRISPR v2-hygro vector containing gene specific sgRNA followed by selection with 600 μg/ml hygromycin for 14 days. For the p150/Bax DKOs, clonal p150 KOs were transduced with a lentiCRISPR v2-neo vector containing the gene specific sgRNA followed by selection in 600 μg/ml neomycin for 14 days. The RIG-I/MDA5/p150 and MAVS/MDA5/p150 TKO A549s were generated by transducing the p150/MDA5 DKOs with the lentiCRISPR v2-neo vector containing gene specific sgRNA followed by selection in 600 μg/ml neomycin for 14 days. Individual KO clones were isolated as described above and screened by western blot and Sanger sequencing.

To generate complemented cell lines, p150 cDNA was cloned into the pLX304 lentivirus vector. p150 KO and p150/MDA5 DKOs were transduced with lentivirus carrying either empty vector or p150 cDNA, and selected with 15 μg/ml blasticidin for 14 days. Polyclonal population were seeded at limiting dilutions and individual clones were isolated and confirmed via western. After selection, complemented clones were maintained in 5 μg/ml blasticidin.

Virus Infections

To assess viral replication, CTRL A549s or KOs were seeded at a density of $1.2x10^6$ cells per well in triplicate in a 6-well dish. For IAV infection, cells were washed twice with phosphate buffer saline (PBS) and 500 μl of infection media (DMEM supplemented with 0.2% bovine serum albumin (BSA) and 1μg/ml TPCK-treated trypsin (T1426, Sigma)) was added per well. Cells were infected at indicated MOI based on cell numbers determined prior to infection and incubated for 1 hour at 37°C. After the 1 hour incubation, the inoculum was removed and the cells were washed twice in PBS and placed in 2 ml of fresh infection media. Supernatants were harvested at the indicated times and titered by plaque assay in MDCK cells (Han et al., 2018). For VSV, infections were performed as described above with DMEM supplemented with 2% FBS. VSV titers were assessed by plaque assay in Vero cells using 1% methylcellulose. To examine viral replication following inhibition of IFN signaling, cells were seeded at a density of $1.2x10^6$ cells per well in a 6-well dish in DMEM supplemented with 10% FBS, 1% P/S, and either DMSO or 0.2 μM Ruxolitinib (INCB018424 Selleckchem). IAV infection was performed as described above using infection media containing DMSO or 0.2 μM Ruxolitinib. Viral titers were assessed as described above. All infection experiments were performed with biological triplicates and data is presented as the mean titer of the triplicate samples(±SD).

For western blotting and qPCR, cells were seeded at a density of $1.2x10^6$ cells per well in a 6-well dish. Cell numbers were calculated the next day prior to infection. Cells were mock treated or inoculated with H1N1 at MOI of 1 or SeV at a 1:100 dilution in DMEM

supplemented with 0.2% BSA and 1% P/S at 37°C. Cells were harvested at the indicated time points for RNA or protein isolation.

QPCR Analysis of Host Gene Expression

Total RNA from pooled triplicates was isolated by TRIzol (Invitrogen) extraction method. Residual genomic DNA contamination was removed by treatment with recombinant DNAse I (Roche). cDNA was generated using Superscript II reverse transcriptase and Oligo d(T) (Invitrogen). Using SYBR Green PCR Master Mix (Applied Biosystems), qPCR was performed with technical duplicates and gene specific primers. Tubulin was used as an endogenous housekeeping gene to calculate delta delta cycle thresholds. Results are represented as fold expression relative to mock vector CTRL A549s.

RT and qPCR primers: hIFN-β: forward TCTGGCACAACAGGTAGTAGGC and reverse GAGAAGCACAACAGGAGAGCAA; hTub: forward GCCTGGACCACAAGTTTGAC and reverse TGAAATTCTGGGAGCATGAC.

Western Blot Analysis

To confirm ADAR1 isoform specific KO and MDA5 KOs, CTRL A549s and various KOs cells were treated with 1000U/ml of universal type I IFN (PBL Assay Science) for 24 hours and lysed for western blot analysis. To confirm RIG-I KO, vector control and KO cells were infected with SeV for 16 hours and then lysed for western blot analysis. Whole cell lysates for western blot analysis was prepared using RIPA buffer (50 mM

Tris pH 7.8, 150 mM NaCl, 0.1% SDS, 0.5% Sodium deoxycholate, 1% Triton X-100) containing protease inhibitors and quantified by Bradford protein assay. Approximately 50-80 μg of total protein was loaded on to SDS gel. Antibodies used for western blot analysis: ADAR1 (Abcam 88574; Santa Cruz sc-271854), MDA5 (Alexis Biochemicals AT113), RIG-I ((1C3 clone) (Nistal-Villan et al., 2010)), IRF3 (Santa Cruz sc-9082), V5 (Bio-Rad), cleaved PARP (Cell Signaling 5625), total PARP (Cell Signaling 9542), and Ku (#K2882 Sigma).

RLR agonist transfection

For vRNA transfection, IAV vRNA from H1N1 was extracted using the QIAamp Viral RNA Mini Kit per the manufacturer's recommendations. Cells were seeded at a density of $1.2x10^6$ cells per well in a 6-well dish a day prior to transfection. Cells were transfected with vRNA using polyethylenimine reagent (PEI) in OptiMem (OMEM) and were collected at the indicated time points for RNA or protein extraction. For low molecular weight (LMW) and high molecular weight (HMW) poly(I:C) (pI:C) transfections, 1μg of LMW or HMW pI:C (Invivogen) was transfected into cells

For siRNA transfection, cells were seeded at a density of $1.5x10^5$ cells per well in a 12-well dish. 50 nM pooled siRNA (Dharmacon) was transfected using RNAiMAx reagent (2.4 μl per well). At 48 hours post siRNA transfection, cells were transfected with H1N1 vRNA and cell lysates were collected 24 hours post vRNA transfection for western blot.

IFN-β reporter assay

p150 KO 293s was transfected with a plasmid mixture containing p150 (100ng), IFN-β-Firefly reporter (100ng), and SV40 Renilla (50ng) using PEI (1:5 DNA:PEI ratio). A GFP expressing plasmid was included in place of p150 as controls. To measure p150 and NS1 mediated suppression of IFN-β-Firefly reporter activity, 293s were transfected with a PEI and plasmid mixture containing p150 (100ng), NS1 (2ng), IFN-β-Firefly reporter (100ng) and SV40 Renilla (50ng). A GFP expressing plasmid was included in place of p150 or NS1 as a control. IFN-β-Firefly reporter activity was induced by infecting cells with SeV (1:100) at 6 hours post transfection. At 48 hours post transfection, cells were lysed in 1x Passive Lysis Buffer (Promega), and firefly and renilla luciferase activity in the lysates were measured using Dual-Luciferase Reporter Assay System (Promega) in GloMax 20/20 luminometer (Promega). Data from biological triplicates is presented as percent luciferase activity relative to GFP + SeV control.

ANNEXIN V Staining

ADAR1 KOs were seeded at a density of $1.0x10^6$ cells per well in a 6-well dish. The following day, cells were transfected with H1N1 vRNA as described above. At 40 hours post transfection, cells were stained with Annexin V-PE (BD Pharmingen) per the manufacturer's recommendations. Annexin V staining was analyzed by flow cytometer. Data analysis was performed using FlowJo Software

Immunofluorescence

To analyze p150 and NS1 localization, cells were seeded at a density of $8x10^5$ cells per well on a glass coverslip in a 24-well dish. Cells were infected at a MOI of 5 on ice for 1 hour in OMEM, allowing virus to bind to the cells. After 1 hour incubation on ice, cells were washed twice with PBS and 0.5 mL of OMEM was added per well. After 16 hours, cells were fixed with 4% formaldehyde for 10 minutes, washed with PBS twice, and permeabilized with 0.1% Triton-X for 15 minutes. Cells were then incubated with blocking buffered for 1 hour. After blocking, cells were incubated with a mixture of NS1 (anti-rabbit clone 155) and ADAR1 or Flag (M2, Sigma) antibodies in blocking buffer for 1 hour and then washed three times with blocking buffer. A mixture of Alex-488 and Alexa-546 secondary antibodies with DAPI was added to the cells and incubated for 1 hour. Following incubation with secondary antibodies and wash steps, slides were mounted onto coverslips with Prolong and then visualized using a confocal microscope.

For FlAsh staining, cells were incubated with FlAsH staining solution (1-1.5μM FlAsH (Invitrogen) and 10 μM 1,2-ethanedithiol (Sigma)) one hour prior to fixation. After incubating cells in FlAsH solution for 30 minutes at 37°C, cells were washed with PBS once. Cells were then incubated in wash buffer (500 μM 1,2-ethanedithiol diluted in DMSO and 1x 2,3-dimercapto-1-propanol (Sigma)) for 7 minutes at 37°C. Incubations with wash buffer were repeated twice and then cells were washed with PBS and fixed in 4% formaldehyde. Staining for ADAR1 and Flag was performed as described above.

CHAPTER III

The p150 Isoform of ADAR1 Suppresses RLR Signaling during Infection

Some of this chapter includes text adapted from an article that is under review 'The p150 Isoform of ADAR1 Blocks Sustained RLR signaling and Apoptosis during Influenza Virus Infection'. Olivia Vogel performed all of the experiments in this chapter, except for the basal ISG experiments in Figure III.5 panels A and C as well as the IFN-β kinetics experiments in Figure III.7 panels C-E which were performed by Dr. Jasmine Perez. The FACS experiment in Figure III.7 panel H was performed by Chieh-Yu Liang.

Introduction

The cell intrinsic response to viral infection activated through PRRs is essential for restricting viral infection. For many RNA viruses, detection of viral nucleic acids in the cytoplasm are primarily mediated by the RLR family of PRRs, which include RIG-I and MDA5. RIG-I has been demonstrated to detect the 5'triphosphate or 5'diphosphate with short dsRNA structures and MDA5 has been shown to detect long dsRNA (Pichlmair et al., 2006; Hornung et al., 2006; Schlee et al., 2009; Goubau et al., 2014; Kato et al., 2008; Pichlmair et al., 2009; Peisley et al., 2012). Following binding of IAV viral (genomic) RNA, RIG-I is activated through dephosphorylation and ubiquitination processes, which enables interaction with MAVS at the mitochondrial membrane via the CARD domains (Kawai et al., 2005). At this junction, activated RIG-I and MAVS can either stimulate the IRF3 transcriptional pathway or IRF3 mediated apoptosis pathway, both of which are crucial aspects of the host responses to control viral infection. For the

transcriptional pathway, Tank binding kinase (TBK1) and inhibitor of nuclear factor kappa B kinase (IKKb) are recruited by the E3 ligase TNFR associated factor 3 (TRAF3) to the RIG-I-MAVS complex to phosphorylate and activate the transcription factors IRF3 and NF-kB. Phosphorylated IRF3 and NF-kB, translocate to the nucleus to initiate transcription of IFN-β and other proinflammatory cytokines, respectively (Xu et al., 2005; Seth et al., 2005; Hou et al., 2011; Goubau et al., 2013; Loo et al., 2011). This transcriptional upregulation of antiviral genes is critical for generating an antiviral environment within the cell and surrounding cells through the induction of IFN stimulated gene (ISG) expression (Schneider et al., 2014). The IRF3-mediated apoptosis pathway is activated by the recruitment of LUBAC complex to the RIG-I–MAVS complex and subsequent linear ubiquitination of IRF3. Ubiquitinylated IRF3 in complex with the pro-apoptotic protein Bax translocate to the mitochondrial membrane and stimulate the release of cytochrome C, triggering cell intrinsic apoptosis process (Chattopadhyay et al., 2016; Chattopadhyay et al., 2010; Chattopadhyay et al., 2017). Intrinsic apoptosis is immunologically silent and plays an important role in clearing infected cells from the site of infection (Elmore 2007).

While robust activation of cell intrinsic immune responses is necessary for effective control of viral infection, timely downregulation of these processes is also important to prevent hyperactive inflammatory responses. In addition, recent studies demonstrate that endogenous RNA ligands can stimulate antiviral responses through RLRs under physiological conditions. As a result, many proteins involved in RNA sensing and RNA metabolism have been implicated in preventing activation of RLR signaling under basal

conditions (Crow, Chase, Schmidt, et al., 2015). The RNA editing enzyme ADAR1 has been shown to prevent various RNA sensors, such as MDA5, PKR, and RNaseL, from aberrant activation through endogenous dsRNA ligands (Pestal et al., 2015; Liddicoat et al., 2015; Mannion et al., 2014; Chung et al., 2018; Li et al., 2017). By inhibiting the sensing of endogenous RNA ligands, ADAR1 aids in preventing erroneous activation of antiviral signaling pathways within the cell under basal conditions.

In addition to the regulation of basal cell intrinsic immunity, ADAR1 has also been shown to modulate viral replication. Both proviral and antiviral roles have been attributed to ADAR1, depending upon the virus family (Samuel 2011). In regards to IAV replication, the contribution of ADAR1 and its different isoforms are less defined, with conflicting findings as to whether ADAR1 demonstrates a proviral or antiviral role during IAV infection (Ward et al., 2011; de Chassey et al., 2013). IAV belongs to an unique group of RNA viruses that replicate in the nucleus (Fields et al., 2013). Considering the differential intracellular localization of the ADAR1 isoforms, with p110 localizing in the nucleus and p150 predominantly localizing in the cytoplasm, we sought to determine how these two isoforms of ADAR1 may contribute to the replication of IAV.

Here, we investigated the role of ADAR1 in the life-cycle of IAV by generating ADAR1 and isoform specific KOs in A549s using the CRISPR/Cas9 technology. We demonstrate that the loss of ADAR1 or the p150 isoform resulted in increased expression of ISGs under homeostatic conditions, due to activation of MDA5 by endogenous dsRNA ligands. Although concurrent deletion of p150 and MDA5 reduced

basal IFN-β expression, IAV replication was significantly reduced in p150/MDA5 double KOs (DKOs) due to sustained IFN-β expression and increased cell intrinsic apoptosis. Furthermore, stimulation of the RIG-I pathway through RIG-I agonists, demonstrated that both IFN-β expression and apoptosis induction are increased in the p150/MDA5 DKO A549s compared to control A549s. Together, these studies illuminate another aspect of p150 mediated suppression of innate immune signaling, with p150 suppressing RLR signaling during viral infection.

Results

ADAR1 is a proviral factor for IAV replication

To assess the role of ADAR1 in IAV replication, we generated CRISPR/Cas9 knockouts of ADAR1 in A549s (ADAR1 KOs) using a single guide RNA (gRNA) targeting the open reading frame shared by both isoforms (Figure III.1A). Individual ADAR1 KO clones were identified by Sanger sequencing of the region flanking the sgRNA target site. To confirm the loss of ADAR1 protein expression, we performed western blot analysis for the p110 and p150 isoforms in ADAR1 KOs, vector control A549s (CTRL), and parental wild-type A549s (WT A549) under mock and universal interferon (IFN-I) treatment conditions, which induces p150 expression (Figure III.1B). ADAR1 KOs showed loss of expression for both p110 and p150 under mock and IFN-I treated conditions, confirming successful knockout of both isoforms. Next, to assess the importance of ADAR1 in IAV replication, ADAR1 KOs and CTRL A549s were infected at a low MOI with different strains of IAV (A/Puerto Rico/8/1934 H1N1, A/Vietnam/1203/04 H5N1-low pathogenic, and A/HongKong/1/1968 H3N2) and observed decreased IAV replication in ADAR1

KOs as compared to CTRL A549s (Figure III.1C; Figure III.2.A). Interestingly, the replication of vesicular stomatitis virus (VSV), also an RNA virus, was similar in both ADAR1 KOs and CTRL A549s (Figure III.1C). These results suggest that ADAR1 is important for optimal IAV replication.

The p150 isoform of ADAR1 is important for optimal IAV replication

Next, to identify the isoform of ADAR1 promoting IAV replication, we generated isoform specific KO A549s by deleting either the p110 or p150 promoter (p110 KOs or p150 KOs, respectively) using sgRNA (Figure III.3A). Individual KO clones were identified by PCR screening for deletion and the loss of specific ADAR1 isoforms was analyzed by western blot analysis following IFN-I treatment (Figure III.3B). Under mock conditions, p110 expression was abolished in p110 KOs but not in p150 KOs or CTRL A549s. Following treatment with IFN-I, p150 KOs did not show induction of p150 expression, confirming successful deletion of the p150 promoter. In the p110 KOs, treatment with IFN-I led to induction of both p110 and p150 expression, albeit at lower levels as compared to p150 KOs and CTRL A549s. This is in accordance with a prior study suggesting that p110 can be expressed from a cryptic promoter present before exon 1C (Figure III.3A) (Chung et al., 2018; Nachmani et al., 2014).

Next, we assessed IAV replication in the isoform specific KOs, ADAR1 KOs, and CTRL A549s (Figure III.3C; Figure III.4A). The replication of all three IAV strains was decreased in p150 KOs to levels similar to ADAR1 KOs, demonstrating that the p150 isoform is critical for optimal IAV replication. In a multi-cycle growth kinetics assay, we also observed reduced viral titers in the p150 KOs as compared to CTRL A549s at all

tested time points (Figure III.4B). In contrast, IAV replication was increased in p110 KOs as compared to CTRL A549s, indicating a potential antiviral role for p110 during IAV infection (Figure III.3C; Figure III.4A). However, VSV replication was mostly unaffected by the loss of either the p110 or p150 isoform.

Next, to confirm that the reduction in IAV replication observed in p150 KOs was due to loss of p150 expression, as well as to rule out any off-target effects, we complemented the p150 KO with V5-tagged wildtype p150 (p150 KO/p150) and confirmed the expression of exogenous p150 by western blot analysis of clonal cells (Figure III.3D). As anticipated, IAV replication was increased in p150 KO/p150 clones as compared to empty vector p150 KOs for three different IAV strains, indicating that the decreased IAV replication observed in p150 KOs was due to loss of p150 expression (Figure III.3E; Figure III.4C). Together, these results demonstrate that the two isoforms of ADAR1 have opposing roles during IAV replication, with the p150 isoform of ADAR1 being important for efficient IAV replication, and the p110 isoform playing a potential antiviral role in IAV replication.

p150 promotes IAV replication independent of MDA5 suppression

Prior studies indicate that loss of ADAR1 results in increased upregulation of IFN-β and ISGs due to MDA5 mediated sensing of endogenous dsRNA (Liddicoat et al., 2015; Pestal et al., 2015). To test this, we first assessed basal IFN-β expression in ADAR1 and isoform specific KOs by qRT-PCR (Figure III.5A). As compared to CTRL A549s, ADAR1 KOs and p150 KOs exhibited elevated levels of basal IFN-β expression,

confirming the role of p150 in suppressing MDA5 activation by endogenous ligands (Pestal et al., 2015; Liddicoat et al., 2015; Mannion et al., 2014). To determine whether the elevated basal IFN-β expression observed in p150 KOs contributed to reduced IAV replication, we generated p150 and MDA5 double knockout A549s as well as MDA5 single KO A549s (p150/MDA5 DKOs or MDA5 KOs). We confirmed successful knockout of MDA5 expression by western blot analysis (Figure III.5B). As expected, p150/MDA5 DKOs exhibited reduced basal IFN-β expression as compared to p150 KOs (Figure III.5C), further confirming that p150 suppresses sensing of endogenous ligands by MDA5. Next, to determine if the reduced basal IFN-β levels rendered p150/MDA5 DKOs more permissive to IAV replication, we assessed IAV replication in various MDA5 KOs. Interestingly, IAV replication was reduced in p150/MDA5 DKOs to levels similar to p150 KOs (Figure III.5D; Figure III.6A). We observed a similar reduction in IAV replication in p150/MDA5 DKOs in multicycle replication assays for both H1N1 and H5N1 strains (Figure III.6B). Complementation of p150/MDA5 DKOs with V5-p150 restored IAV replication to levels similar to CTRL A549s, demonstrating that the reduction in viral titer in p150/MDA5 DKOs was due to loss of p150 expression (Figure III.5E). Taken together, these results demonstrate that p150 promotes IAV replication independent of MDA5 suppression.

<u>p150 suppresses exogenous RLR ligand induced IFN-β expression and apoptosis</u>

Prior studies indicate that RLR-mediated sensing of viral PAMPS activates both IRF3 mediated transcriptional upregulation of antiviral genes as well as apoptosis through the RIPA pathway as means to control viral replication (Figure III.7A) (Chattopadhyay et al.,

2010; Chattopadhyay et al., 2011; Chattopadhyay et al., 2016; Chattopadhyay et al., 2017). As we observed decreased IAV replication in p150/MDA5 DKOs, we next investigated the role of p150 in RIG-I mediated induction of IFN-β expression and apoptosis. We first examined IFN-β expression in p150/MDA5 DKOs following transfection of low molecular weight (LMW) pI:C and high molecular weight (HMW) pI:C, which predominantly stimulate RLRs RIG-I and MDA5, respectively (Figure III.7B). Transfection of LMW pI:C showed elevated IFN-β expression in p150/MDA5 DKO as compared to CTRL cells; however, transfection of HMW pI:C did not result in higher IFN-β expression in p150/MDA5 DKOs due to the lack of MDA5. These results suggest that, in addition to suppressing MDA5 sensing of endogenous ligands, p150 also suppresses RIG-I mediated induction of IFN-β expression from exogenous stimuli. Next, we examined the kinetics of IFN-β expression during SeV infection, a potent activator of RLRs, in various A549 KO cells (Figure III.7C). At 8 hpi, IFN-β expression levels were similar in all cell types analyzed; however, starting at 16 hpi, IFN-β expression remained elevated in p150/MDA5 DKOs and p150 KOs; in contrast, MDA5 KOs and CTRL A549s showed down regulation of IFN-β expression. To rule out altered viral replication contributing to the observed differences in IFN-β expression, we performed IAV vRNA transfections and observed sustained IFN-β expression in p150/MDA5 DKOs as compared to CTRL A549s (Figure III.7D). For further validation, we generated human embryonic kidney cells lacking p150 (p150 KO 293) and examined IFN-β expression following Sendai virus (SeV) (Figure III.7E; Figure III.8A). IFN-β expression in the p150 KO 293s was elevated at each time point, further confirming the importance of p150 in suppressing sustained RIG-I mediated induction of IFN-β expression. Taken together,

these results reveal a novel role for p150 in suppressing sustained RIG-I activation during viral infection.

To assess the contribution of apoptosis via the RIPA pathway in p150 deficient cells, we examined the levels of PARP cleavage, a byproduct of apoptosis, by western blot in p150 KOs and CTRL A549s cells following stimulation with various RLR agonists (Figure III.8B-D). p150 KOs exhibited increased PARP cleavage in response to IAV vRNA transfection, H1N1 infection and pI:C transfection; in contrast, little or no PARP cleavage was observed in CTRL A549s (Figure III.8B-D). Similarly, p150 KO 293s exhibited increased PARP cleavage following IAV vRNA transfection (Figure III.8E). These data indicate that loss of p150 results increased apoptosis upon stimulation with RLR agonists.

Next, we examined PARP cleavage in p150/MDA5 DKOs following IAV vRNA transfection or H1N1 infection (Figure III.7F-G). p150/MDA5 DKOs also showed increased PARP cleavage as compared to CTRL A549s in response to both vRNA transfection and H1N1 infection. We also examined apoptosis by staining with Annexin V, which binds phosphatidylserine, an early marker for apoptosis (Figure III.7H). Flow cytometric analysis of ADAR1 KOs transfected with IAV vRNA showed increased binding of Annexin V as compared to CTRL A549s. Taken together, these results demonstrate that p150 is critical for suppressing RLR induced apoptosis.

Discussion

Here, we investigated the role of ADAR1 in IAV replication and revealed opposing functions for the two isoforms, with the cytoplasmic p150 isoform acting as a negative regulator of RIG-I signaling and the nuclear p110 isoform acting as an IAV restriction factor. Additionally, we show that p150 promotes IAV replication independent of its role in the suppression of MDA5 mediated sensing of endogenous dsRNA. Through concurrent deletion of p150 and RLR pathway components, we demonstrate that p150 suppresses sustained activation of the RLR signaling cascade, resulting in decreased levels of IFN-β expression and apoptosis.

ADAR1, a member of the ADAR family, has been implicated in several cellular functions including editing of dsRNA from repetitive elements, miRNA biogenesis/processing and regulation of cell intrinsic immunity (Athanasiadis et al., 2004; Kim et al., 2004; Blow et al., 2004; Levanon et al., 2004; Ramaswami et al., 2012; Bazak et al., 2014; Yang et al., 2006; Kawahara et al., 2008; Zipeto et al., 2016; Lamers et al., 2019). Moreover, ADAR1 has been shown to have both proviral and antiviral roles during viral infection (Samuel 2011). One well characterized proviral function of ADAR1 is in the hepatitis delta virus life cycle, where ADAR1 editing of viral RNA is critical for production of the large delta antigen (Jayan et al., 2002; Wong et al., 2002). Similarly, ADAR1 editing is critical for polyomavirus replication as it facilitates the switch from early to late gene expression (Gu et al., 2009; Kumar et al., 1997). As these viruses replicate in the nucleus, ADAR1 mediated editing of viral RNA has been mostly attributed to the p110 isoform. Our studies with IAV show that p110 isoform of ADAR1 is antiviral, as evidenced by increased viral titers in p110 KOs. It should be noted that the p110 KOs

showed low levels of p110 induction upon treatment with IFN likely due to a cryptic promoter, as previously reported (Figure III.3B) (Chung et al., 2018; Nachmani et al., 2014). Despite low levels of p110, replication of different IAV strains was 5-10 fold higher in p110 KOs to CTRL A549s (Figure III.3C – Figure III.4A). In agreement, prior studies suggest that p110 is relocalized from the nucleoplasm to the nucleolus during IAV infection, perhaps to prevent antiviral activity (de Chassey et al., 2013; Emmott et al., 2010). Future studies will determine if the RNA editing activity or other functional domains in p110 is critical for antiviral activity.

Recently, several studies have focused on understanding the role of ADAR1 in regulating cell intrinsic immunity (Lamers et al., 2019). Loss of ADAR1 or p150 results in embryonic lethality in mice, due to aberrant upregulation of ISGs and increased apoptosis in hematopoietic cells (Liddicoat et al., 2015; Pestal et al., 2015; Mannion et al., 2014; Ward et al., 2011). Embryonic lethality from ADAR1 deficiency can be rescued by concurrent deletion of RLR components MDA5 or MAVS, as doubly deficient mice show decreased ISG expression; however, ADAR1/MDA5 DKO mice display early lethality after birth (Pestal et al., 2015; Liddicoat et al., 2015; Mannion et al., 2014). In agreement, our studies in p150 KOs showed elevated basal IFN-β expression, which was reduced with concurrent deletion of MDA5, demonstrating the role of p150 in suppressing MDA5 mediated sensing of endogenous ligands under physiological conditions (Figure III.5A and III.5C). Despite displaying reduced basal IFN-β expression, the p150/MDA5 DKOs were unable to support robust IAV replication, suggesting that the role of p150 during IAV replication is independent of MDA5 suppression. Thus, our

studies reveal an additional role for p150 in the suppression of RLR signaling during viral infection.

In addition to genetic deletion studies in mice, previous studies show increased ISG expression upon deletion of ADAR1 or p150 in transformed cell lines (Li et al., 2017; Chung et al., 2018; Li et al., 2012; George et al., 2016). Furthermore, treatment of these cells with exogenous type I IFN enhanced endogenous dsRNA induced antiviral responses, including activation of dsRNA protein kinase (PKR) and the OAS-RNase L pathway, resulting in shutdown of global protein translation by eIF2α phosphorylation and indiscriminate RNA degradation, respectively (Chung et al., 2018; Li et al., 2017; Pfaller et al., 2018). In this system, siRNA KD of PKR in ADAR1 KO cells or concurrent deletion of ADAR1 with RNase L resulted in restoration of protein translation and abrogation of RNA degradation, respectively. However, in our studies in p150 KOs and p150/MDA5 DKOs without addition of exogenous IFN, VSV replication was mostly unaffected, suggesting that restriction of IAV replication occurred via a mechanism independent of PKR and RNase L (Figure III.3C and III.5D). These results are in agreement with prior studies demonstrating that VSV replication is unaffected by loss of ADAR1 alone (Ward et al., 2011).

In addition to viral restriction through IRF3-mediated transcriptional upregulation of IFN-β and ISGs, viral spread can be restricted by cell death through cell intrinsic and extrinsic pathways (Elmore 2007). The RIPA pathway is a cell intrinsic apoptosis process that is triggered by activation of RLRs and subsequent linear

polyubiqutinylation of IRF3 (Chattopadhyay et al., 2016). Polyubiquitinylated IRF3 in complex with Bax associates on the mitochondrial membrane and initiates apoptosis by promoting the release of Cytochrome C. Prior studies in ADAR1 deficient mice showed increased cell death in hematopoietic cell compartments along with elevated ISG expression (Qiu et al., 2013; Hartner et al., 2009). Moreover, measles virus infection of ADAR1 KD cells showed increased apoptosis (Toth et al., 2009). In our studies, ADAR1 KOs, p150 KOs, and p150/MDA5 DKOs showed elevated apoptosis upon IAV infection or stimulation with RLR agonist as compared to CTRL A549 (Figure III.7F-H; Figure III.8B-E). These results demonstrate that loss of p150 predisposes cells to RLR induced apoptosis.

In conclusion, we demonstrate that p150 is a negative regulator of RLR signaling during viral infection, expanding upon the previously established role of p150 as a negative regulator of RLR signaling under basal conditions. While our studies confirm p150 suppresses MDA5 sensing of endogenous ligands, we also highlight the potential for p150 as a negative regulator of RIG-I signaling. Following stimulation with RLR agonists or IAV, p150/MDA5 DKOs exhibit elevated IFN-β expression and apoptosis compared to CTRL A549s, suggesting that p150 also suppresses RIG-I mediated induction of IFN-β expression and apoptosis. Together, these studies broaden the role of p150 as a negative regulator of RLR signaling, demonstrating p150 suppresses both MDA5 and RIG-I signaling pathways.

CHAPTER IV

The p150 Isoform of ADAR1 Suppresses RIG-I Mediated Induction of IFN-β and Apoptosis

Some of this chapter includes text adapted from an article that is under review 'The p150 Isoform of ADAR1 Blocks Sustained RLR signaling and Apoptosis during Influenza Virus Infection'. Olivia Vogel performed all of the experiments in this chapter.

Introduction

The detection of cytoplasmic viral RNA is mediated by the RLR family of cytoplasmic PRRs, which includes RIG-I and MDA5 (Rehwinkel et al., 2020). MDA5 has been shown to sense long dsRNA, while RIG-I senses short vRNA containing a 5'-triphoshate or 5'-diphosphate with a duplex structure lacking 2'-O-methylation (Pichlmair et al., 2009; Peisley et al., 2012; Pichlmair et al., 2006; Hornung et al., 2006; Schlee et al., 2009; Schmidt et al., 2009; Schuberth-Wagner et al., 2015). Upon binding to cognate ligands, RIG-I and MDA5 are activated through dephosphorylation and ubiquitination, which allows their interaction with the adaptor protein MAVS at the mitochondrial membrane (Kawai et al., 2005). This interaction then leads to the aggregation and activation of MAVS, enabling the initiation of downstream signaling (Hou et al., 2011).

Following activation of the RIG-I-MAVS pathway, one of two cell intrinsic signaling cascades are initiated: a transcriptional pathway or an apoptosis pathway. In the

transcriptional pathway, RIG-I-MAVS interactions leads to the recruitment of signaling molecules necessary for the activation of transcription factors IRF3 and NFκB (Kawai et al., 2005; Xu et al., 2005; Seth et al., 2005). For IRF3 transcriptional responses, phosphorylated IRF3 dimerizes and translocates to the nucleus to initiate the expression of type I IFN and a small subset of ISGs (Schneider et al., 2014). These secreted IFN bind to the type I IFN receptor (IFNAR) expressed on the cell surface, and activate intracellular JAK kinases to phosphorylate IFNAR (Schneider et al., 2014). Subsequently, STAT proteins are recruited to the IFN receptor, phosphorylated by JAKs and released from the IFN receptor for downstream signaling (Schneider et al., 2014). Phosphorylated STAT1 and STAT2 heterodimerize and interact with IRF9 to form the ISG factor 3 (ISGF3) complex, which translocates to the nucleus and stimulates the transcription of genes containing IFN-stimulated regulatory elements (ISREs) (Schneider et al., 2014).

In the apoptosis pathway, RIG-I activation and interaction with MAVS can result in an alternative mode of activation for IRF3 which pivots the cells towards apoptosis, rather than the IRF3 transcriptional pathway (Chattopadhyay et al., 2010; Chattopadhyay et al., 2016). In this RIPA pathway, IRF3 is activated through linear ubiquitination of specific lysine residues on IRF3 by the LUBAC, which is composed of the enzymes SHARPIN, HOIP, and HOIL-1L (Kirisako et al., 2006; Tokunaga et al., 2009; Ikeda et al., 2011; Gerlach et al., 2011; Tokunaga et al., 2011; Chattopadhyay et al., 2016). In addition to LUBAC, IRF3 activation has been shown to require the E3 ligases TRAF2 and TRAF6 (Chattopadhyay et al., 2016). The exact function of these E3 ligases in the

RIPA signaling pathway is unknown; however, lack of TRAF2 or TRAF6 expression results in reduced interaction between LUBAC and IRF3, indicating a role for these proteins in the RIPA pathway (Chattopadhyay et al., 2016). Following linear ubiquitination, IRF3 interacts with the pro-apoptotic protein Bax through the BH3 domains (Chattopadhyay et al., 2010). This IRF3:Bax complex translocate to mitochondria and triggering the release of cytochrome C, thereby initiating the induction of cell intrinsic apoptosis (Chattopadhyay et al., 2010).

Although viral nucleic acids are potent stimulators of RLRs, recent studies suggest that endogenous RNA encoded from the host genome can bind and stimulate RLRs. As such, RLRs are tightly regulated and are prevented from aberrant activation through negative regulation under homeostatic conditions. The RNA editing enzyme ADAR1 has been implicated as a negative regulator of RLR signaling and has been show to suppress MDA5 sensing of endogenous dsRNA transcribed from the *Alu* elements in the genome (Mannion et al., 2014; Pestal et al., 2015; Liddicoat et al., 2015). ADAR1 is expressed as two isoforms: p110 and p150. Both isoforms are composed of three central dsRNA binding domains and a C-terminal deaminase domain, which is responsible for ADAR1 RNA editing activity (Lamers et al., 2019). The full length p150 isoform also contains two Z DNA binding domains at the N-terminus, while the N-terminally truncated p110 isoform contains a single Z DNA binding domain (George et al., 1999; Poulsen et al., 2001).

The RNA editing activity of ADAR1 is postulated to contribute to the role of ADAR1 as a negative regulator of RLR signaling by editing and destabilizing dsRNA structures on endogenous RNA ligands (Liddicoat et al., 2016; Vitali et al., 2010). This was confirmed through murine genetics studies using ADAR1 editing deficient knock-in mice carrying the ADAR1 editing deficient allele ADAR1^{E861A}, which is homologous to the editing deficient human ADAR1^{E912A} allele (Liddicoat et al., 2015; Lai et al., 1995). The elevated ISG expression and embryonic lethality associated with ADAR1 and p150 KO mice was also observed in the ADAR1 editing deficient mice and was only rescued by concurrent deletion of MDA5, demonstrating that ADAR1 editing of endogenous RNA is necessary to prevent activation of MDA5 under physiological conditions (Liddicoat et al., 2015).

While murine genetics studies have described a role for ADAR1 and the p150 isoform of ADAR1 in suppressing MDA5 signaling, these studies could not fully examine the relationship between ADAR1 and RIG-I in mice due to the embryonic lethality associated with the ablation of ADAR1 or RIG-I expression (Pestal et al., 2015; Kato et al., 2005). However, several studies have begun addressing the impact of ADAR1 expression on RIG-I mediated signaling through the use of primary and transformed cell lines. Using primary macrophages, it was demonstrated that knockdown of ADAR1 expression led to an increase in MDA5, RIG-I, and STAT1 phosphorylation, suggesting a role for ADAR1 in suppressing RLR mediated IFN signaling (Pujantell et al., 2017). Similarly, increased IFN-α and IFN-β expression was observed in ADAR1 knockdown hepatocytes following hypoxia and reoxygenation and this was reduced following concurrent knockdown of RIG-I and ADAR1 (Wang, Wang, et al., 2016). Knockdown of

RIG-I and ADAR1 in these cells also increased cell viability following hypoxia and reoxygenation when compared to ADAR1 knockdown hepatocytes (Wang, Wang, et al., 2016). Finally, experiments in human embryonic kidney cells (HEK293) demonstrated that increased expression of ADAR1 resulted in a reduction in the amount of RIG-I pulled down by poly(I:C) (pI:C), suggesting that ADAR1 may also have a role in preventing the sensing of viral and cellular RNA by RIG-I (Yang et al., 2014). Together, these results demonstrate the potential for ADAR1 as a negative regulator of the RIG-I signaling pathway; however, these studies provide limited ADAR1 isoform specific data regarding the ADAR1 mediated down regulation of the RIG-I pathway.

In the previous chapter, we demonstrate that p150 isoform of ADAR1 suppresses RLR mediated signaling during infection, resulting in reduced IFN-β expression and apoptosis. Here, we demonstrate that p150 suppresses IFN-β expression and apoptosis through the RIG-I-MAVS-IRF3 pathway. Both elevated IFN receptor signaling via the JAK-STAT pathway and increased apoptosis contributed to restriction of IAV replication in various cells deficient in p150. The restoration of IAV replication in p150/MDA5/RIG-I and p150/MDA5/MAVS triple KOs (TKOs) demonstrate that p150 prevents sustained RIG-I activation induced IFN-β expression and apoptosis. Importantly, we demonstrate that the RNA binding activity, not the editing activity, of p150 is critical for the suppression of RIG-I signaling during IAV infection. Together, these results demonstrate that p150-mediated suppression of RIG-I signaling creates a more hospitable environment for efficient IAV replication.

Results

p150 suppresses induction of IFN-β and apoptosis via the RIG-I-MAVS-IRF3 pathway

In the previous chapter, we demonstrated that p150 suppresses RLR signaling during infection. To investigate if the RIG-I signaling cascade through IRF3 results in increased apoptosis in p150/MDA5 DKOs, we performed siRNA knockdown of RIG-I or IRF3 and assessed PARP cleavage after IAV vRNA transfection (Figure IV.1A). Knockdown of RIG-I or IRF3 in p150/MDA5 DKOs led to reduced PARP cleavage as compared to control siRNA transfected p150/MDA5 DKOs, demonstrating that the RIG-I signaling cascade through IRF3 leads to increased apoptosis in p150 deficient cells. To further validate our findings, we generated p150/MDA5/RIG-I and p150/MDA5/MAVS triple knockout (TKO) A549s and assessed IFN-β expression and apoptosis. Following SeV infection, both the p150/MDA5/RIG-I and p150/MDA5/MAVS TKOs showed reduced IFN-β expression as compared to p150/MDA5 DKOs (Figure IV.1B). Similarly, both TKOs showed reduced PARP cleavage during IAV infection as compared to p150/MDA5 DKOs (Figure IV.1C). These data demonstrate that p150 is critical for suppressing RIG-I induced IFN-β expression and apoptosis. As expected, IAV replication in both p150/MDA5/RIG-I and p150/MDA5/MAVS TKOs increased to levels similar CTRL A549s, while replication remained lower in p150/MDA5 DKOs (Figure IV.1D). Taken together, these results demonstrate that the p150 isoform of ADAR1 promotes IAV replication through suppression of the RIG-I signaling cascade via MAVS-IRF3.

Inhibition of apoptosis and JAK-STAT signaling restores IAV replication in p150 deficient cells

To determine the relative contribution of elevated IFN-β expression versus increased apoptosis to IAV restriction in p150 deficient cells, we generated p150/Bax DKO A549s using the CRISPR/Cas9 technology. Bax is a pro-apoptotic protein in the Bcl-2 protein family and has also been implicated in the RIPA pathway (Figure III.7A) (Chattopadhyay et al., 2016; Chattopadhyay et al., 2017). We first assessed apoptosis in p150/Bax DKOs by PARP cleavage following IAV vRNA transfection and observed reduced PARP cleavage as compared to p150 KOs (Figure IV.2A). As anticipated, while PARP cleavage was reduced, IFN-β expression remained elevated in p150/Bax DKOs as compared to CTRL A549s (Figure IV.2B). IAV replication was increased in the p150/Bax DKOs as compared to p150 KOs yet remained lower than CTRL A549s (Figure IV.2C). These results indicate that inhibition of apoptosis via Bax deletion partially restores IAV replication in p150 deficient cells. Next, to assess the contribution of elevated IFN-β signaling through the IFN receptor to reduced IAV replication in p150 deficient cells, we treated various A549 KO cells with Ruxolitinib, an inhibitor of Janus kinases 1 and 2 (JAK 1/2), to block IFN receptor signaling. Treatment of p150 KOs with Ruxolitinib showed a modest increase in IAV viral titers, while Ruxolitinib treatment had no significant impact on viral replication in CTRL A549s (Figure IV.2D). In contrast, treatment of p150/Bax DKOs with Ruxolitinib led to a greater increase in viral titers as compared to DMSO treated p150/Bax DKOs (Figure IV.2D). Taken together, these results demonstrate that both increased apoptosis and elevated IFN receptor signaling contribute to the inhibition of IAV replication in the absence of p150.

RNA binding activity of p150 is required for suppression of the RIG-I pathway

To identify the functional domains in p150 important for suppression of RIG-I signaling, we generated V5-tagged p150 mutant constructs including (1) Z alpha mutant (p150 Zα) with K169A/Y177A mutations in Z DNA/RNA binding domain, (2) RNA binding mutant (p150 RBM) with KKxxK→EAxxA mutations in all three RNA binding domains, and (3) a catalytic mutant that lacks the deaminase domain (p150 Cat) (Figure IV.3A) (Valente et al., 2007) (Ng et al., 2013). We first assessed the ability of these mutants to suppress RIG-I signaling in IFN-β reporter assay in p150 KO 293s. Different p150 mutant constructs were co-transfected with the IFN-β-firefly reporter and the RIG-I pathway was stimulated with SeV. As compared to GFP control, wildtype (WT) p150, p150 Zα, and p150 Cat transfected cells showed decreased IFN-β reporter activity (Figure IV.3B); in contrast, p150 RBM transfected cells showed increased IFN-β reporter activity. Next, we complemented the p150/MDA5 DKO A549s with different p150 mutant constructs (DKO/WT, DKO/ Zα, DKO/RBM, and DKO/Cat) and generated clonal populations (Figure IV.3C). Following IAV vRNA transfection in complemented DKOs, IFN-β expression was elevated in DKO/RBMs at levels similar to p150/MDA5 DKOs, demonstrating that the RNA binding activity of p150 is required for suppression of IFN-β expression (Figure IV.3D). Similarly, DKO/RBMs showed increased PARP cleavage following IAV vRNA transfection, suggesting that the RNA binding activity of p150 is also required for suppression of apoptosis (Figure IV.3E). Finally, we assessed IAV replication in complemented DKOs and observed increased viral titers in DKO/WTs and DKO/Cats yet not in DKO/RBMs (Figure IV.3F). Interestingly, DKO/Zαs showed

decreased replication despite showing decreased IFN-β expression and apoptosis upon vRNA transfection. Taken together, these results demonstrate that the RNA binding activity and not the catalytic activity of p150 is required for the suppression of RIG-I mediated induction of IFN-β expression and apoptosis.

Discussion

Here, we investigated whether p150 suppresses IFN-β expression and apoptosis via the RIG-I-MAVS signaling pathways. In p150 deficient cells, we observed increased IAV replication only upon inhibition of both apoptosis and IFN receptor signaling. p150 mediated suppression of RLR signaling was dependent on RNA binding functions but independent of RNA editing activity. Taken together, our studies illustrate a broad role for p150 in preventing the hyperactivation of innate immune responses, with p150 suppressing both the MDA5 pathway under basal conditions and the RIG-I pathway during viral infection.

As previously mentioned, murine genetic studies have been unable to fully examine the relationship between ADAR1 and RIG-I in mice due to the unrelated embryonic lethality associated with RIG-I ablation (Pestal et al., 2015). A study in human embryonic kidney cells (HEK293) showed that over expression of p110 or p150 resulted in decreased association of pI:C with RIG-I, suggesting that ADAR1 may prevent the sensing of dsRNA by RIG-I (Yang et al., 2014). Our studies in p150/MDA5/RIG-I or p150/MDA5/MAVS TKOs showed restoration of IAV replication and reduced IFN-β expression to levels similar to CTRL A549s, demonstrating that the p150 isoform is

critical for suppressing RIG-I signaling during IAV infection (Figure IV.1D). We observed sustained IFN-β expression in p150/MDA5 DKOs, whereas IFN-β expression declined after initial induction in CTRL A549s (Figure III.7C-D). Furthermore, the differences in IAV replication between p150/MDA5 DKOs and CTRL A549s, were more pronounced at later times during infection (Figure III.6B). Together, these results indicate that p150 acts as a negative regulator for ramping down RIG-I signaling during viral infection.

In the previous chapter, we demonstrated that loss of p150 expression predisposes cells to RIPA mediated apoptosis. As further validation, concurrent deletion of Bax with p150 as well as p150/MDA5/RIG-I and p150/MDA5/MAVS TKOs showed decreased apoptosis upon vRNA transfection or IAV infection, demonstrating that p150 suppresses apoptosis via the RIPA pathway (Figure IV.2A; Figure IV.1C). A recent study shows that concurrent deletion of Bax with ADAR1 is not sufficient to rescue mice from embryonic lethality (Walkley et al., 2019). In our studies with p150/Bax DKOs, we observed reduced apoptosis yet high IFN-β expression upon RLR stimulation (Figure IV.2A-B). As such, treatment of p150/Bax DKOs with Ruxolitinib, a JAK inhibitor, resulted in significantly higher viral replication, demonstrating that restriction of IAV replication in p150 deficient cells occurred due to both elevated IFN receptor signaling and increased apoptosis via the RIPA pathway.

Both editing dependent and independent ADAR1 functions have been implicated in the suppression of innate immunity. Previous studies show that the RNA binding functions and editing functions of p110 and p150 were necessary for suppressing endogenous

dsRNA or pI:C induced RLR signaling (Liddicoat et al., 2015; Yang et al., 2014). Similarly, in the context of measles virus infection, ADAR1 KO cells complemented with a catalytic mutant of p150 showed a modest increase in viral replication as compared to control ADAR1 KO, whereas wildtype p150 completely restored viral replication (Pfaller et al., 2018). Moreover, murine genetic studies also highlight the importance of ADAR1 mediated editing of endogenous dsRNA in the suppression of MDA5 activation (Liddicoat et al., 2015). However, in another study, overexpression of p110 or p150 catalytic mutants was sufficient to suppress RIG-I activation upon SeV infection (Yang et al., 2014). Our studies with p150/MDA5 DKOs complemented with different p150 mutants demonstrated that the RNA binding ability of p150 but not the catalytic activity was critical for suppression of RIG-I signaling. We hypothesize that p150 may function upstream of RIG-I activation, possibly by binding and sequestering cellular or viral RNA to prevent sustained RIG-I sensing and activation.

Our data shows that the role of p150 in promoting viral replication is specific to IAV, as VSV replication was unaffected in p150 deficient cells (Fig III.5D). The NS1 of IAV has been show to interact with ADAR1 in yeast-2-hybrid screening and immunoprecipitation assays, as well as to increase the editing activity of ADAR1 in reporter assays (de Chassey et al., 2013; Ngamurulert et al., 2009). However, the significance of these interactions has yet to be determined. Importantly, NS1 has been shown to antagonize several host antiviral pathways, including activation of the RIG-I pathway via its interactions with the E3 ligases TRIM25 and RIPLET (Gack et al., 2009; Mibayashi et al., 2007; Rajsbaum et al., 2012). Despite the presence of this viral antagonist, we

observed decreased IAV replication in p150 deficient cells due to increased RIG-I signaling, suggesting that NS1 is likely incapable of suppressing the amplification of RIG-I signaling in cells lacking p150 (Fig IV.1B). Future studies will determine the importance of NS1:ADAR1 interactions in suppression of the RIG-I pathway.

In conclusion, our studies demonstrate the importance of p150 as a negative regulator of RLR signaling. p150 prevents endogenous dsRNA mediated activation of the innate immune sensor MDA5 under basal conditions (Liddicoat et al., 2015; Pestal et al., 2015; Chung et al., 2018). Our studies demonstrate that p150 also functions to dampen host antiviral signaling via suppression of RIG-I during IAV infection. This dampening of RIG-I mediated signaling by p150 enables efficient IAV replication. Future studies are required to determine the exact mechanism of p150 mediated suppression of the RIG-I pathway and the significance of NS1-p150 interactions in this process.

CHAPTER V

The p150 Isoform of ADAR1 and Influenza A Virus Nonstructural Protein 1 Suppress Antiviral Signaling

Introduction

To effectively establish infection and replicate within a host, IAV must evade host innate immune responses mediated by pattern recognition receptors (PRRs). Given the ssRNA nature of the IAV genome, IAV viral RNA (vRNA) is primarily detected by the cytoplasmic PRR retinoic acid-inducible gene-I (RIG-I) (Pichlmair et al., 2006). RIG-I is a member of the RIG-I like receptor (RLR) family, which also includes the melanoma differentiation-associated protein 5 (MDA5). Both RIG-I and MDA5 detect cytoplasmic vRNA, with RIG-I sensing the 5'triphosphate or 5'diphosphate on vRNA and MDA5 sensing long dsRNA (Pichlmair et al., 2006; Hornung et al., 2006; Schlee et al., 2009; Goubau et al., 2014; Kato et al., 2008; Pichlmair et al., 2009). These RLRs are a crucial aspect of the host response to viral infection, enabling the production of type I interferons (IFN) and inflammatory cytokines through activation of downstream signaling cascades that culminate in the activation of transcription factors IRF3 and NFκB (Schneider et al., 2014).

To overcome host innate immune responses, IAV encodes the nonstructural protein 1 (NS1) that antagonizes several host antiviral pathways. NS1 is composed of two domains: an N-terminal RNA binding domain (RBM) and a C-terminal effector domain

(Fields et al., 2013). Although NS1 is non-essential for viral genome replication, NS1 has been shown to promote efficient viral replication through its interactions with several host proteins/pathways (Fields et al., 2013). The best characterized role of NS1 in regulating innate immune signaling revolves around the ability of NS1 to inhibit RIG-I mediated signaling, thereby preventing transcription of type I IFNs and interferon stimulated genes (ISG). It has been demonstrated that NS1 interacts directly with RIG-I via the RIG-I caspase activation and recruitment domains (CARDs) to inhibit RIG-I mediated signaling (Pichlmair et al., 2006; Mibayashi et al., 2007; Jureka et al., 2020). Additionally, NS1 has been shown to interact with the E3 ligases TRIM25 and Riplet, which are necessary for the ubiquitination and activation of RIG-I (Gack et al., 2007; Oshiumi et al., 2009; Gack et al., 2008; Gack et al., 2009; Rajsbaum et al., 2012). By interacting with TRIM25 and Riplet, NS1 inhibits the E3 ligase activity of these proteins, thereby preventing the activation of RIG-I and the induction of type I IFN. Indeed, recombinant IAV strains that lack NS1 expression are more susceptible to host IFN signaling (Garcia-Sastre et al., 1998). Through interactions with cleavage and polyadenylation specificity factor 30 (CPSF30), NS1 also interferes and blocks host antiviral gene expression at a post-transcriptional step (Nemeroff et al., 1998; Noah et al., 2003; Twu et al., 2006).

In addition to restriction of viruses through upregulation of IFN and ISG, viral replication and spread can be blocked by apoptosis of infected cells. Several viruses encode factors to directly promote or block apoptosis for efficient viral replication. The NS1 of IAV has been shown to downregulate apoptosis by upregulating phosphoinositide-3-

kinase (PI3K) and Akt signaling, which provides a pro-survival signal to the cells (Ehrhardt et al., 2007; Zhirnov et al., 2002). NS1 upregulates PI3K signaling by binding to the PI3K regulatory subunit p85 thus releasing PI3K from an inhibitory conformation and enabling interaction with the PI3K effector protein Akt for downstream signaling (Hale et al., 2006; Hale et al., 2008; Hale et al., 2010; Shin et al., 2007; Zhirnov et al., 2007). While several studies have established a relationship between NS1 and the suppression of apoptosis, NS1 expression has also been shown to stimulate the induction of apoptosis late in IAV infection, supposedly for efficient release of viral ribonucleoprotein complexes from the nucleus (Zhirnov et al., 2007; Schultz-Cherry et al., 2001).

Previous studies examining the interactome of NS1 via yeast two-hybrid screens identified adenosine deaminase acting on RNA (ADAR1) as an additional host interactor of NS1 (de Chassey et al., 2013; Ngamurulert et al., 2009). ADAR1 is a cellular RNA editing enzyme that catalyzes the deamination of adenosine to inosine and is expressed as two isoforms: p110 and p150. The p110 isoform is constitutively expressed within the nucleus, while p150 has an IFN inducible promoter and is expressed in both the cytoplasm and the nucleus. The ADAR1 and NS1 interaction was found to be partially mediated by the RNA binding domains of ADAR1 and NS1 in immunoprecipitation experiments using RNA binding mutants of both ADAR1 and NS1 (de Chassey et al., 2013). Furthermore, immunofluorescence experiments demonstrated that ADAR1 relocalized during IAV infection and colocalized with NS1 in the nucleolus (de Chassey et al., 2013). While these studies highlight the potential for a relationship between

ADAR1 and NS1 during IAV infection, they did not examine the ADAR1 isoform specific contributions involved in the relationship between ADAR1 and NS1.

Our previous studies using p150 KO human lung adenocarcinoma (A549) cells demonstrated that during IAV infection both RIG-I mediated induction of IFN-β and apoptosis were elevated despite the expression of NS1. This suggests that in the absence of p150 expression NS1 is unable to sufficiently suppress RIG-I mediated signaling. Therefore, we sought to determine whether p150 and NS1 may cooperate to suppress RIG-I mediated signaling during IAV infection. Utilizing a reporter virus that encodes a tetracysteine-tagged NS1 as well as p110 and p150 overexpressing A549s, we were able visualize isoform specific localization of ADAR1 and NS1 during IAV infection through fluorescent microscopy. Following infection, we demonstrated that p110 and NS1 relocalized to the nucleolus, while p150 and NS1 colocalized in punctate structures in the cytoplasm. Furthermore, overexpression of p150 and NS1 showed increased suppression of IFN-β luciferase reporter activity. Together, these results suggest that p150 and NS1 could potentially cooperate in order to suppress RIG-I mediated signaling during IAV infection.

Results

ADAR1 Relocalizes during IAV Infection

To examine the relationship between ADAR1 and NS1 during IAV infection, we first assessed the localization of ADAR1 and NS1 using fluorescent microscopy. Under mock conditions, ADAR1 is expressed throughout the nucleus in wild-type (WT) A549s

(Fig V.1A). Following A/Puerto Rico/8/1934 (PR8) infection, we observed relocalization of ADAR1 into the nucleolus and to punctate structures in the cytoplasm were ADAR1 colocalized with NS1 (Fig V.1A). To further examine the requirements for ADAR1 and NS1 colocalization, we infected WT A549s with mutant strains of PR8 that express a NS1 RNA binding mutant (PR8 RBM) or that lack NS1 expression (PR8 ΔNS1). Following infection with PR8 RBM or PR8 ΔNS1, ADAR1 (p110) did not relocalize to the nucleolus and instead remained dispersed throughout the nucleus (Fig V.1B). This suggests that NS1 is required for ADAR1 relocalization to the nucleolus and that this relocalization is dependent upon the RNA binding ability of NS1.

Differential Localization of ADAR1 Isoforms during IAV Infection

To further examine ADAR1 and NS1 localization we used a recombinant PR8 expressing a tetracysteine-tagged NS1 (PR8-Tc) (Fig V.1C). To generate the PR8-Tc reporter virus, the splice acceptor site on the IAV NS segment, which encodes NS1 and the nuclear export protein (NEP), was mutated to enable incorporation of the tetracysteine-tag on the C-terminus of NS1 (Manicassamy et al., 2010). To ensure expression of the NEP, the splice acceptor site was duplicated to allow for NEP expression along with the NS1 Tc tag. The NS1-Tc tag localization can then be visualized through fluorescent microscopy by staining with fluorescein arsenical hairpin binder–ethanedithiol (FlAsH-EDT2), which fluoresces upon binding to the tetracysteine motif. Utilization of PR8-Tc enabled improved visualization of NS1, particularly in the nucleolus, which we were unable to visualize through regular antibody staining of NS1.

To specifically examine relocalization of the different ADAR1 isoforms, we infected A549s overexpressing Flag-tagged p150 and Flag-tagged p110 with PR8-Tc (Fig V.1D). As with wildtype PR8, ADAR1 relocalized to the nucleolus following infection with PR8-Tc. In the Flag-p110 overexpressing A549s, p110 relocalized to the nucleolus where it colocalized with NS1. In contrast, Flag-p150 relocalized to cytoplasmic puncta colocalized with NS1. These results demonstrate that the ADAR1 isoforms colocalize with NS1 in distinct regions of the cell during IAV infection, with p110 in the nucleolus and p150 in punctate structures within the cytoplasm.

Co-expression of p150 and NS1 show increased suppression of IFN-β Expression

Next, we assessed the impact of NS1 and p150 co-expression in an IFN-β-firefly reporter assay following stimulation with SeV. As expected, IFN-β-firefly reporter activity was reduced following expression of NS1 alone (Fig V.2A). Interestingly, co-expression of NS1 with p150 led to a greater reduction in IFN-β-firefly reporter activity than that observed with either NS1 or p150 alone (Fig V.2A). We also sought to determine the functional domains of p150 required to suppress IFN-β-firefly reporter activity in the presence of NS1. Reflecting the results of our previous IFN-β-firefly reporter assay, the p150 RBM was unable to suppress IFN-β-firefly reporter activity when co-expressed with NS1, with suppression levels resembling that of NS1 alone (Fig V.2B). Together, these results suggest that p150 and NS1 may work together to suppress the activation of RIG-I pathway during IAV infection.

Discussion

NS1 of IAV is critical for the evasion host innate immune signaling by targeting several cellular processes to generate an optimal host environment for viral replication. As a result, lack of NS1 expression during IAV infection severely attenuates IAV replication in immune competent cells (Garcia-Sastre et al., 1998). Amongst the several host processes targeted by NS1, NS1 inhibition of RIG-I mediated signaling is critical for the suppression type I IFN production (Pichlmair et al., 2006; Mibayashi et al., 2007; Jureka et al., 2020; Oshiumi et al., 2009; Gack et al., 2009; Rajsbaum et al., 2012). Likewise, NS1 has been shown to downregulate apoptosis induction, enabling efficient IAV replication (Ehrhardt et al., 2007; Zhirnov et al., 2002). Despite the well characterized role of NS1 in suppressing IFN-β expression and apoptosis, our studies demonstrate that these processes remain elevated during IAV infection in the absence of p150 expression. This suggests that without the expression of p150, NS1 is unable to completely suppress the induction of IFN-β expression and apoptosis.

Here, we assess the relationship between ADAR1 and NS1 by first examining ADAR1 and NS1 localization during IAV infection. We demonstrate that during IAV infection ADAR1 relocalizes to the nucleolus and colocalizes with NS1, confirming previous studies (de Chassey et al., 2013). These results suggest that NS1 restricts the antiviral functions of ADAR1 in the nucleus. We also demonstrate that ADAR1 relocalizes to punctate structures within the cytoplasm where it colocalizes with NS1. Through the utilization of p110 and 150 overexpressing A549s, we were able to confirm that the p150 isoform of ADAR1 relocalized to cytoplasmic puncta and colocalized with NS1 while p110 and NS1 relocalized to the nucleolus. This illuminates the differential

localization of the ADAR1 isoforms during IAV infection, with NS1 colocalizing with each isoform despite the different locations within the cell. These results mirror our previous studies using p110 KO and p150 KO A549s, in which we observed an increase in IAV replication in the p110 KO A549s and a reduction in IAV replication in the p150 KO A549s. This is of particular interest considering that IAV replicates within the nucleus where p110 localizes; while RIG-I mediated signaling occurs within the cytoplasm where p150 localizes during infection. Together, these results highlight the potential for opposing roles of the ADAR1 isoforms during IAV infection, with p150 acting as a proviral factor and p110 acting as an antiviral factor. However, further studies are necessary to characterize the nature of the interaction between NS1 and the different ADAR1 isoforms.

To further examine the relationship between p150, NS1, and IFN signaling, we examined the impact of p150 and NS1 expression on IFN-β luciferase reporter activity. IFN-β luciferase reporter experiments demonstrate that p150 and NS1 together suppress IFN-β luciferase reporter activity to a greater extent than when expressed alone. In addition, we demonstrate that this enhanced suppression of IFN-β luciferase reporter activity is mediated by p150 RNA binding activity. Together, these results suggest that p150 and NS1 may work together to suppress IFN-β expression during infection in a manner that is dependent upon RNA binding. We hypothesize that NS1 may recruit p150 to cytoplasmic puncta where they then work together to sequester IAV vRNA, preventing RIG-I activation. Alternatively, NS1 and p150 may both work independently to suppress RIG-I mediated signaling, with both NS1 and p150 mediated

suppression of RIG-I being necessary for optimal IAV replication. However, further studies are required to conclusively determine the nature of NS1 and p150 suppression. Considering that NS1 is unable to efficiently suppress IFN-β expression and apoptosis in the absence of p150 expression, these studies highlight the potential for a cooperative interaction between p150 and NS1 to ensure an optimal cellular environment for IAV replication.

CHAPTER VI

Discussion

Some of this chapter includes text adapted from an article that is under review 'The p150 Isoform of ADAR1 Blocks Sustained RLR signaling and Apoptosis during Influenza Virus Infection'

Viral pandemics pose a significant public health and economic burden, as evidenced by past Influenza virus pandemics and the current SARS-CoV-2 pandemic. While the development of vaccines is crucial for the containment of viral outbreaks and the prevention of further viral spread, it is also necessary to develop antiviral therapeutics to improve disease outcomes following viral infection. To do so, it is necessary to understand how the host responds to viral infection and the strategies utilized by different viruses to evade these host responses.

The innate immune response is a crucial first line of defense against viral infection, helping to generate an antiviral environment within the cell as well as alerting and recruiting immune cells to the sight of infection. For RNA viruses, detection of cytoplasmic nucleic acids is primarily mediated by the RLR family of PRRs, including RIG-I and MDA5. By detecting specific viral RNA motifs, activated RIG-I and MDA5 stimulate downstream signaling cascades that ultimately lead to the production of type I IFNs and inflammatory cytokines. These cytokines can then be secreted from the cell to signal in an autocrine or paracrine manner, stimulating the induction of ISGs via the JAK-STAT pathway (Schneider et al., 2014). In addition to the IFN signaling arm of the

cell intrinsic response, apoptotic cell death is an important component involved in the host response to viral infection. Immunologically silent, apoptosis serves as a method of removing infected cells for viral clearance and can be induced following activation of RIG-I via RIPA (Elmore 2007; Chattopadhyay et al., 2010; Chattopadhyay et al., 2011; Chattopadhyay et al., 2016). Together, these pathways are crucial for restricting viral replication.

The p150 Isoform of ADAR1 Negatively Regulates RLR Signaling

Cell intrinsic signaling cascades are tightly regulated through a combination of posttranslational modifications and structural changes, enabling timely and rapid responses to viral infection. Similarly, the ramping down of these signaling cascades is crucial for the prevention of overactive inflammatory responses. While finely tuned for the detection of viral RNA, RLRs can also sense endogenous RNA ligands that, when unregulated, can lead to the initiation of inflammatory antiviral responses under basal conditions (Mannion et al., 2014; Pestal et al., 2015; Liddicoat et al., 2015). As a result, mutations in proteins involved in RNA metabolism or RNA sensing are often associated with the development of autoimmune disorders, such as AGS, which is characterized by elevated IFN activity reminiscent of viral infection (Crow, Chase, Lowenstein Schmidt, et al., 2015; Rice et al., 2013). In studies examining host proteins involved in the development of AGS, mutations within ADAR1 were shown to be one of the causes of AGS, demonstrating a role for ADAR1 in the downregulation of cell intrinsic immunity (Crow, Chase, Lowenstein Schmidt, et al., 2015; Rice et al., 2012). Similarly, loss of ADAR1 expression in hematopoietic cells leads to an upregulation of ISG expression

and apoptosis (Hartner et al., 2009). The role of ADAR1 as key regulator of cell intrinsic immunity was further highlighted through murine genetics studies that demonstrated that the embryonic lethality and elevated ISG expression in ADAR1 KO and p150 KO mice could be rescued by concurrent deletion of MDA5 or MAVS (Mannion et al., 2014; Pestal et al., 2015; Liddicoat et al., 2015). Studies using transformed cell lines, have described additional roles for ADAR1 in suppressing activation of PKR and OAS-RNaseL pathways by endogenous RNA ligands (Chung et al., 2018; Li et al., 2017). Together, these studies underscore the importance of ADAR1 as a negative regulator of cell intrinsic immunity during uninfected conditions.

While several studies have established that ADAR1 downregulates basal innate immune signaling, examining ADAR1 during viral infection has also served to broaden our knowledge about the role of ADAR1 as a negative regulator of cell intrinsic immunity. By examining the role of the ADAR1 in IAV infection, we were able to gain important insights into one of the many mechanisms utilized by IAV to subvert host innate immune defenses while also unveiling an additional aspect of ADAR1 mediated suppression of RLR signaling. Through concurrent deletion of p150 and RLR signaling molecules, we were able to demonstrate that p150 suppresses sustained RIG-I mediated signaling which ultimately results in decreased IFN signaling and apoptosis. Upon examination of IFN-β expression kinetics following SeV infection or H1N1 vRNA transfection, we observed a similar induction of IFN-β expression between the p150/MDA5 DKO, MDA5 KOs, and CTRLs. However, at later time points the p150/MDA5 DKOs exhibited elevated IFN-β expression while the MDA5 KOs and

CTRLs showed a down regulation of IFN-β expression. These results suggest that p150 is important for down regulating IFN-β expression at later time points during infection as cells lacking p150 were unable to rapidly turn-off IFN-β expression. Considering the IFN-inducible nature of p150, we hypothesize that p150 expression is induced later during infection after initial IFN signaling has begun in order to begin the process of ramping down the RIG-I pathway so that the cell may return to normal homeostatic conditions.

Additionally, we demonstrate that the RNA binding activity and not the RNA editing activity of p150 is necessary for suppression of RIG-I mediated induction of IFN-β expression and apoptosis. This is in contrast to what is known about p150 mediated suppression of MDA5 and PKR, both of which have been shown to require p150 RNA editing activity (Liddicoat et al., 2015; Chung et al., 2018; Okonski et al., 2013). While further studies are required to determine the exact mechanism of p150 mediated suppression of RIG-I, we hypothesize that p150 may act upstream of RIG-I activation by preventing RIG-I sensing of viral RNA. Previous studies have demonstrated that, like MDA5, RIG-I can also sense endogenous RNA ligands (Chiang et al., 2018). Likewise, ADAR1 has been shown to sense mitochondrial RNA, which can be released following mitochondrial destabilization and trigger antiviral signaling within the cell (Cai et al., 2014). Therefore, it also possible that p150 could prevent RIG-I from sensing endogenous RNA ligands released over the course of infection and the ensuing cellular stress. Sequestration of these endogenous RNA ligands could be a crucial step in the ramping down of antiviral responses post infection. Future studies examining the nature

of the RNA bound by p150 during viral infection could provide intriguing details into the mechanism by which p150 suppresses RLR signaling during infection.

Together, these studies underscore the importance of p150 as a negative regulator of cell intrinsic immunity. We demonstrate that p150 crucial is for the suppression of RLR mediated signaling, both under physiological conditions through the inhibition of the MDA5 pathway and during viral infection through the inhibition of the RIG-I pathway. As mentioned previously, mutations in ADAR1 are associated with the development of the autoimmune disorder AGS. These mutations have been mostly attributed to the role of p150 in suppressing MDA5 mediated sensing of endogenous RNA ligands under basal conditions. However, our studies unveil an additional facet of p150 mediated regulation of cell intrinsic immunity, where p150 plays an important role in ramping down the RIG-I pathway after the initiation of antiviral signaling, thus enabling the cells to return to physiological conditions after viral infection. Without p150 expression, IFN signaling and apoptosis remain unregulated and could potentially contribute to the development of pathological immune responses and consequent tissue damage.

The p150 Isoform of ADAR1 is Required for Optimal IAV Replication

As described previously, ADAR1 has also been demonstrated to promote or inhibit viral replication for several different viruses (Samuel 2011). Prior to our study, the role of ADAR1 in IAV replication was not completely understood (Ward et al., 2011; de Chassey et al., 2013). Using CRISPR/cas9 technology, we were able to examine the individual contributions of the ADAR1 isoforms during IAV replication. This was of

particular interest considering the differing localization of the ADAR1 isoforms. By examining IAV replication in the isoform specific KOs we demonstrated opposing roles for the isoforms during IAV replication, with p110 restricting IAV replication and p150 promoting IAV replication via inhibition of RIG-I mediated signaling. This differential utilization of the ADAR1 isoforms during IAV replication is mirrored in their localization during infection, with p150 relocalizing in cytoplasmic puncta and p110 relocalizing to the nucleolus. In each instance, the respective ADAR1 isoform colocalizes with the IAV innate immune antagonist NS1. Previous yeast 2-hybrid and immunoprecipitation experiments have demonstrated that ADAR1 and NS1 interact and colocalize in the nucleolus during infection (de Chassey et al., 2013; Ngamurulert et al., 2009; Emmott et al., 2010). Our results confirm this colocalization while also expanding upon the nature of this interaction through the use of p150 and p110 overexpressing cells, demonstrating an isoform specific localization during infection. Considering that our studies suggest an antiviral role for p110 during IAV replication, it is possible that NS1 may work to sequester p110 within the nucleolus in order to prevent p110 antiviral activity within the nucleus, the site of IAV replication. Under basal conditions, p110 KOs do not exhibit the elevated ISG expression like that observed in the p150 KOs, suggesting that p110 does not have a role in editing and suppressing sensing of endogenous dsRNA. However, further studies are required to conclusively determine whether p110 RNA editing is required to suppress IAV replication. These results provide interesting avenues for further discovery regarding the nature of the antiviral role for p110.

Our studies also reveal the cytoplasmic colocalization of p150 with NS1, reflecting the role of p150 a negative regulator of the cytoplasmic sensor RIG-I. NS1 is a well characterized innate immune antagonist, preventing RIG-I activation either through direction interaction with RIG-I or inhibition of the E3 ligases TRIM25 and Riplet, both of which are important for ubiquitination and activation of RIG-I (Gack et al., 2009; Mibayashi et al., 2007; Rajsbaum et al., 2012). Despite the presence of NS1, IAV replication is reduced in cells deficient in p150 expression due to increased RIG-I mediated induction of IFN-β and apoptosis. This suggests that in the absence of p150 expression NS1 is unable to sufficiently suppress RIG-I mediated signaling. To further explore the relationship between p150 and NS1, we examined the impact of p150 and NS1 expression on IFN-β reporter activity. We demonstrate that p150 and NS1 co-expression reduce IFN-β reporter activity to a greater extent than when either construct is expressed alone, underscoring the potential for a cooperative interaction between p150 and NS1 to suppress RIG-I mediated signaling.

Our studies establish that p150 is important for ramping down RIG-I signaling during infection; therefore, it is possible that in the absence of p150 expression NS1 is unable to efficiently suppress amplification of RIG-I mediated signaling and that NS1 requires the action of p150 to ensure sufficient suppression. As a cytoplasmic RNA sensor, RIG-I has been shown to localize to antiviral stress granules in the cytoplasm which have been suggested to act as signaling platforms for amplifying antiviral signaling (Onomoto et al., 2012; Kim et al., 2019). In contrast, NS1 has been shown to prevent antiviral stress granule formation, inhibiting RIG-I recruitment to these signaling platforms

(Onomoto et al., 2012). Similarly, knockdown of ADAR1 expression has been shown to increase measles induced stress granule formation (Okonski et al., 2013). As previous studies have demonstrated a partial RNA dependent interaction between ADAR1 and NS1 (de Chassey et al., 2013), it is possible NS1 may achieve optimal suppression of RIG-I by recruiting p150 to prevent sensing of viral RNA and amplification of RIG-I signaling within the cytoplasm. Alternatively, p150 and NS1 may work independently of one another, with expression of both p150 and NS1 necessary for optimal IAV replication. Future studies are necessary to fully elucidate the nature of the interaction between the different isoforms of ADAR1 and NS1; however, our studies highlight the exciting potential for the differential utilization of the ADAR1 isoforms by NS1 during infection.

In addition to exploring the relationship between ADAR1 and NS1, our studies also revealed that both the p150 RNA binding and Z DNA/RNA binding activity are required for optimal IAV replication. This is of particular interest given that p150/MDA5 DKOs complemented with the Zα mutant of p150 were able to suppress PARP cleavage and IFN-β expression following stimulation with H1N1 vRNA; nevertheless, IAV replication was inhibited in these cells. While the majority of ADAR1 mutations associated with the development of AGS are found within the deaminase domain, a small number of mutations were also found around the Z DNA/RNA binding domains, suggesting that the Z DNA/RNA binding activity of ADAR1 may also be important for the suppression of cell intrinsic immunity (Rice et al., 2012). Previous studies have demonstrated that IAV vRNA can be bound by the Zα domain of an another RNA sensor, Z-DNA binding

protein 1 (ZBP1), demonstrating the potential for IAV vRNA to form Z-form RNA and be bound by proteins with similar Z DNA/RNA binding domains (Thapa et al., 2016). ZBP1 sensing of IAV vRNA has also been shown to induce RIPK3-dependent necroptosis to suppress IAV replication, highlighting an alternative cell death pathway p150 could suppress to promote IAV replication (Thapa et al., 2016). The utilization of Z DNA/RNA binding domains to promote viral replication is not unprecedented, as mutations within the Zα domain of the vaccinia virus protein E3L resulted in reduced viral pathogenicity (Kim et al., 2003). The Zα domain of E3L was also shown to be necessary for inhibition of ZBP1-medaited necroptosis (Koehler et al., 2017). Given the similarities between the Zα domains of ADAR1, ZBP1, and E3L, it has been proposed that proviral proteins, like vaccinia E3L, may compete with ZBP1 for binding of RNA to prevention activation of ZBP1 induced necroptosis (Rothenburg et al., 2002; Ng et al., 2013). It is possible that during IAV infection, p150 may compete with ZBP1 for binding of IAV vRNA, thereby inhibiting the induction of necroptosis. Further studies examining the localization of the p150 mutant constructs during infection as well as investigating the activation of RIPK3-dependent cell death in cells deficient in p150 expression may shed more light upon the utilization of p150 Z DNA/RNA binding activity during IAV replication.

Our data also suggests that the role of p150 in promoting viral replication is specific to IAV. VSV replication, despite being sensitive to IFN, was unaffected in cells deficient in p150 expression. It is possible that the rapid replication kinetics of VSV do not allow ample time for p150 expression to be induced and dampen the RIG-I signaling cascade in a manner that would be impactful for VSV replication. Despite the apparent specificity

to IAV, future studies examining replication of other RNA viruses predominantly sensed by RIG-I are necessary to conclusively determine whether p150 mediated suppression of RIG-I signaling promotes replication of other RNA viruses. The relationship between p150 and flaviviruses, such as Dengue virus, is of particular interest due to previous studies that demonstrate an interaction between Dengue virus nonstructural protein 3 (NS3) and ADAR1, highlighting the potential for a similar relationship to that observed between IAV NS1 and p150 (de Chassey et al., 2013).

Concluding Remarks

Taken together, our studies highlight the importance of p150 as a negative regulator of RLR signaling, with p150 preventing the hyperactivation of innate immune responses through the inhibition of MDA5 signaling under basal conditions and RIG-I signaling during viral infection. While necessary for the prevention of autoimmunity, p150 mediated suppression of RLR signaling may prove detrimental during IAV infection by inadvertently generating a more hospitable environment for IAV replication. As a result, these studies highlight the potential of p150 as a therapeutic target that when inhibited could improve cell intrinsic responses to IAV infection. Current ADAR1 inhibitors, such as 8-Adzaadenosine, target the RNA editing activity of ADAR1; however, our studies demonstrate that p150 RNA binding and not p150 RNA editing is crucial for suppression of RIG-I signaling during viral infection. As result, novel inhibitors would need to be developed to target RNA binding functions of ADAR1. While the therapeutic potential for inhibiting p150 remains to be explored, this work unveils an additional aspect of p150 mediated suppression of cell intrinsic immunity. These studies provide important insight

into the mechanisms of negative regulation of cell intrinsic immunity, which may be exploited by viruses to promote efficient replication.

Bibliography

Aglietti, R. A., A. Estevez, A. Gupta, M. G. Ramirez, P. S. Liu, N. Kayagaki, C. Ciferri, V. M. Dixit, and E. C. Dueber. 2016. 'GsdmD p30 elicited by caspase-11 during pyroptosis forms pores in membranes', *Proc Natl Acad Sci U S A*, 113: 7858-63.

Alexopoulou, L., A. C. Holt, R. Medzhitov, and R. A. Flavell. 2001. 'Recognition of double-stranded RNA and activation of NF-kappaB by Toll-like receptor 3', *Nature*, 413: 732-8.

Arimoto, K., H. Takahashi, T. Hishiki, H. Konishi, T. Fujita, and K. Shimotohno. 2007. 'Negative regulation of the RIG-I signaling by the ubiquitin ligase RNF125', *Proc Natl Acad Sci U S A*, 104: 7500-5.

Athanasiadis, A., A. Rich, and S. Maas. 2004. 'Widespread A-to-I RNA editing of Alu-containing mRNAs in the human transcriptome', *PLoS Biol*, 2: e391.

Baczko, K., J. Lampe, U. G. Liebert, U. Brinckmann, V. ter Meulen, I. Pardowitz, H. Budka, S. L. Cosby, S. Isserte, and B. K. Rima. 1993. 'Clonal expansion of hypermutated measles virus in a SSPE brain', *Virology*, 197: 188-95.

Barrangou, R., C. Fremaux, H. Deveau, M. Richards, P. Boyaval, S. Moineau, D. A. Romero, and P. Horvath. 2007. 'CRISPR provides acquired resistance against viruses in prokaryotes', *Science*, 315: 1709-12.

Bass, B. L., and H. Weintraub. 1987. 'A developmentally regulated activity that unwinds RNA duplexes', *Cell*, 48: 607-13.

———. 1988. 'An unwinding activity that covalently modifies its double-stranded RNA substrate', *Cell*, 55: 1089-98.

Bazak, L., A. Haviv, M. Barak, J. Jacob-Hirsch, P. Deng, R. Zhang, F. J. Isaacs, G. Rechavi, J. B. Li, E. Eisenberg, and E. Y. Levanon. 2014. 'A-to-I RNA editing occurs at over a hundred million genomic sites, located in a majority of human genes', *Genome Res*, 24: 365-76.

Blow, M., P. A. Futreal, R. Wooster, and M. R. Stratton. 2004. 'A survey of RNA editing in human brain', *Genome Res*, 14: 2379-87.

Brouns, S. J., M. M. Jore, M. Lundgren, E. R. Westra, R. J. Slijkhuis, A. P. Snijders, M. J. Dickman, K. S. Makarova, E. V. Koonin, and J. van der Oost. 2008. 'Small CRISPR RNAs guide antiviral defense in prokaryotes', *Science*, 321: 960-4.

Cai, Z., S. Jitkaew, J. Zhao, H. C. Chiang, S. Choksi, J. Liu, Y. Ward, L. G. Wu, and Z. G. Liu. 2014. 'Plasma membrane translocation of trimerized MLKL protein is required for TNF-induced necroptosis', *Nat Cell Biol*, 16: 55-65.

Cattaneo, R., A. Schmid, D. Eschle, K. Baczko, V. ter Meulen, and M. A. Billeter. 1988. 'Biased hypermutation and other genetic changes in defective measles viruses in human brain infections', *Cell*, 55: 255-65.

Cattaneo, R., A. Schmid, G. Rebmann, K. Baczko, V. Ter Meulen, W. J. Bellini, S. Rozenblatt, and M. A. Billeter. 1986. 'Accumulated measles virus mutations in a case of subacute sclerosing panencephalitis: interrupted matrix protein reading frame and transcription alteration', *Virology*, 154: 97-107.

Chan, Y. K., and M. U. Gack. 2016. 'A phosphomimetic-based mechanism of dengue virus to antagonize innate immunity', *Nat Immunol*, 17: 523-30.

Chattopadhyay, S., T. Kuzmanovic, Y. Zhang, J. L. Wetzel, and G. C. Sen. 2016. 'Ubiquitination of the transcription factor IRF-3 activates RIPA, the apoptotic pathway that protects mice from viral pathogenesis', *Immunity*, 44: 1151-61.

Chattopadhyay, S., J. T. Marques, M. Yamashita, K. L. Peters, K. Smith, A. Desai, B. R. G. Williams, and G. C. Sen. 2010. 'Viral apoptosis is induced by IRF-3-mediated activation of Bax.' in, *Embo j*.

Chattopadhyay, S., and G. C. Sen. 2017. 'RIG-I-like receptor-induced IRF3 mediated pathway of apoptosis (RIPA): a new antiviral pathway.' in, *Protein Cell*.

Chattopadhyay, S., M. Yamashita, Y. Zhang, and G. C. Sen. 2011. 'The IRF-3/Bax-Mediated Apoptotic Pathway, Activated by Viral Cytoplasmic RNA and DNA, Inhibits Virus Replication ▿ †.' in, *J Virol*.

Chen, C. X., D. S. Cho, Q. Wang, F. Lai, K. C. Carter, and K. Nishikura. 2000. 'A third member of the RNA-specific adenosine deaminase gene family, ADAR3, contains both single- and double-stranded RNA binding domains', *Rna*, 6: 755-67.

Chen, X., W. Li, J. Ren, D. Huang, W. T. He, Y. Song, C. Yang, X. Zheng, P. Chen, and J. Han. 2014. 'Translocation of mixed lineage kinase domain-like protein to plasma membrane leads to necrotic cell death', *Cell Res*, 24: 105-21.

Chiang, J. J., K. M. Sparrer, M. van Gent, C. Lässig, T. Huang, N. Osterrieder, K. P. Hopfner, and M. U. Gack. 2018. 'Viral unmasking of cellular 5S rRNA pseudogene transcripts induces RIG-I mediated immunity', *Nat Immunol*, 19: 53-62.

Choe, J., M. S. Kelker, and I. A. Wilson. 2005. 'Crystal structure of human toll-like receptor 3 (TLR3) ectodomain', *Science*, 309: 581-5.

Chung, H., J. J. A. Calis, X. Wu, T. Sun, Y. Yu, S. L. Sarbanes, V. L. Dao Thi, A. R. Shilvock, H. H. Hoffmann, B. R. Rosenberg, and C. M. Rice. 2018. 'Human ADAR1 Prevents Endogenous RNA from Triggering Translational Shutdown', *Cell*, 172: 811-24.e14.

Clerzius, G., J. F. Gelinas, A. Daher, M. Bonnet, E. F. Meurs, and A. Gatignol. 2009. 'ADAR1 interacts with PKR during human immunodeficiency virus infection of lymphocytes and contributes to viral replication', *J Virol*, 83: 10119-28.

Crow, Y. J., D. S. Chase, J. Lowenstein Schmidt, M. Szynkiewicz, G. M. Forte, H. L. Gornall, A. Oojageer, B. Anderson, A. Pizzino, G. Helman, M. S. Abdel-Hamid, G. M. Abdel-Salam, S. Ackroyd, A. Aeby, G. Agosta, C. Albin, S. Allon-Shalev, M. Arellano, G. Ariaudo, V. Aswani, R. Babul-Hirji, E. M. Baildam, N. Bahi-Buisson, K. M. Bailey, C. Barnerias, M. Barth, R. Battini, M. W. Beresford, G. Bernard, M. Bianchi, T. Billette de Villemeur, E. M. Blair, M. Bloom, A. B. Burlina, M. L. Carpanelli, D. R. Carvalho, M. Castro-Gago, A. Cavallini, C. Cereda, K. E. Chandler, D. A. Chitayat, A. E. Collins, C. Sierra Corcoles, N. J. Cordeiro, G. Crichiutti, L. Dabydeen, R. C. Dale, S. D'Arrigo, C. G. De Goede, C. De Laet, L. M. De Waele, I. Denzler, I. Desguerre, K. Devriendt, M. Di Rocco, M. C. Fahey, E. Fazzi, C. D. Ferrie, A. Figueiredo, B. Gener, C. Goizet, N. R. Gowrinathan, K. Gowrishankar, D. Hanrahan, B. Isidor, B. Kara, N. Khan, M. D. King, E. P. Kirk, R. Kumar, L. Lagae, P. Landrieu, H. Lauffer, V. Laugel, R. La Piana, M. J. Lim, J. P. Lin, T. Linnankivi, M. T. Mackay, D. R. Marom, C. Marques Lourenco, S. A. McKee, I. Moroni, J. E. Morton, M. L. Moutard, K. Murray, R. Nabbout, S. Nampoothiri, N. Nunez-Enamorado, P. J. Oades, I. Olivieri, J. R. Ostergaard, B. Perez-Duenas, J. S. Prendiville, V. Ramesh, M. Rasmussen, L. Regal, F. Ricci, M. Rio, D. Rodriguez, A. Roubertie, E. Salvatici, K. A. Segers, G. P. Sinha, D. Soler, R. Spiegel, T. I. Stodberg, R. Straussberg, K. J. Swoboda, M. Suri, U. Tacke, T. Y. Tan, J. te Water Naude, K. Wee Teik, M. M. Thomas, M. Till, D. Tonduti, E. M. Valente, R. N. Van Coster, M. S. van der Knaap, G. Vassallo, R. Vijzelaar, J. Vogt, G. B. Wallace, E. Wassmer, H. J. Webb, W. P. Whitehouse, R. N. Whitney, M. S. Zaki, S. M. Zuberi, J. H. Livingston, F. Rozenberg, P. Lebon, A. Vanderver, S. Orcesi, and G. I. Rice. 2015. 'Characterization of human disease phenotypes associated with mutations in TREX1, RNASEH2A, RNASEH2B, RNASEH2C, SAMHD1, ADAR, and IFIH1', *Am J Med Genet A*, 167a: 296-312.

Crow, Y. J., D. S. Chase, J. L. Schmidt, M. Szynkiewicz, G. M. Forte, H. L. Gornall, A. Oojageer, B. Anderson, A. Pizzino, G. Helman, M. S. Abdel-Hamid, G. M. Abdel-Salam, S. Ackroyd, A. Aeby, G. Agosta, C. Albin, S. Allon-Shalev, M. Arellano, G. Ariaudo, V. Aswani, R. Babul-Hirji, E. M. Baildam, N. Bahi-Buisson, K. M. Bailey, C. Barnerias, M. Barth, R. Battini, M. W. Beresford, G. Bernard, M. Bianchi, T. B. de Villemeur, E. M. Blair, M. Bloom, A. B. Burlina, M. L. Carpanelli, D. R.

Carvalho, M. Castro-Gago, A. Cavallini, C. Cereda, K. E. Chandler, D. A. Chitayat, A. E. Collins, C. S. Corcoles, N. J. Cordeiro, G. Crichiutti, L. Dabydeen, R. C. Dale, S. D'Arrigo, C. G. De Goede, C. De Laet, L. M. De Waele, I. Denzler, I. Desguerre, K. Devriendt, M. Di Rocco, M. C. Fahey, E. Fazzi, C. D. Ferrie, A. Figueiredo, B. Gener, C. Goizet, N. R. Gowrinathan, K. Gowrishankar, D. Hanrahan, B. Isidor, B. Kara, N. Khan, M. D. King, E. P. Kirk, R. Kumar, L. Lagae, P. Landrieu, H. Lauffer, V. Laugel, R. La Piana, M. J. Lim, Jpsm Lin, T. Linnankivi, M. T. Mackay, D. R. Marom, C. M. Lourenço, S. A. McKee, I. Moroni, J. E. Morton, M. L. Moutard, K. Murray, R. Nabbout, S. Nampoothiri, N. Nunez-Enamorado, P. J. Oades, I. Olivieri, J. R. Ostergaard, B. Pérez-Dueñas, J. S. Prendiville, V. Ramesh, M. Rasmussen, L. Régal, F. Ricci, M. Rio, D. Rodriguez, A. Roubertie, E. Salvatici, K. A. Segers, G. P. Sinha, D. Soler, R. Spiegel, T. I. Stödberg, R. Straussberg, K. J. Swoboda, M. Suri, U. Tacke, T. Y. Tan, W. Naude Jte, K. W. Teik, M. M. Thomas, M. Till, D. Tonduti, E. M. Valente, R. N. Van Coster, M. S. van der Knaap, G. Vassallo, R. Vijzelaar, J. Vogt, G. B. Wallace, E. Wassmer, H. J. Webb, W. P. Whitehouse, R. N. Whitney, M. S. Zaki, S. M. Zuberi, J. H. Livingston, F. Rozenberg, P. Lebon, A. Vanderver, S. Orcesi, and G. I. Rice. 2015. 'Characterization of Human Disease Phenotypes Associated with Mutations in TREX1, RNASEH2A, RNASEH2B, RNASEH2C, SAMHD1, ADAR, and IFIH1', *Am J Med Genet A*, 0: 296-312.

Cui, J., Y. Song, Y. Li, Q. Zhu, P. Tan, Y. Qin, H. Y. Wang, and R. F. Wang. 2014. 'USP3 inhibits type I interferon signaling by deubiquitinating RIG-I-like receptors', *Cell Res*, 24: 400-16.

de Chassey, B., A. Aublin-Gex, A. Ruggieri, L. Meyniel-Schicklin, F. Pradezynski, N. Davoust, T. Chantier, L. Tafforeau, P. E. Mangeot, C. Ciancia, L. Perrin-Cocon, R. Bartenschlager, P. Andre, and V. Lotteau. 2013. 'The interactomes of influenza virus NS1 and NS2 proteins identify new host factors and provide insights for ADAR1 playing a supportive role in virus replication', *PLoS Pathog*, 9: e1003440.

Deltcheva, E., K. Chylinski, C. M. Sharma, K. Gonzales, Y. Chao, Z. A. Pirzada, M. R. Eckert, J. Vogel, and E. Charpentier. 2011. 'CRISPR RNA maturation by trans-encoded small RNA and host factor RNase III', *Nature*, 471: 602-7.

Desterro, J. M., L. P. Keegan, M. Lafarga, M. T. Berciano, M. O'Connell, and M. Carmo-Fonseca. 2003. 'Dynamic association of RNA-editing enzymes with the nucleolus', *J Cell Sci*, 116: 1805-18.

Deveau, H., R. Barrangou, J. E. Garneau, J. Labonte, C. Fremaux, P. Boyaval, D. A. Romero, P. Horvath, and S. Moineau. 2008. 'Phage response to CRISPR-encoded resistance in Streptococcus thermophilus', *J Bacteriol*, 190: 1390-400.

Diebold, S. S., T. Kaisho, H. Hemmi, S. Akira, and C. Reis e Sousa. 2004. 'Innate antiviral responses by means of TLR7-mediated recognition of single-stranded RNA', *Science*, 303: 1529-31.

Dondelinger, Y., W. Declercq, S. Montessuit, R. Roelandt, A. Goncalves, I. Bruggeman, P. Hulpiau, K. Weber, C. A. Sehon, R. W. Marquis, J. Bertin, P. J. Gough, S. Savvides, J. C. Martinou, M. J. Bertrand, and P. Vandenabeele. 2014. 'MLKL compromises plasma membrane integrity by binding to phosphatidylinositol phosphates', *Cell Rep*, 7: 971-81.

Eckmann, C. R., A. Neunteufl, L. Pfaffstetter, and M. F. Jantsch. 2001. 'The human but not the Xenopus RNA-editing enzyme ADAR1 has an atypical nuclear localization signal and displays the characteristics of a shuttling protein', *Mol Biol Cell*, 12: 1911-24.

Ehrhardt, C., T. Wolff, S. Pleschka, O. Planz, W. Beermann, J. G. Bode, M. Schmolke, and S. Ludwig. 2007. 'Influenza A virus NS1 protein activates the PI3K/Akt pathway to mediate antiapoptotic signaling responses', *J Virol*, 81: 3058-67.

Elmore, S. 2007. 'Apoptosis: A Review of Programmed Cell Death', *Toxicol Pathol*, 35: 495-516.

Emmott, E., H. Wise, E. M. Loucaides, D. A. Matthews, P. Digard, and J. A. Hiscox. 2010. 'Quantitative proteomics using SILAC coupled to LC-MS/MS reveals changes in the nucleolar proteome in influenza A virus-infected cells', *J Proteome Res*, 9: 5335-45.

Endo, T. A., M. Masuhara, M. Yokouchi, R. Suzuki, H. Sakamoto, K. Mitsui, A. Matsumoto, S. Tanimura, M. Ohtsubo, H. Misawa, T. Miyazaki, N. Leonor, T. Taniguchi, T. Fujita, Y. Kanakura, S. Komiya, and A. Yoshimura. 1997. 'A new protein containing an SH2 domain that inhibits JAK kinases', *Nature*, 387: 921-4.

Fields, Bernard N., David M. Knipe, and Peter M. Howley. 2013. *Fields virology* (Lippincott-Raven Publishers: Philadelphia).

Frank, D., and J. E. Vince. 2019. 'Pyroptosis versus necroptosis: similarities, differences, and crosstalk', *Cell Death Differ*, 26: 99-114.

Gack, M. U., R. A. Albrecht, T. Urano, K. S. Inn, I. C. Huang, E. Carnero, M. Farzan, S. Inoue, J. U. Jung, and A. Garcia-Sastre. 2009. 'Influenza A virus NS1 targets the ubiquitin ligase TRIM25 to evade recognition by the host viral RNA sensor RIG-I', *Cell Host Microbe*, 5: 439-49.

Gack, M. U., A. Kirchhofer, Y. C. Shin, K. S. Inn, C. Liang, S. Cui, S. Myong, T. Ha, K. P. Hopfner, and J. U. Jung. 2008. 'Roles of RIG-I N-terminal tandem CARD and

splice variant in TRIM25-mediated antiviral signal transduction', *Proc Natl Acad Sci U S A*, 105: 16743-8.

Gack, M. U., E. Nistal-Villan, K. S. Inn, A. Garcia-Sastre, and J. U. Jung. 2010. 'Phosphorylation-mediated negative regulation of RIG-I antiviral activity', *J Virol*, 84: 3220-9.

Gack, M. U., Y. C. Shin, C. H. Joo, T. Urano, C. Liang, L. Sun, O. Takeuchi, S. Akira, Z. Chen, S. Inoue, and J. U. Jung. 2007. 'TRIM25 RING-finger E3 ubiquitin ligase is essential for RIG-I-mediated antiviral activity.' in, *Nature* (England).

Garcia-Sastre, A., A. Egorov, D. Matassov, S. Brandt, D. E. Levy, J. E. Durbin, P. Palese, and T. Muster. 1998. 'Influenza A virus lacking the NS1 gene replicates in interferon-deficient systems', *Virology*, 252: 324-30.

Garneau, J. E., M. E. Dupuis, M. Villion, D. A. Romero, R. Barrangou, P. Boyaval, C. Fremaux, P. Horvath, A. H. Magadan, and S. Moineau. 2010. 'The CRISPR/Cas bacterial immune system cleaves bacteriophage and plasmid DNA', *Nature*, 468: 67-71.

Gasiunas, G., R. Barrangou, P. Horvath, and V. Siksnys. 2012. 'Cas9-crRNA ribonucleoprotein complex mediates specific DNA cleavage for adaptive immunity in bacteria', *Proc Natl Acad Sci U S A*, 109: E2579-86.

George, C. X., G. Ramaswami, J. B. Li, and C. E. Samuel. 2016. 'Editing of Cellular Self-RNAs by Adenosine Deaminase ADAR1 Suppresses Innate Immune Stress Responses', *J Biol Chem*, 291: 6158-68.

George, C. X., and C. E. Samuel. 1999. 'Human RNA-specific adenosine deaminase ADAR1 transcripts possess alternative exon 1 structures that initiate from different promoters, one constitutively active and the other interferon inducible', *Proc Natl Acad Sci U S A*, 96: 4621-6.

Gerlach, B., S. M. Cordier, A. C. Schmukle, C. H. Emmerich, E. Rieser, T. L. Haas, A. I. Webb, J. A. Rickard, H. Anderton, W. W. Wong, U. Nachbur, L. Gangoda, U. Warnken, A. W. Purcell, J. Silke, and H. Walczak. 2011. 'Linear ubiquitination prevents inflammation and regulates immune signalling', *Nature*, 471: 591-6.

Goubau, D., S. Deddouche, and C. Reis e Sousa. 2013. 'Cytosolic Sensing of Viruses.' in, *Immunity*.

Goubau, D., M. Schlee, S. Deddouche, A. J. Pruijssers, T. Zillinger, M. Goldeck, C. Schuberth, A. G. Van der Veen, T. Fujimura, J. Rehwinkel, J. A. Iskarpatyoti, W. Barchet, J. Ludwig, T. S. Dermody, G. Hartmann, and C. Reis e Sousa. 2014. 'Antiviral immunity via RIG-I-mediated recognition of RNA bearing 5'-diphosphates', *Nature*, 514: 372-75.

Gu, R., Z. Zhang, J. N. DeCerbo, and G. G. Carmichael. 2009. 'Gene regulation by sense-antisense overlap of polyadenylation signals', *Rna*, 15: 1154-63.

Hale, B. G., I. H. Batty, C. P. Downes, and R. E. Randall. 2008. 'Binding of influenza A virus NS1 protein to the inter-SH2 domain of p85 suggests a novel mechanism for phosphoinositide 3-kinase activation', *J Biol Chem*, 283: 1372-80.

Hale, B. G., D. Jackson, Y. H. Chen, R. A. Lamb, and R. E. Randall. 2006. 'Influenza A virus NS1 protein binds p85beta and activates phosphatidylinositol-3-kinase signaling', *Proc Natl Acad Sci U S A*, 103: 14194-9.

Hale, B. G., P. S. Kerry, D. Jackson, B. L. Precious, A. Gray, M. J. Killip, R. E. Randall, and R. J. Russell. 2010. 'Structural insights into phosphoinositide 3-kinase activation by the influenza A virus NS1 protein', *Proc Natl Acad Sci U S A*, 107: 1954-9.

Han, J., J. T. Perez, C. Chen, Y. Li, A. Benitez, M. Kandasamy, Y. Lee, J. Andrade, B. tenOever, and B. Manicassamy. 2018. 'Genome-wide CRISPR/Cas9 Screen Identifies Host Factors Essential for Influenza Virus Replication', *Cell Rep*, 23: 596-607.

Hartner, J. C., C. R. Walkley, J. Lu, and S. H. Orkin. 2009. 'ADAR1 is essential for maintenance of hematopoiesis and suppression of interferon signaling', *Nat Immunol*, 10: 109-15.

Heil, F., H. Hemmi, H. Hochrein, F. Ampenberger, C. Kirschning, S. Akira, G. Lipford, H. Wagner, and S. Bauer. 2004. 'Species-specific recognition of single-stranded RNA via toll-like receptor 7 and 8', *Science*, 303: 1526-9.

Horner, S. M., H. M. Liu, H. S. Park, J. Briley, and M. Gale, Jr. 2011. 'Mitochondrial-associated endoplasmic reticulum membranes (MAM) form innate immune synapses and are targeted by hepatitis C virus', *Proc Natl Acad Sci U S A*, 108: 14590-5.

Hornung, V., A. Ablasser, M. Charrel-Dennis, F. Bauernfeind, G. Horvath, D. R. Caffrey, E. Latz, and K. A. Fitzgerald. 2009. 'AIM2 recognizes cytosolic dsDNA and forms a caspase-1-activating inflammasome with ASC', *Nature*, 458: 514-8.

Hornung, V., J. Ellegast, S. Kim, K. Brzozka, A. Jung, H. Kato, H. Poeck, S. Akira, K. K. Conzelmann, M. Schlee, S. Endres, and G. Hartmann. 2006. '5'-Triphosphate RNA is the ligand for RIG-I', *Science*, 314: 994-7.

Hou, F., L. Sun, H. Zheng, B. Skaug, Q. X. Jiang, and Z. J. Chen. 2011. 'MAVS forms functional prion-like aggregates to activate and propagate antiviral innate immune response', *Cell*, 146: 448-61.

Ikeda, F., Y. L. Deribe, S. S. Skanland, B. Stieglitz, C. Grabbe, M. Franz-Wachtel, S. J. van Wijk, P. Goswami, V. Nagy, J. Terzic, F. Tokunaga, A. Androulidaki, T. Nakagawa, M. Pasparakis, K. Iwai, J. P. Sundberg, L. Schaefer, K. Rittinger, B. Macek, and I. Dikic. 2011. 'SHARPIN forms a linear ubiquitin ligase complex regulating NF-kappaB activity and apoptosis', *Nature*, 471: 637-41.

Jacobs, M. M., R. L. Fogg, R. B. Emeson, and G. D. Stanwood. 2009. 'ADAR1 and ADAR2 expression and editing activity during forebrain development', *Dev Neurosci*, 31: 223-37.

Jayan, G. C., and J. L. Casey. 2002. 'Increased RNA editing and inhibition of hepatitis delta virus replication by high-level expression of ADAR1 and ADAR2', *J Virol*, 76: 3819-27.

Jinek, M., K. Chylinski, I. Fonfara, M. Hauer, J. A. Doudna, and E. Charpentier. 2012. 'A programmable dual-RNA-guided DNA endonuclease in adaptive bacterial immunity', *Science*, 337: 816-21.

Jureka, A. S., A. B. Kleinpeter, J. L. Tipper, K. S. Harrod, and C. M. Petit. 2020. 'The influenza NS1 protein modulates RIG-I activation via a strain-specific direct interaction with the second CARD of RIG-I', *J Biol Chem*, 295: 1153-64.

Kamura, T., K. Maenaka, S. Kotoshiba, M. Matsumoto, D. Kohda, R. C. Conaway, J. W. Conaway, and K. I. Nakayama. 2004. 'VHL-box and SOCS-box domains determine binding specificity for Cul2-Rbx1 and Cul5-Rbx2 modules of ubiquitin ligases', *Genes Dev*, 18: 3055-65.

Kato, H., S. Sato, M. Yoneyama, M. Yamamoto, S. Uematsu, K. Matsui, T. Tsujimura, K. Takeda, T. Fujita, O. Takeuchi, and S. Akira. 2005. 'Cell type-specific involvement of RIG-I in antiviral response', *Immunity*, 23: 19-28.

Kato, H., O. Takeuchi, E. Mikamo-Satoh, R. Hirai, T. Kawai, K. Matsushita, A. Hiiragi, T. S. Dermody, T. Fujita, and S. Akira. 2008. 'Length-dependent recognition of double-stranded ribonucleic acids by retinoic acid-inducible gene-I and melanoma differentiation-associated gene 5', *J Exp Med*, 205: 1601-10.

Kawahara, Y., M. Megraw, E. Kreider, H. Iizasa, L. Valente, A. G. Hatzigeorgiou, and K. Nishikura. 2008. 'Frequency and fate of microRNA editing in human brain', *Nucleic Acids Res*, 36: 5270-80.

Kawai, T., K. Takahashi, S. Sato, C. Coban, H. Kumar, H. Kato, K. J. Ishii, O. Takeuchi, and S. Akira. 2005. 'IPS-1, an adaptor triggering RIG-I- and Mda5-mediated type I interferon induction', *Nat Immunol*, 6: 981-8.

Kim, D. D., T. T. Kim, T. Walsh, Y. Kobayashi, T. C. Matise, S. Buyske, and A. Gabriel. 2004. 'Widespread RNA editing of embedded alu elements in the human transcriptome', *Genome Res*, 14: 1719-25.

Kim, S. S. Y., L. Sze, and K. P. Lam. 2019. 'The stress granule protein G3BP1 binds viral dsRNA and RIG-I to enhance interferon-β response.' in, *J Biol Chem*.

Kim, U., Y. Wang, T. Sanford, Y. Zeng, and K. Nishikura. 1994. 'Molecular cloning of cDNA for double-stranded RNA adenosine deaminase, a candidate enzyme for nuclear RNA editing', *Proc Natl Acad Sci U S A*, 91: 11457-61.

Kim, Y. G., M. Muralinath, T. Brandt, M. Pearcy, K. Hauns, K. Lowenhaupt, B. L. Jacobs, and A. Rich. 2003. 'A role for Z-DNA binding in vaccinia virus pathogenesis.' in, *Proc Natl Acad Sci U S A*.

Kirisako, T., K. Kamei, S. Murata, M. Kato, H. Fukumoto, M. Kanie, S. Sano, F. Tokunaga, K. Tanaka, and K. Iwai. 2006. 'A ubiquitin ligase complex assembles linear polyubiquitin chains', *Embo j*, 25: 4877-87.

Koehler, H., S. Cotsmire, J. Langland, K. V. Kibler, D. Kalman, J. W. Upton, E. S. Mocarski, and B. L. Jacobs. 2017. 'Inhibition of DAI-dependent necroptosis by the Z-DNA binding domain of the vaccinia virus innate immune evasion protein, E3.' in, *Proc Natl Acad Sci U S A*.

Kowalinski, E., T. Lunardi, A. A. McCarthy, J. Louber, J. Brunel, B. Grigorov, D. Gerlier, and S. Cusack. 2011. 'Structural basis for the activation of innate immune pattern-recognition receptor RIG-I by viral RNA', *Cell*, 147: 423-35.

Kumar, M., and G. G. Carmichael. 1997. 'Nuclear antisense RNA induces extensive adenosine modifications and nuclear retention of target transcripts', *Proc Natl Acad Sci U S A*, 94: 3542-7.

Lai, F., R. Drakas, and K. Nishikura. 1995. 'Mutagenic analysis of double-stranded RNA adenosine deaminase, a candidate enzyme for RNA editing of glutamate-gated ion channel transcripts', *J Biol Chem*, 270: 17098-105.

Lamers, M. M., B. G. van den Hoogen, and B. L. Haagmans. 2019. 'ADAR1: "Editor-in-Chief" of Cytoplasmic Innate Immunity', *Front Immunol*, 10: 1763.

Lander, E. S., L. M. Linton, B. Birren, C. Nusbaum, M. C. Zody, J. Baldwin, K. Devon, K. Dewar, M. Doyle, W. FitzHugh, R. Funke, D. Gage, K. Harris, A. Heaford, J. Howland, L. Kann, J. Lehoczky, R. LeVine, P. McEwan, K. McKernan, J. Meldrim, J. P. Mesirov, C. Miranda, W. Morris, J. Naylor, C. Raymond, M. Rosetti, R. Santos, A. Sheridan, C. Sougnez, Y. Stange-Thomann, N. Stojanovic, A. Subramanian, D. Wyman, J. Rogers, J. Sulston, R. Ainscough, S. Beck, D. Bentley, J. Burton, C. Clee, N. Carter, A. Coulson, R. Deadman, P. Deloukas, A.

Dunham, I. Dunham, R. Durbin, L. French, D. Grafham, S. Gregory, T. Hubbard, S. Humphray, A. Hunt, M. Jones, C. Lloyd, A. McMurray, L. Matthews, S. Mercer, S. Milne, J. C. Mullikin, A. Mungall, R. Plumb, M. Ross, R. Shownkeen, S. Sims, R. H. Waterston, R. K. Wilson, L. W. Hillier, J. D. McPherson, M. A. Marra, E. R. Mardis, L. A. Fulton, A. T. Chinwalla, K. H. Pepin, W. R. Gish, S. L. Chissoe, M. C. Wendl, K. D. Delehaunty, T. L. Miner, A. Delehaunty, J. B. Kramer, L. L. Cook, R. S. Fulton, D. L. Johnson, P. J. Minx, S. W. Clifton, T. Hawkins, E. Branscomb, P. Predki, P. Richardson, S. Wenning, T. Slezak, N. Doggett, J. F. Cheng, A. Olsen, S. Lucas, C. Elkin, E. Uberbacher, M. Frazier, R. A. Gibbs, D. M. Muzny, S. E. Scherer, J. B. Bouck, E. J. Sodergren, K. C. Worley, C. M. Rives, J. H. Gorrell, M. L. Metzker, S. L. Naylor, R. S. Kucherlapati, D. L. Nelson, G. M. Weinstock, Y. Sakaki, A. Fujiyama, M. Hattori, T. Yada, A. Toyoda, T. Itoh, C. Kawagoe, H. Watanabe, Y. Totoki, T. Taylor, J. Weissenbach, R. Heilig, W. Saurin, F. Artiguenave, P. Brottier, T. Bruls, E. Pelletier, C. Robert, P. Wincker, D. R. Smith, L. Doucette-Stamm, M. Rubenfield, K. Weinstock, H. M. Lee, J. Dubois, A. Rosenthal, M. Platzer, G. Nyakatura, S. Taudien, A. Rump, H. Yang, J. Yu, J. Wang, G. Huang, J. Gu, L. Hood, L. Rowen, A. Madan, S. Qin, R. W. Davis, N. A. Federspiel, A. P. Abola, M. J. Proctor, R. M. Myers, J. Schmutz, M. Dickson, J. Grimwood, D. R. Cox, M. V. Olson, R. Kaul, N. Shimizu, K. Kawasaki, S. Minoshima, G. A. Evans, M. Athanasiou, R. Schultz, B. A. Roe, F. Chen, H. Pan, J. Ramser, H. Lehrach, R. Reinhardt, W. R. McCombie, M. de la Bastide, N. Dedhia, H. Blocker, K. Hornischer, G. Nordsiek, R. Agarwala, L. Aravind, J. A. Bailey, A. Bateman, S. Batzoglou, E. Birney, P. Bork, D. G. Brown, C. B. Burge, L. Cerutti, H. C. Chen, D. Church, M. Clamp, R. R. Copley, T. Doerks, S. R. Eddy, E. E. Eichler, T. S. Furey, J. Galagan, J. G. Gilbert, C. Harmon, Y. Hayashizaki, D. Haussler, H. Hermjakob, K. Hokamp, W. Jang, L. S. Johnson, T. A. Jones, S. Kasif, A. Kaspryzk, S. Kennedy, W. J. Kent, P. Kitts, E. V. Koonin, I. Korf, D. Kulp, D. Lancet, T. M. Lowe, A. McLysaght, T. Mikkelsen, J. V. Moran, N. Mulder, V. J. Pollara, C. P. Ponting, G. Schuler, J. Schultz, G. Slater, A. F. Smit, E. Stupka, J. Szustakowki, D. Thierry-Mieg, J. Thierry-Mieg, L. Wagner, J. Wallis, R. Wheeler, A. Williams, Y. I. Wolf, K. H. Wolfe, S. P. Yang, R. F. Yeh, F. Collins, M. S. Guyer, J. Peterson, A. Felsenfeld, K. A. Wetterstrand, A. Patrinos, M. J. Morgan, P. de Jong, J. J. Catanese, K. Osoegawa, H. Shizuya, S. Choi, and Y. J. Chen. 2001. 'Initial sequencing and analysis of the human genome', *Nature*, 409: 860-921.

Lebon, P., J. Badoual, G. Ponsot, F. Goutieres, F. Hemeury-Cukier, and J. Aicardi. 1988. 'Intrathecal synthesis of interferon-alpha in infants with progressive familial encephalopathy', *J Neurol Sci*, 84: 201-8.

Levanon, E. Y., E. Eisenberg, R. Yelin, S. Nemzer, M. Hallegger, R. Shemesh, Z. Y. Fligelman, A. Shoshan, S. R. Pollock, D. Sztybel, M. Olshansky, G. Rechavi, and M. F. Jantsch. 2004. 'Systematic identification of abundant A-to-I editing sites in the human transcriptome', *Nat Biotechnol*, 22: 1001-5.

Li, B., S. M. Clohisey, B. S. Chia, B. Wang, A. Cui, T. Eisenhaure, L. D. Schweitzer, P. Hoover, N. J. Parkinson, A. Nachshon, N. Smith, T. Regan, D. Farr, M. U. Gutmann, S. I. Bukhari, A. Law, M. Sangesland, I. Gat-Viks, P. Digard, S. Vasudevan, D. Lingwood, D. H. Dockrell, J. G. Doench, J. K. Baillie, and N. Hacohen. 2020. 'Genome-wide CRISPR screen identifies host dependency factors for influenza A virus infection', *Nat Commun*, 11: 164.

Li, X. D., L. Sun, R. B. Seth, G. Pineda, and Z. J. Chen. 2005. 'Hepatitis C virus protease NS3/4A cleaves mitochondrial antiviral signaling protein off the mitochondria to evade innate immunity', *Proc Natl Acad Sci U S A*, 102: 17717-22.

Li, Y., S. Banerjee, S. A. Goldstein, B. Dong, C. Gaughan, S. Rath, J. Donovan, A. Korennykh, R. H. Silverman, and S. R. Weiss. 2017. 'Ribonuclease L mediates the cell-lethal phenotype of double-stranded RNA editing enzyme ADAR1 deficiency in a human cell line', *Elife*, 6.

Li, Z., K. M. Okonski, and C. E. Samuel. 2012. 'Adenosine deaminase acting on RNA 1 (ADAR1) suppresses the induction of interferon by measles virus', *J Virol*, 86: 3787-94.

Liddicoat, B. J., A. M. Chalk, and C. R. Walkley. 2016. 'ADAR1, inosine and the immune sensing system: distinguishing self from non-self', *Wiley Interdiscip Rev RNA*, 7: 157-72.

Liddicoat, B. J., R. Piskol, A. M. Chalk, G. Ramaswami, M. Higuchi, J. C. Hartner, J. B. Li, P. H. Seeburg, and C. R. Walkley. 2015. 'RNA editing by ADAR1 prevents MDA5 sensing of endogenous dsRNA as nonself', *Science*, 349: 1115-20.

Lin, J. P., Y. K. Fan, and H. M. Liu. 2019. 'The 14-3-3eta chaperone protein promotes antiviral innate immunity via facilitating MDA5 oligomerization and intracellular redistribution', *PLoS Pathog*, 15: e1007582.

Lindqvist, L. M., D. Frank, K. McArthur, T. A. Dite, M. Lazarou, J. S. Oakhill, B. T. Kile, and D. L. Vaux. 2018. 'Autophagy induced during apoptosis degrades mitochondria and inhibits type I interferon secretion', *Cell Death Differ*, 25: 784-96.

Liu, H. M., Y. M. Loo, S. M. Horner, G. A. Zornetzer, M. G. Katze, and M. Gale, Jr. 2012. 'The mitochondrial targeting chaperone 14-3-3epsilon regulates a RIG-I translocon that mediates membrane association and innate antiviral immunity', *Cell Host Microbe*, 11: 528-37.

Liu, L., I. Botos, Y. Wang, J. N. Leonard, J. Shiloach, D. M. Segal, and D. R. Davies. 2008. 'Structural basis of toll-like receptor 3 signaling with double-stranded RNA', *Science*, 320: 379-81.

Liu, X., Z. Zhang, J. Ruan, Y. Pan, V. G. Magupalli, H. Wu, and J. Lieberman. 2016. 'Inflammasome-activated gasdermin D causes pyroptosis by forming membrane pores', *Nature*, 535: 153-8.

Liu, Y., R. B. Emeson, and C. E. Samuel. 1999. 'Serotonin-2C receptor pre-mRNA editing in rat brain and in vitro by splice site variants of the interferon-inducible double-stranded RNA-specific adenosine deaminase ADAR1', *J Biol Chem*, 274: 18351-8.

Liu, Y., and C. E. Samuel. 1999. 'Editing of glutamate receptor subunit B pre-mRNA by splice-site variants of interferon-inducible double-stranded RNA-specific adenosine deaminase ADAR1', *J Biol Chem*, 274: 5070-7.

Loo, Y. M., and M. Gale. 2011. 'Immune signaling by RIG-I-like receptors', *Immunity*, 34: 680-92.

Ma, Y., M. J. Walsh, K. Bernhardt, C. W. Ashbaugh, S. J. Trudeau, I. Y. Ashbaugh, S. Jiang, C. Jiang, B. Zhao, D. E. Root, J. G. Doench, and B. E. Gewurz. 2017. 'CRISPR/Cas9 Screens Reveal Epstein-Barr Virus-Transformed B Cell Host Dependency Factors', *Cell Host Microbe*, 21: 580-91.e7.

Maelfait, J., L. Liverpool, and J. Rehwinkel. 2020. 'Nucleic Acid Sensors and Programmed Cell Death', *J Mol Biol*, 432: 552-68.

Magadan, A. H., M. E. Dupuis, M. Villion, and S. Moineau. 2012. 'Cleavage of phage DNA by the Streptococcus thermophilus CRISPR3-Cas system', *PLoS One*, 7: e40913.

Maharaj, N. P., E. Wies, A. Stoll, and M. U. Gack. 2012. 'Conventional protein kinase C-alpha (PKC-alpha) and PKC-beta negatively regulate RIG-I antiviral signal transduction', *J Virol*, 86: 1358-71.

Manicassamy, B., S. Manicassamy, A. Belicha-Villanueva, G. Pisanelli, B. Pulendran, and A. García-Sastre. 2010. 'Analysis of in vivo dynamics of influenza virus infection in mice using a GFP reporter virus.' in, *Proc Natl Acad Sci U S A*.

Mannion, N., S. M. Greenwood, R. Young, S. Cox, J. Brindle, D. Read, C. Nellåker, C. Vesely, C. Ponting, P. McLaughlin, M. Jantsch, J. Dorin, I. Adams, A. Scadden, M. Öhman, L. Keegan, and M. O'Connell. 2014. 'The RNA-Editing Enzyme ADAR1 Controls Innate Immune Responses to RNA.' in, *Cell Rep*.

Marceau, C. D., A. S. Puschnik, K. Majzoub, Y. S. Ooi, S. M. Brewer, G. Fuchs, K. Swaminathan, M. A. Mata, J. E. Elias, P. Sarnow, and J. E. Carette. 2016. 'Genetic dissection of Flaviviridae host factors through genome-scale CRISPR screens', *Nature*, 535: 159-63.

Marraffini, L. A., and E. J. Sontheimer. 2008. 'CRISPR interference limits horizontal gene transfer in staphylococci by targeting DNA', *Science*, 322: 1843-5.

———. 2010. 'Self versus non-self discrimination during CRISPR RNA-directed immunity', *Nature*, 463: 568-71.

Melcher, T., S. Maas, A. Herb, R. Sprengel, M. Higuchi, and P. H. Seeburg. 1996. 'RED2, a brain-specific member of the RNA-specific adenosine deaminase family', *J Biol Chem*, 271: 31795-8.

Melcher, T., S. Maas, A. Herb, R. Sprengel, P. H. Seeburg, and M. Higuchi. 1996. 'A mammalian RNA editing enzyme', *Nature*, 379: 460-4.

Meylan, E., J. Curran, K. Hofmann, D. Moradpour, M. Binder, R. Bartenschlager, and J. Tschopp. 2005. 'Cardif is an adaptor protein in the RIG-I antiviral pathway and is targeted by hepatitis C virus', *Nature*, 437: 1167-72.

Mibayashi, M., L. Martinez-Sobrido, Y. M. Loo, W. B. Cardenas, M. Gale, Jr., and A. Garcia-Sastre. 2007. 'Inhibition of retinoic acid-inducible gene I-mediated induction of beta interferon by the NS1 protein of influenza A virus', *J Virol*, 81: 514-24.

Nachmani, D., A. Zimmermann, E. Oiknine Djian, Y. Weisblum, Y. Livneh, V. T. Khanh Le, E. Galun, V. Horejsi, O. Isakov, N. Shomron, D. G. Wolf, H. Hengel, and O. Mandelboim. 2014. 'MicroRNA Editing Facilitates Immune Elimination of HCMV Infected Cells.' in, *PLoS Pathog*.

Naka, T., M. Narazaki, M. Hirata, T. Matsumoto, S. Minamoto, A. Aono, N. Nishimoto, T. Kajita, T. Taga, K. Yoshizaki, S. Akira, and T. Kishimoto. 1997. 'Structure and function of a new STAT-induced STAT inhibitor', *Nature*, 387: 924-9.

Nemeroff, M. E., S. M. Barabino, Y. Li, W. Keller, and R. M. Krug. 1998. 'Influenza virus NS1 protein interacts with the cellular 30 kDa subunit of CPSF and inhibits 3'end formation of cellular pre-mRNAs', *Mol Cell*, 1: 991-1000.

Ng, S. K., R. Weissbach, G. E. Ronson, and A. D. J. Scadden. 2013. 'Proteins that contain a functional Z-DNA-binding domain localize to cytoplasmic stress granules.' in, *Nucleic Acids Res*.

Ngamurulert, S., T. Limjindaporn, and P. Auewaraku. 2009. 'Identification of cellular partners of Influenza A virus (H5N1) non-structural protein NS1 by yeast two-hybrid system', *Acta Virol*, 53: 153-9.

Nistal-Villan, E., M. U. Gack, G. Martinez-Delgado, N. P. Maharaj, K. S. Inn, H. Yang, R. Wang, A. K. Aggarwal, J. U. Jung, and A. Garcia-Sastre. 2010. 'Negative role of

RIG-I serine 8 phosphorylation in the regulation of interferon-beta production', *J Biol Chem*, 285: 20252-61.

Noah, D. L., K. Y. Twu, and R. M. Krug. 2003. 'Cellular antiviral responses against influenza A virus are countered at the posttranscriptional level by the viral NS1A protein via its binding to a cellular protein required for the 3' end processing of cellular pre-mRNAS', *Virology*, 307: 386-95.

Okonski, K. M., and C. E. Samuel. 2013. 'Stress granule formation induced by measles virus is protein kinase PKR dependent and impaired by RNA adenosine deaminase ADAR1', *J Virol*, 87: 756-66.

Onomoto, K., M. Jogi, J. S. Yoo, R. Narita, S. Morimoto, A. Takemura, S. Sambhara, A. Kawaguchi, S. Osari, K. Nagata, T. Matsumiya, H. Namiki, M. Yoneyama, and T. Fujita. 2012. 'Critical Role of an Antiviral Stress Granule Containing RIG-I and PKR in Viral Detection and Innate Immunity.' in, *PLoS One*.

Oshiumi, H., M. Matsumoto, S. Hatakeyama, and T. Seya. 2009. 'Riplet/RNF135, a RING finger protein, ubiquitinates RIG-I to promote interferon-beta induction during the early phase of viral infection', *J Biol Chem*, 284: 807-17.

Park, R. J., T. Wang, D. Koundakjian, J. F. Hultquist, P. Lamothe-Molina, B. Monel, K. Schumann, H. Yu, K. M. Krupzcak, W. Garcia-Beltran, A. Piechocka-Trocha, N. J. Krogan, A. Marson, D. M. Sabatini, E. S. Lander, N. Hacohen, and B. D. Walker. 2017. 'A genome-wide CRISPR screen identifies a restricted set of HIV host dependency factors', *Nat Genet*, 49: 193-203.

Patterson, J. B., and C. E. Samuel. 1995. 'Expression and regulation by interferon of a double-stranded-RNA-specific adenosine deaminase from human cells: evidence for two forms of the deaminase', *Mol Cell Biol*, 15: 5376-88.

Patterson, J. B., D. C. Thomis, S. L. Hans, and C. E. Samuel. 1995. 'Mechanism of interferon action: double-stranded RNA-specific adenosine deaminase from human cells is inducible by alpha and gamma interferons', *Virology*, 210: 508-11.

Paz-Yaacov, N., E. Y. Levanon, E. Nevo, Y. Kinar, A. Harmelin, J. Jacob-Hirsch, N. Amariglio, E. Eisenberg, and G. Rechavi. 2010. 'Adenosine-to-inosine RNA editing shapes transcriptome diversity in primates', *Proc Natl Acad Sci U S A*, 107: 12174-9.

Peisley, A., M. H. Jo, C. Lin, B. Wu, M. Orme-Johnson, T. Walz, S. Hohng, and S. Hur. 2012. 'Kinetic mechanism for viral dsRNA length discrimination by MDA5 filaments', *Proc Natl Acad Sci U S A*, 109: E3340-9.

Pestal, K., C. C. Funk, J. M. Snyder, N. D. Price, P. M. Treuting, and D. B. Stetson. 2015. 'Isoforms of RNA-Editing Enzyme ADAR1 Independently Control Nucleic

Acid Sensor MDA5-Driven Autoimmunity and Multi-organ Development', *Immunity*, 43: 933-44.

Pfaller, C. K., R. C. Donohue, S. Nersisyan, L. Brodsky, and R. Cattaneo. 2018. 'Extensive editing of cellular and viral double-stranded RNA structures accounts for innate immunity suppression and the proviral activity of ADAR1p150', *PLoS Biol*, 16: e2006577.

Pichlmair, A., O. Schulz, C. P. Tan, T. I. Naslund, P. Liljestrom, F. Weber, and C. Reis e Sousa. 2006. 'RIG-I-mediated antiviral responses to single-stranded RNA bearing 5'-phosphates', *Science*, 314: 997-1001.

Pichlmair, A., O. Schulz, C. P. Tan, J. Rehwinkel, H. Kato, O. Takeuchi, S. Akira, M. Way, G. Schiavo, and C. Reis e Sousa. 2009. 'Activation of MDA5 requires higher-order RNA structures generated during virus infection', *J Virol*, 83: 10761-9.

Piganis, R. A., N. A. De Weerd, J. A. Gould, C. W. Schindler, A. Mansell, S. E. Nicholson, and P. J. Hertzog. 2011. 'Suppressor of cytokine signaling (SOCS) 1 inhibits type I interferon (IFN) signaling via the interferon alpha receptor (IFNAR1)-associated tyrosine kinase Tyk2', *J Biol Chem*, 286: 33811-8.

Poulsen, H., J. Nilsson, C. K. Damgaard, J. Egebjerg, and J. Kjems. 2001. 'CRM1 mediates the export of ADAR1 through a nuclear export signal within the Z-DNA binding domain', *Mol Cell Biol*, 21: 7862-71.

Pujantell, M., E. Riveira-Munoz, R. Badia, M. Castellvi, E. Garcia-Vidal, G. Sirera, T. Puig, C. Ramirez, B. Clotet, J. A. Este, and E. Ballana. 2017. 'RNA editing by ADAR1 regulates innate and antiviral immune functions in primary macrophages', *Sci Rep*, 7: 13339.

Qiu, W., X. Wang, M. Buchanan, K. He, R. Sharma, L. Zhang, Q. Wang, and J. Yu. 2013. 'ADAR1 is essential for intestinal homeostasis and stem cell maintenance.' in, *Cell Death Dis*.

Rajsbaum, R., R. A. Albrecht, M. K. Wang, N. P. Maharaj, G. A. Versteeg, E. Nistal-Villán, A. García-Sastre, and M. U. Gack. 2012. 'Species-Specific Inhibition of RIG-I Ubiquitination and IFN Induction by the Influenza A Virus NS1 Protein.' in, *PLoS Pathog*.

Ramaswami, G., W. Lin, R. Piskol, M. H. Tan, C. Davis, and J. B. Li. 2012. 'Accurate identification of human Alu and non-Alu RNA editing sites', *Nat Methods*, 9: 579-81.

Ran, F. A., P. D. Hsu, J. Wright, V. Agarwala, D. A. Scott, and F. Zhang. 2013. 'Genome engineering using the CRISPR-Cas9 system', *Nat Protoc*, 8: 2281-308.

Reading, P. C., A. Khanna, and G. L. Smith. 2002. 'Vaccinia virus CrmE encodes a soluble and cell surface tumor necrosis factor receptor that contributes to virus virulence', *Virology*, 292: 285-98.

Rebagliati, M. R., and D. A. Melton. 1987. 'Antisense RNA injections in fertilized frog eggs reveal an RNA duplex unwinding activity', *Cell*, 48: 599-605.

Rehwinkel, J., and M. U. Gack. 2020. 'RIG-I-like receptors: their regulation and roles in RNA sensing', *Nat Rev Immunol*.

Rice, G. I., G. M. Forte, M. Szynkiewicz, D. S. Chase, A. Aeby, M. S. Abdel-Hamid, S. Ackroyd, R. Allcock, K. M. Bailey, U. Balottin, C. Barnerias, G. Bernard, C. Bodemer, M. P. Botella, C. Cereda, K. E. Chandler, L. Dabydeen, R. C. Dale, C. De Laet, C. G. De Goede, M. Del Toro, L. Effat, N. N. Enamorado, E. Fazzi, B. Gener, M. Haldre, J. P. Lin, J. H. Livingston, C. M. Lourenco, W. Marques, Jr., P. Oades, P. Peterson, M. Rasmussen, A. Roubertie, J. L. Schmidt, S. A. Shalev, R. Simon, R. Spiegel, K. J. Swoboda, S. A. Temtamy, G. Vassallo, C. N. Vilain, J. Vogt, V. Wermenbol, W. P. Whitehouse, D. Soler, I. Olivieri, S. Orcesi, M. S. Aglan, M. S. Zaki, G. M. Abdel-Salam, A. Vanderver, K. Kisand, F. Rozenberg, P. Lebon, and Y. J. Crow. 2013. 'Assessment of interferon-related biomarkers in Aicardi-Goutieres syndrome associated with mutations in TREX1, RNASEH2A, RNASEH2B, RNASEH2C, SAMHD1, and ADAR: a case-control study', *Lancet Neurol*, 12: 1159-69.

Rice, G. I., P. R. Kasher, G. M. Forte, N. M. Mannion, S. M. Greenwood, M. Szynkiewicz, J. E. Dickerson, S. S. Bhaskar, M. Zampini, T. A. Briggs, E. M. Jenkinson, C. A. Bacino, R. Battini, E. Bertini, P. A. Brogan, L. A. Brueton, M. Carpanelli, C. De Laet, P. de Lonlay, M. del Toro, I. Desguerre, E. Fazzi, A. Garcia-Cazorla, A. Heiberg, M. Kawaguchi, R. Kumar, J. P. Lin, C. M. Lourenco, A. M. Male, W. Marques, Jr., C. Mignot, I. Olivieri, S. Orcesi, P. Prabhakar, M. Rasmussen, R. A. Robinson, F. Rozenberg, J. L. Schmidt, K. Steindl, T. Y. Tan, W. G. van der Merwe, A. Vanderver, G. Vassallo, E. L. Wakeling, E. Wassmer, E. Whittaker, J. H. Livingston, P. Lebon, T. Suzuki, P. J. McLaughlin, L. P. Keegan, M. A. O'Connell, S. C. Lovell, and Y. J. Crow. 2012. 'Mutations in ADAR1 cause Aicardi-Goutieres syndrome associated with a type I interferon signature', *Nat Genet*, 44: 1243-8.

Riedl, W., D. Acharya, J. H. Lee, G. Liu, T. Serman, C. Chiang, Y. K. Chan, M. S. Diamond, and M. U. Gack. 2019. 'Zika Virus NS3 Mimics a Cellular 14-3-3-Binding Motif to Antagonize RIG-I- and MDA5-Mediated Innate Immunity', *Cell Host Microbe*, 26: 493-503.e6.

Rongvaux, A., R. Jackson, C. C. Harman, T. Li, A. P. West, M. R. de Zoete, Y. Wu, B. Yordy, S. A. Lakhani, C. Y. Kuan, T. Taniguchi, G. S. Shadel, Z. J. Chen, A.

Iwasaki, and R. A. Flavell. 2014. 'Apoptotic caspases prevent the induction of type I interferons by mitochondrial DNA', *Cell*, 159: 1563-77.

Rothenburg, S., T. Schwartz, F. Koch-Nolte, and F. Haag. 2002. 'Complex regulation of the human gene for the Z-DNA binding protein DLM-1.' in, *Nucleic Acids Res*.

Samuel, C. E. 2011. 'Adenosine deaminases acting on RNA (ADARs) are both antiviral and proviral', *Virology*, 411: 180-93.

Sanjana, N. E., O. Shalem, and F. Zhang. 2014. 'Improved vectors and genome-wide libraries for CRISPR screening', *Nat Methods*, 11: 783-84.

Sapranauskas, R., G. Gasiunas, C. Fremaux, R. Barrangou, P. Horvath, and V. Siksnys. 2011. 'The Streptococcus thermophilus CRISPR/Cas system provides immunity in Escherichia coli', *Nucleic Acids Res*, 39: 9275-82.

Sasaki, A., H. Yasukawa, A. Suzuki, S. Kamizono, T. Syoda, I. Kinjyo, M. Sasaki, J. A. Johnston, and A. Yoshimura. 1999. 'Cytokine-inducible SH2 protein-3 (CIS3/SOCS3) inhibits Janus tyrosine kinase by binding through the N-terminal kinase inhibitory region as well as SH2 domain', *Genes Cells*, 4: 339-51.

Savidis, G., W. M. McDougall, P. Meraner, J. M. Perreira, J. M. Portmann, G. Trincucci, S. P. John, A. M. Aker, N. Renzette, D. R. Robbins, Z. Guo, S. Green, T. F. Kowalik, and A. L. Brass. 2016. 'Identification of Zika Virus and Dengue Virus Dependency Factors using Functional Genomics', *Cell Rep*, 16: 232-46.

Sborgi, L., S. Ruhl, E. Mulvihill, J. Pipercevic, R. Heilig, H. Stahlberg, C. J. Farady, D. J. Muller, P. Broz, and S. Hiller. 2016. 'GSDMD membrane pore formation constitutes the mechanism of pyroptotic cell death', *Embo j*, 35: 1766-78.

Schlee, M., A. Roth, V. Hornung, C. A. Hagmann, V. Wimmenauer, W. Barchet, C. Coch, M. Janke, A. Mihailovic, G. Wardle, S. Juranek, H. Kato, T. Kawai, H. Poeck, K. A. Fitzgerald, O. Takeuchi, S. Akira, T. Tuschl, E. Latz, J. Ludwig, and G. Hartmann. 2009. 'Recognition of 5' triphosphate by RIG-I helicase requires short blunt double-stranded RNA as contained in panhandle of negative-strand virus', *Immunity*, 31: 25-34.

Schmidt, A., T. Schwerd, W. Hamm, J. C. Hellmuth, S. Cui, M. Wenzel, F. S. Hoffmann, M. C. Michallet, R. Besch, K. P. Hopfner, S. Endres, and S. Rothenfusser. 2009. '5'-triphosphate RNA requires base-paired structures to activate antiviral signaling via RIG-I', *Proc Natl Acad Sci U S A*, 106: 12067-72.

Schneider, W. M., M. D. Chevillotte, and C. M. Rice. 2014. 'Interferon-stimulated genes: a complex web of host defenses', *Annu Rev Immunol*, 32: 513-45.

Schuberth-Wagner, C., J. Ludwig, A. K. Bruder, A. M. Herzner, T. Zillinger, M. Goldeck, T. Schmidt, J. L. Schmid-Burgk, R. Kerber, S. Wolter, J. P. Stumpel, A. Roth, E. Bartok, C. Drosten, C. Coch, V. Hornung, W. Barchet, B. M. Kummerer, G. Hartmann, and M. Schlee. 2015. 'A Conserved Histidine in the RNA Sensor RIG-I Controls Immune Tolerance to N1-2'O-Methylated Self RNA', *Immunity*, 43: 41-51.

Schultz-Cherry, S., N. Dybdahl-Sissoko, G. Neumann, Y. Kawaoka, and V. S. Hinshaw. 2001. 'Influenza virus ns1 protein induces apoptosis in cultured cells', *J Virol*, 75: 7875-81.

Seth, R. B., L. Sun, C. K. Ea, and Z. J. Chen. 2005. 'Identification and characterization of MAVS, a mitochondrial antiviral signaling protein that activates NF-kappaB and IRF 3', *Cell*, 122: 669-82.

Shin, Y. K., Q. Liu, S. K. Tikoo, L. A. Babiuk, and Y. Zhou. 2007. 'Influenza A virus NS1 protein activates the phosphatidylinositol 3-kinase (PI3K)/Akt pathway by direct interaction with the p85 subunit of PI3K', *J Gen Virol*, 88: 13-8.

Slee, E. A., C. Adrain, and S. J. Martin. 2001. 'Executioner caspase-3, -6, and -7 perform distinct, non-redundant roles during the demolition phase of apoptosis', *J Biol Chem*, 276: 7320-6.

Stojdl, D. F., B. D. Lichty, B. R. tenOever, J. M. Paterson, A. T. Power, S. Knowles, R. Marius, J. Reynard, L. Poliquin, H. Atkins, E. G. Brown, R. K. Durbin, J. E. Durbin, J. Hiscott, and J. C. Bell. 2003. 'VSV strains with defects in their ability to shutdown innate immunity are potent systemic anti-cancer agents', *Cancer Cell*, 4: 263-75.

Sun, L., J. Wu, F. Du, X. Chen, and Z. J. Chen. 2013. 'Cyclic GMP-AMP synthase is a cytosolic DNA sensor that activates the type I interferon pathway', *Science*, 339: 786-91.

Sun, Z., H. Ren, Y. Liu, J. L. Teeling, and J. Gu. 2011. 'Phosphorylation of RIG-I by casein kinase II inhibits its antiviral response', *J Virol*, 85: 1036-47.

Suspène, R., V. Petit, D. Puyraimond-Zemmour, M. M. Aynaud, M. Henry, D. Guétard, C. Rusniok, S. Wain-Hobson, and J. P. Vartanian. 2011. 'Double-Stranded RNA Adenosine Deaminase ADAR-1-Induced Hypermutated Genomes among Inactivated Seasonal Influenza and Live Attenuated Measles Virus Vaccines ▿ .' in, *J Virol*.

Suspene, R., M. Renard, M. Henry, D. Guetard, D. Puyraimond-Zemmour, A. Billecocq, M. Bouloy, F. Tangy, J. P. Vartanian, and S. Wain-Hobson. 2008. 'Inversing the natural hydrogen bonding rule to selectively amplify GC-rich ADAR-edited RNAs', *Nucleic Acids Res*, 36: e72.

Takashima, K., H. Oshiumi, H. Takaki, M. Matsumoto, and T. Seya. 2015. 'RIOK3-mediated phosphorylation of MDA5 interferes with its assembly and attenuates the innate immune response', *Cell Rep*, 11: 192-200.

Tan, Y. X., T. H. P. Tan, M. J. R. Lee, P. Y. Tham, V. Gunalan, J. Druce, C. Birch, M. Catton, N. Y. Fu, V. C. Yu, and Y. J. Tan. 2007. 'Induction of Apoptosis by the Severe Acute Respiratory Syndrome Coronavirus 7a Protein Is Dependent on Its Interaction with the Bcl-XL Protein ▿.' in, *J Virol*.

Taylor, D. R., M. Puig, M. E. Darnell, K. Mihalik, and S. M. Feinstone. 2005. 'New antiviral pathway that mediates hepatitis C virus replicon interferon sensitivity through ADAR1', *J Virol*, 79: 6291-8.

Thapa, R. J., J. P. Ingram, K. B. Ragan, S. Nogusa, D. F. Boyd, A. A. Benitez, H. Sridharan, R. Kosoff, M. Shubina, V. J. Landsteiner, M. Andrake, P. Vogel, L. J. Sigal, B. R. tenOever, P. G. Thomas, J. W. Upton, and S. Balachandran. 2016. 'DAI Senses Influenza A Virus Genomic RNA and Activates RIPK3-Dependent Cell Death', *Cell Host Microbe*, 20: 674-81.

Tokunaga, F., T. Nakagawa, M. Nakahara, Y. Saeki, M. Taniguchi, S. Sakata, K. Tanaka, H. Nakano, and K. Iwai. 2011. 'SHARPIN is a component of the NF-kappaB-activating linear ubiquitin chain assembly complex', *Nature*, 471: 633-6.

Tokunaga, F., S. Sakata, Y. Saeki, Y. Satomi, T. Kirisako, K. Kamei, T. Nakagawa, M. Kato, S. Murata, S. Yamaoka, M. Yamamoto, S. Akira, T. Takao, K. Tanaka, and K. Iwai. 2009. 'Involvement of linear polyubiquitylation of NEMO in NF-kappaB activation', *Nat Cell Biol*, 11: 123-32.

Toth, A. M., Z. Li, R. Cattaneo, and C. E. Samuel. 2009. 'RNA-specific Adenosine Deaminase ADAR1 Suppresses Measles Virus-induced Apoptosis and Activation of Protein Kinase PKR*.' in, *J Biol Chem*.

Trengove, M. C., and A. C. Ward. 2013. 'SOCS proteins in development and disease', *Am J Clin Exp Immunol*, 2: 1-29.

Twu, K. Y., D. L. Noah, P. Rao, R. L. Kuo, and R. M. Krug. 2006. 'The CPSF30 Binding Site on the NS1A Protein of Influenza A Virus Is a Potential Antiviral Target.' in, *J Virol*.

Unterholzner, L., S. E. Keating, M. Baran, K. A. Horan, S. B. Jensen, S. Sharma, C. M. Sirois, T. Jin, T. Xiao, K. A. Fitzgerald, S. R. Paludan, and A. G. Bowie. 2010. 'IFI16 is an innate immune sensor for intracellular DNA', *Nat Immunol*, 11: 997-1004.

Valente, L., and K. Nishikura. 2007. 'RNA binding-independent dimerization of adenosine deaminases acting on RNA and dominant negative effects of nonfunctional subunits on dimer functions', *J Biol Chem*, 282: 16054-61.

Vitali, P., and A. D. Scadden. 2010. 'Double-stranded RNAs containing multiple IU pairs are sufficient to suppress interferon induction and apoptosis', *Nat Struct Mol Biol*, 17: 1043-50.

Wagner, R. W., J. E. Smith, B. S. Cooperman, and K. Nishikura. 1989. 'A double-stranded RNA unwinding activity introduces structural alterations by means of adenosine to inosine conversions in mammalian cells and Xenopus eggs', *Proc Natl Acad Sci U S A*, 86: 2647-51.

Walkley, C. R., and B. T. Kile. 2019. 'Cell death following the loss of ADAR1 mediated A-to-I RNA editing is not effected by the intrinsic apoptosis pathway', *Cell Death Dis*, 10: 913.

Wang, H., L. Sun, L. Su, J. Rizo, L. Liu, L. F. Wang, F. S. Wang, and X. Wang. 2014. 'Mixed lineage kinase domain-like protein MLKL causes necrotic membrane disruption upon phosphorylation by RIP3', *Mol Cell*, 54: 133-46.

Wang, H., G. Wang, L. Zhang, J. Zhang, Q. Wang, and T. R. Billiar. 2016. 'ADAR1 Suppresses the Activation of Cytosolic RNA-Sensing Signaling Pathways to Protect the Liver from Ischemia/Reperfusion Injury', *Sci Rep*, 6: 20248.

Wang, W., M. Jiang, S. Liu, S. Zhang, W. Liu, Y. Ma, L. Zhang, J. Zhang, and X. Cao. 2016. 'RNF122 suppresses antiviral type I interferon production by targeting RIG-I CARDs to mediate RIG-I degradation', *Proc Natl Acad Sci U S A*, 113: 9581-6.

Wang, Y., W. Gao, X. Shi, J. Ding, W. Liu, H. He, K. Wang, and F. Shao. 2017. 'Chemotherapy drugs induce pyroptosis through caspase-3 cleavage of a gasdermin', *Nature*, 547: 99-103.

Wang, Y., and C. E. Samuel. 2009. 'Adenosine deaminase ADAR1 increases gene expression at the translational level by decreasing protein kinase PKR-dependent eIF-2alpha phosphorylation', *J Mol Biol*, 393: 777-87.

Ward, S. V., C. X. George, M. J. Welch, L. Y. Liou, B. Hahm, H. Lewicki, J. C. de la Torre, C. E. Samuel, and M. B. Oldstone. 2011. 'RNA editing enzyme adenosine deaminase is a restriction factor for controlling measles virus replication that also is required for embryogenesis', *Proc Natl Acad Sci U S A*, 108: 331-6.

White, M. J., K. McArthur, D. Metcalf, R. M. Lane, J. C. Cambier, M. J. Herold, M. F. van Delft, S. Bedoui, G. Lessene, M. E. Ritchie, D. C. Huang, and B. T. Kile. 2014. 'Apoptotic caspases suppress mtDNA-induced STING-mediated type I IFN production', *Cell*, 159: 1549-62.

Wies, E., M. K. Wang, N. P. Maharaj, K. Chen, S. Zhou, R. W. Finberg, and M. U. Gack. 2013. 'Dephosphorylation of the RNA sensors RIG-I and MDA5 by the phosphatase PP1 is essential for innate immune signaling', *Immunity*, 38: 437-49.

Wong, S. K., and D. W. Lazinski. 2002. 'Replicating hepatitis delta virus RNA is edited in the nucleus by the small form of ADAR1', *Proc Natl Acad Sci U S A*, 99: 15118-23.

Wu, B., A. Peisley, C. Richards, H. Yao, X. Zeng, C. Lin, F. Chu, T. Walz, and S. Hur. 2013. 'Structural basis for dsRNA recognition, filament formation, and antiviral signal activation by MDA5', *Cell*, 152: 276-89.

Wu, J., L. Sun, X. Chen, F. Du, H. Shi, C. Chen, and Z. J. Chen. 2013. 'Cyclic GMP-AMP is an endogenous second messenger in innate immune signaling by cytosolic DNA', *Science*, 339: 826-30.

Xu, L. G., Y. Y. Wang, K. J. Han, L. Y. Li, Z. Zhai, and H. B. Shu. 2005. 'VISA is an adapter protein required for virus-triggered IFN-beta signaling', *Mol Cell*, 19: 727-40.

Yang, S., P. Deng, Z. Zhu, J. Zhu, G. Wang, L. Zhang, A. F. Chen, T. Wang, S. N. Sarkar, T. R. Billiar, and Q. Wang. 2014. 'Adenosine deaminase acting on RNA 1 limits RIG-I RNA detection and suppresses IFN production responding to viral and endogenous RNAs', *J Immunol*, 193: 3436-45.

Yang, W., T. P. Chendrimada, Q. Wang, M. Higuchi, P. H. Seeburg, R. Shiekhattar, and K. Nishikura. 2006. 'Modulation of microRNA processing and expression through RNA editing by ADAR deaminases', *Nat Struct Mol Biol*, 13: 13-21.

Yasukawa, H., H. Misawa, H. Sakamoto, M. Masuhara, A. Sasaki, T. Wakioka, S. Ohtsuka, T. Imaizumi, T. Matsuda, J. N. Ihle, and A. Yoshimura. 1999. 'The JAK-binding protein JAB inhibits Janus tyrosine kinase activity through binding in the activation loop', *Embo j*, 18: 1309-20.

Zhang, H., D. Wang, H. Zhong, R. Luo, M. Shang, D. Liu, H. Chen, L. Fang, and S. Xiao. 2015. 'Ubiquitin-specific Protease 15 Negatively Regulates Virus-induced Type I Interferon Signaling via Catalytically-dependent and -independent Mechanisms', *Sci Rep*, 5: 11220.

Zhang, J. G., A. Farley, S. E. Nicholson, T. A. Willson, L. M. Zugaro, R. J. Simpson, R. L. Moritz, D. Cary, R. Richardson, G. Hausmann, B. T. Kile, S. B. Kent, W. S. Alexander, D. Metcalf, D. J. Hilton, N. A. Nicola, and M. Baca. 1999. 'The conserved SOCS box motif in suppressors of cytokine signaling binds to elongins

B and C and may couple bound proteins to proteasomal degradation', *Proc Natl Acad Sci U S A*, 96: 2071-6.

Zhirnov, O. P., and H. D. Klenk. 2007. 'Control of apoptosis in influenza virus-infected cells by up-regulation of Akt and p53 signaling', *Apoptosis*, 12: 1419-32.

Zhirnov, O. P., T. E. Konakova, T. Wolff, and H. D. Klenk. 2002. 'NS1 protein of influenza A virus down-regulates apoptosis', *J Virol*, 76: 1617-25.

Zipeto, M. A., A. C. Court, A. Sadarangani, N. P. Delos Santos, L. Balaian, H. J. Chun, G. Pineda, S. R. Morris, C. N. Mason, I. Geron, C. Barrett, D. J. Goff, R. Wall, M. Pellecchia, M. Minden, K. A. Frazer, M. A. Marra, L. A. Crews, Q. Jiang, and C. H. M. Jamieson. 2016. 'ADAR1 Activation Drives Leukemia Stem Cell Self-Renewal by Impairing Let-7 Biogenesis', *Cell Stem Cell*, 19: 177-91.

APPENDIX A

Figures

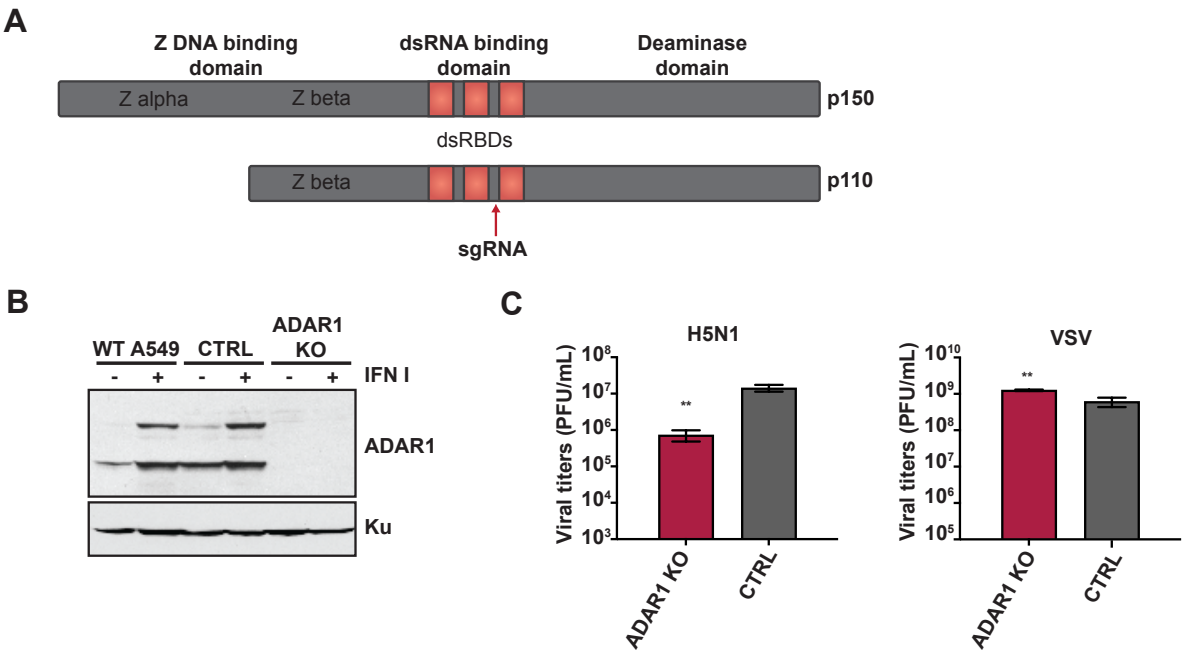

Figure III.1. ADAR1 is an important host factor for IAV replication.
(A) Schematic representation of the p110 and p150 isoforms of ADAR1, including the functional domains in each isoform. The red arrow upstream of the third dsRNA binding domain indicates the region targeted by the sgRNA in ADAR1. (B) Western blot analysis of ADAR1 expression in ADAR1 KO and control cells. ADAR1 KO, CTRL, and WT A549s were mock treated or treated with IFN for 24 hours and expression of ADAR1 was examined by western blot. Expression of Ku is shown as a loading control. (C) IAV replication in ADAR1 KOs. ADAR1 KOs and CTRL A549s were infected with H5N1 (MOI = 0.001) or VSV (MOI = 0.001) and viral titers were measured at 48 hours. Data are represented as mean titer of triplicate samples ± SD. * denotes p-value ≤ 0.5. ** denotes p-value ≤ 0.01. *** denotes p-value ≤ 0.001. NS denotes p-value ≥ 0.05. Data are representative of at least three independent experiments. See also Figure III.2.

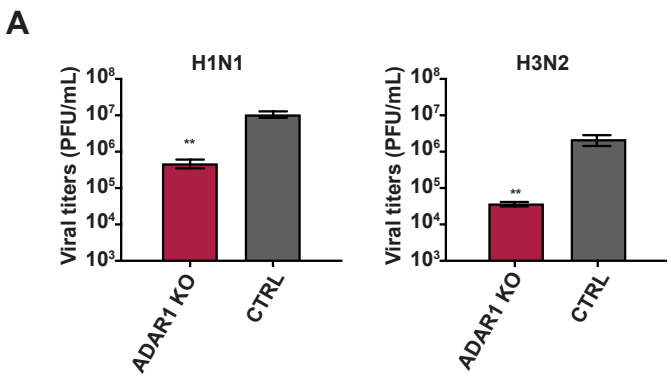

Figure III.2. IAV strains replicate poorly in ADAR1 KOs
(A) ADAR1 KOs and CTRL A549s were infected with H1N1 (MOI = 0.01) and H3N2 (MOI = 0.01). Viral titers were measured at 48 hours. Data are represented as mean titer of triplicate samples ± SD. * denotes p-value ≤ 0.5. ** denotes p-value ≤ 0.01. *** denotes p-value ≤ 0.001. NS denotes p-value ≥ 0.05. Data are representative of at least three independent experiments.

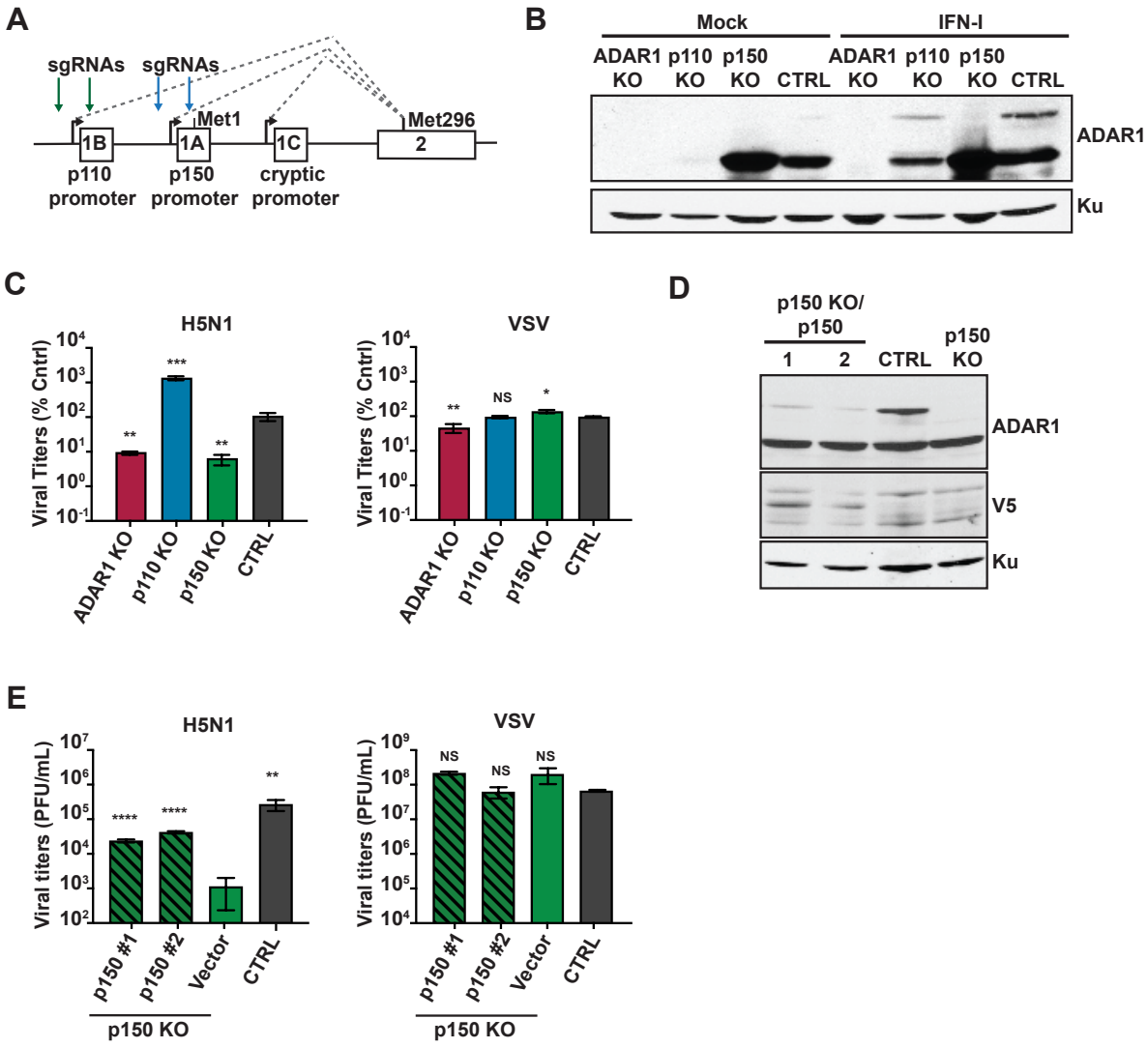

Figure III.3. The p150 isoform of ADAR1 is critical for IAV replication
(A) Schematic representation of the promoters for the p110 and p150 isoforms of ADAR1. The promoter for p110 is upstream of exon 1B and the start methionine for p110 is within exon 2. The promoter for p150 is upstream of exon 1A and the start methionine for p150 is within exon 1A. The green arrows depict the sgRNA target sites for p110 KO and the blue arrows depict the sgRNA target sites for p150 KO. (B) Western blot analysis of ADAR1 expression in isoform specific KO A549s. ADAR1 KO, p110 KOs, p150 KOs, and CTRL A549s were mock treated or treated with IFN for 24 hours and ADAR1 expression was examined by western blot. Expression of Ku is shown as a loading control. (C) IAV replication in isoform specific KO A549s. ADAR1 KOs, p110 KOs, p150 KOs, and CTRL A549s were infected with H5N1 (MOI = 0.001) or VSV (MOI = 0.001) and viral titers were measured at 48 hours. (D) Western blot analysis of V5 tagged p150 in complemented p150 KO A549s. Two clones of p150 complements p150 KO (p150KO/p150 #1, #2), p150 KO/Vector and CTRL A549s were analyzed for expression of ADAR1 and V5 by western blot. Expression of Ku is shown as a loading control. (E) IAV replication in p150 KO/p150#1, p150 KO/p150#2, p150

Figure III.3, continued. KO/Vector, and CTRL A549s were infected with H5N1 (MOI = 0.001) and VSV (MOI = 0.001) and viral titers were measured at 48 hours. Data are represented as mean titer of triplicate samples ± SD. * denotes p-value ≤ 0.5. ** denotes p-value ≤ 0.01. *** denotes p-value ≤ 0.001. NS denotes p-value ≥ 0.05. Data are representative of at least three independent experiments. See also Figure III.4.

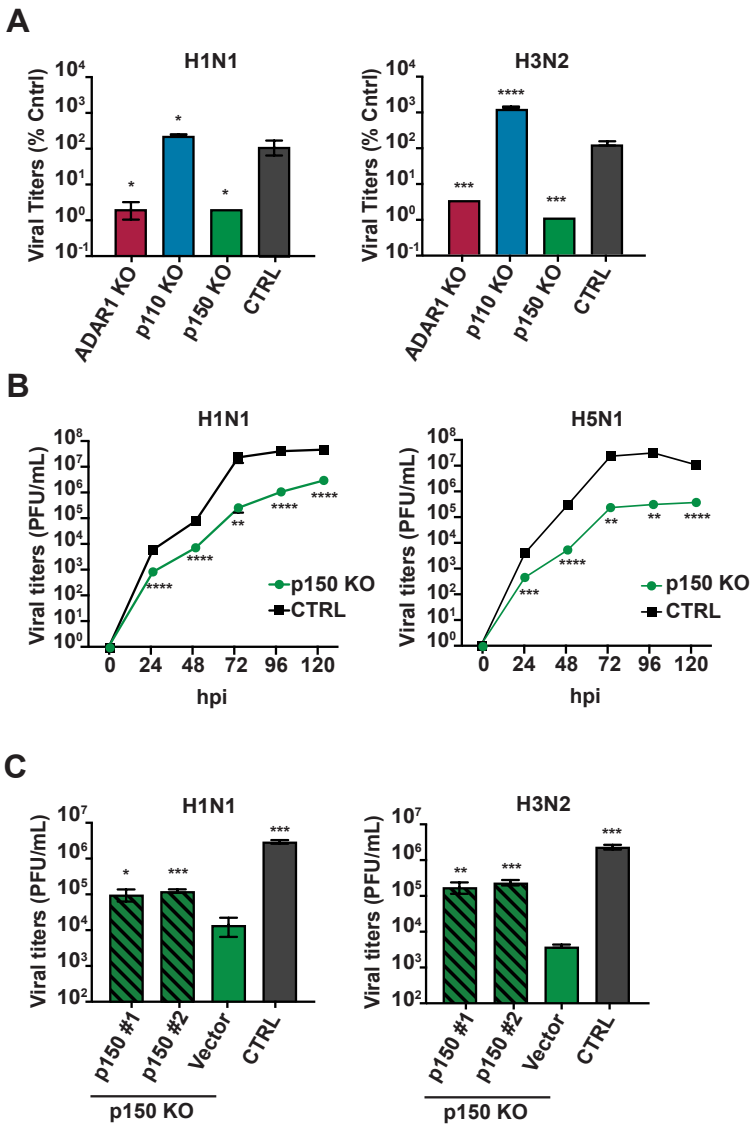

Figure III.4. The p150 isoform of ADAR1 is critical for IAV replication.
(A) Assessment of viral replication in various KO cells lacking ADAR1 isoforms. ADAR1 KOs, isoform specific KOs, and CTRL A549s were infected with H1N1 (MOI = 0.01) and H3N2 (MOI = 0.01) and viral titers were measured at 48 hpi. (B) p150 KOs and CTRL A549s were infected with H1N1 (MOI = 0.01) and H5N1 (MOI = 0.001) and viral titers were measured at the indicated times post infection. (C) Two clones of p150 KOs complemented with wildtype p150, empty vector p150 KOs, and CTRL A549s were infected with H1N1 (MOI = 0.01) and H3N2 (MOI = 0.01) and viral titers were measured at 48 hpi. Data are represented as mean titer of triplicate samples ± SD. * denotes p-value ≤ 0.5. ** denotes p-value ≤ 0.01. *** denotes p-value ≤ 0.001. NS denotes p-value ≥ 0.05. Data are representative of at least three independent experiments.

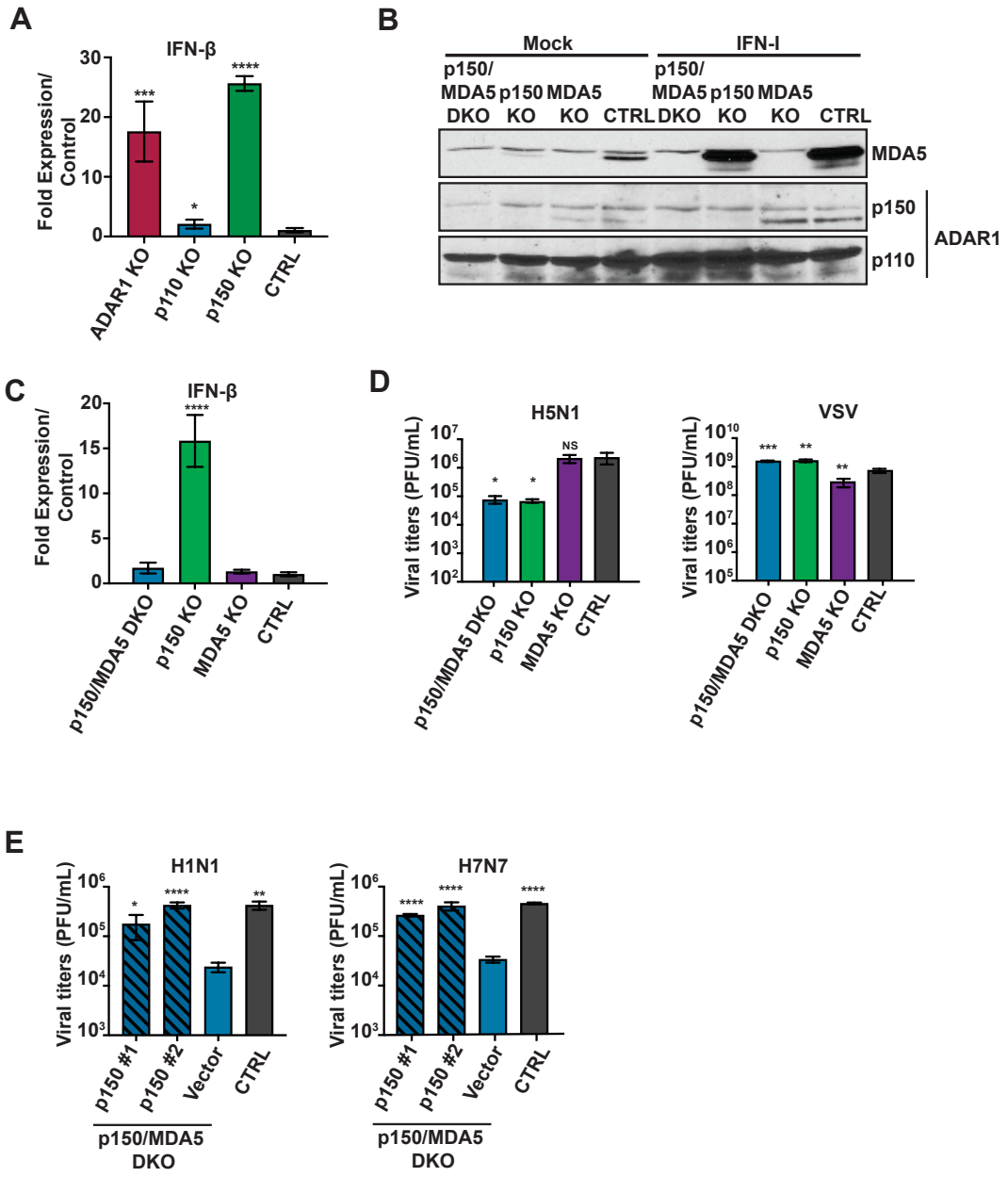

Figure III.5. p150 supports IAV replication independent of MDA5 suppression. (A) qRT-PCR analysis of basal IFN-β expression in ADAR1 KOs, isoform specific KOs, and CTRL A549s. Data are represented as fold expression relative to vector control A549s. (B) Western blot analysis of MDA5 and ADAR1 isoforms in various KOs. p150/MDA5 DKOs, p150 KOs, MDA5 KOs, and CTRL A549s were mock treated or treated with IFN for 24 hours. ADAR1 and MDA5 expression were examined by western blot. (C) qRT-PCR analysis of basal IFN-β expression in p150/MDA5 DKOs. Data are represented as fold expression relative to CTRL A549s. (D) IAV replication in p150/MDA5 DKOs. p150/MDA5 DKOs, p150 KOs, MDA5 KOs, and CTRL A549s were infected with H5N1 (MOI = 0.001) and VSV (MOI = 0.001) and viral titers were measured at 48 hours. Data are represented as mean titer of triplicate samples ± SD. (E) IAV replication in p150/MDA5 DKOs expressing wild-type V5-tagged p150. Two

Figure III.5, continued. clones of p150/MDA5 DKOs complemented with wildtype p150 were infected with H1N1 (MOI = 0.01) and H7N7 (MOI = 0.01). p150/MDA5 DKOs that have been transduced with empty vector and CTRL A549s were also infected. Viral titers were measured at 72 hours. Data are represented as mean titer of triplicate samples $\pm$ SD. * denotes p-value $\leq$ 0.5. ** denotes p-value $\leq$ 0.01. *** denotes p-value $\leq$ 0.001. NS denotes p-value $\geq$ 0.05. Data are representative of at least three independent experiments. See also III.6.

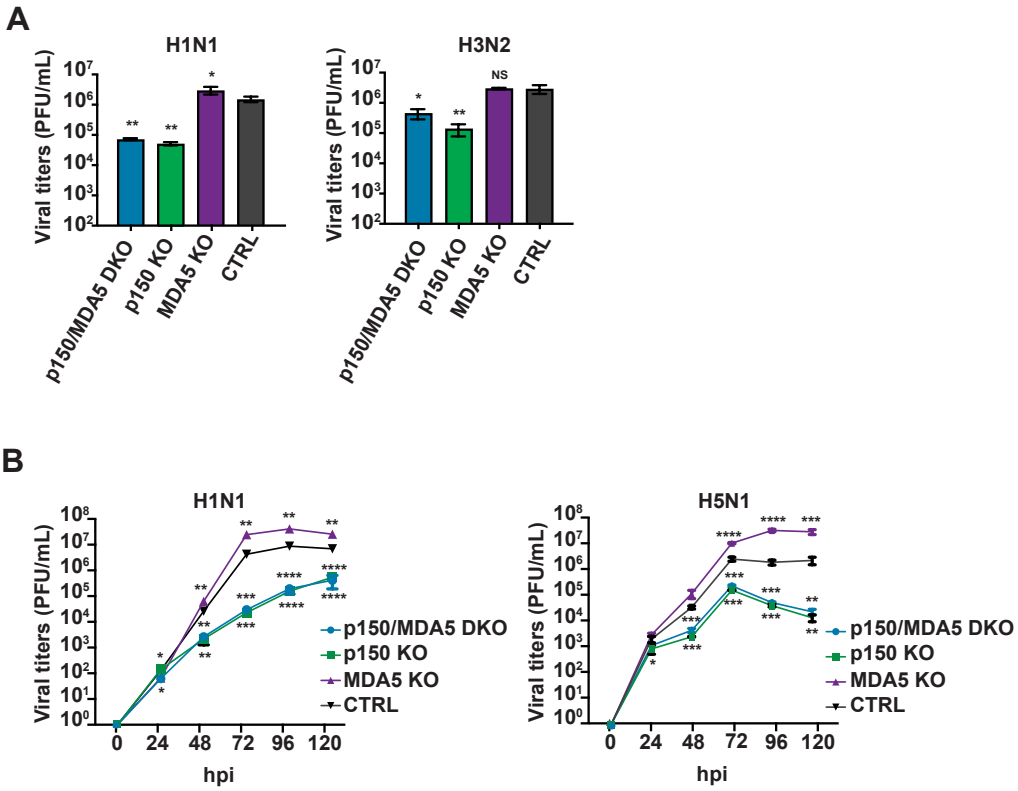

Figure III.6. p150 enhances IAV replication independent of its ability to suppress MDA5

(A) Assessment of viral replication in various KOs. p150/MDA5 DKOs, p150 KOs, MDA5 KOs, and CTRL A549s were infected with H1N1 (MOI = 0.01) and H3N2 (MOI = 0.01). Viral titers were measured at 48 hours. (B) Viral replication kinetics in various KOs. p150/MDA5 DKOs, p150 KOs, MDA5 KOs, and CTRL A549s were infected with H1N1 (MOI = 0.01) and H3N2 (MOI = 0.01). Viral titers were measured at the indicated time points post infection. Data are represented as mean titer of triplicate samples ± SD. * denotes p-value ≤ 0.5. ** denotes p-value ≤ 0.01. *** denotes p-value ≤ 0.001. NS denotes p-value ≥ 0.05. Data are representative of at least three independent experiments.

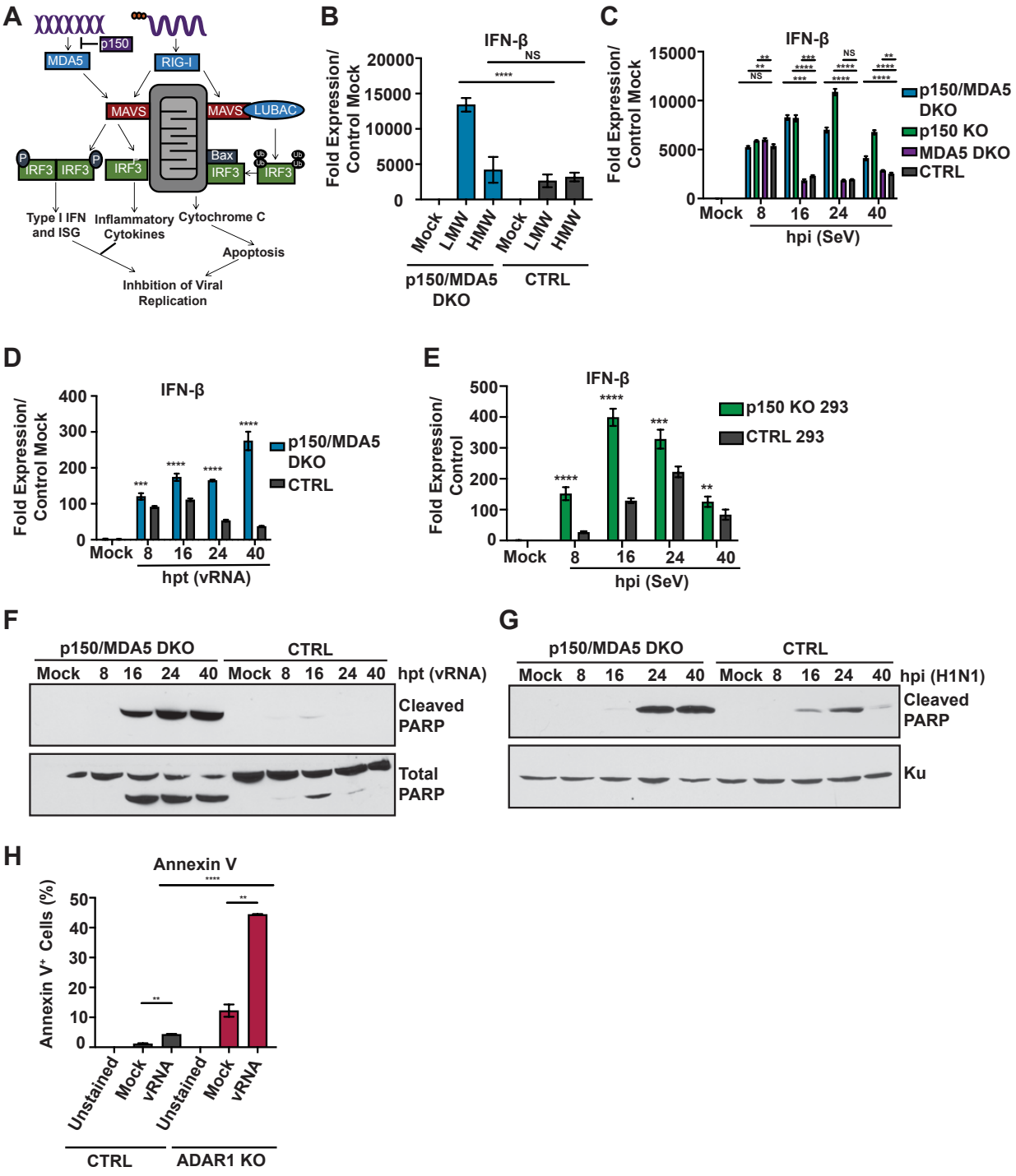

Figure III.7. p150/MDA5 DKO A549s show elevated IFN-β expression and increased apoptosis upon RLR stimulation

(A) Schematic representation of the RLR-Induced IRF3-mediated Pathway of Apoptosis (RIPA) and IRF3 mediated transcriptional upregulation of antiviral genes. (B) qRT-PCR analysis of IFN-β expression in p150/MDA5 DKOs after poly I:C stimulation. p150/MDA5 DKOs and CTRL A549s were transfected with LWM and HMW pI:C for 24 hours and IFN-b expression was analyzed by qRT-PCR analysis. Data are represented

Figure III.7, continued. as fold expression relative to mock transfected CTRL A549s. (C) qRT-PCR analysis of IFN-β expression in p150/MDA5 DKOs following Sendai virus (SeV). p150/MDA5 DKOs, p150 KOs, MDA5 KOs, and CTRL A549s were infected with SeV and mRNA levels were measured at the indicated hours post infection. Data are represented as fold expression relative to mock vector control. (D) qRT-PCR analysis of IFN-β expression in p150/MDA5 DKOs following H1N1 vRNA transfection. p150/MDA5 DKOs and CTRL A549s were transfected with H1N1 vRNA and mRNA levels were measured at the indicated hours post transfection (hpt). (E) qRT-PCR analysis of IFN-β expression in p150 KO and vector control 293s. p150 KO and vector control 293s were infected with SeV and mRNA levels were measured at the indicated hours post infection (hpi). Data are represented as fold expression relative to mock vector control 293s. (F-G) Western blot analysis of PARP cleavage in p150/MDA5 DKOs. (F) p150/MDA5 DKOs and CTRL A549s were transfected with H1N1 vRNA and cell lysates were collected at the indicated time points post transfection. (G) p150/MDA5 DKOs and CTRL A549s were infected with H1N1 (MOI = 1) and cell lysates were collected at the indicated time points post infection. (H) Flow cytometric analysis of Annexin V^+ cells following H1N1 vRNA transfection. ADAR1 KOs and CTRL A549s were transfected with H1N1 vRNA and stained with Annexin V-PE 40 hours post transfection. The levels of Annexin V were analyzed by flow cytometry. * denotes p-value $\leq$ 0.5. ** denotes p-value $\leq$ 0.01. *** denotes p-value $\leq$ 0.001. NS denotes p-value $\geq$ 0.05. Data are representative of at least three independent experiments. See also Figure III.8.

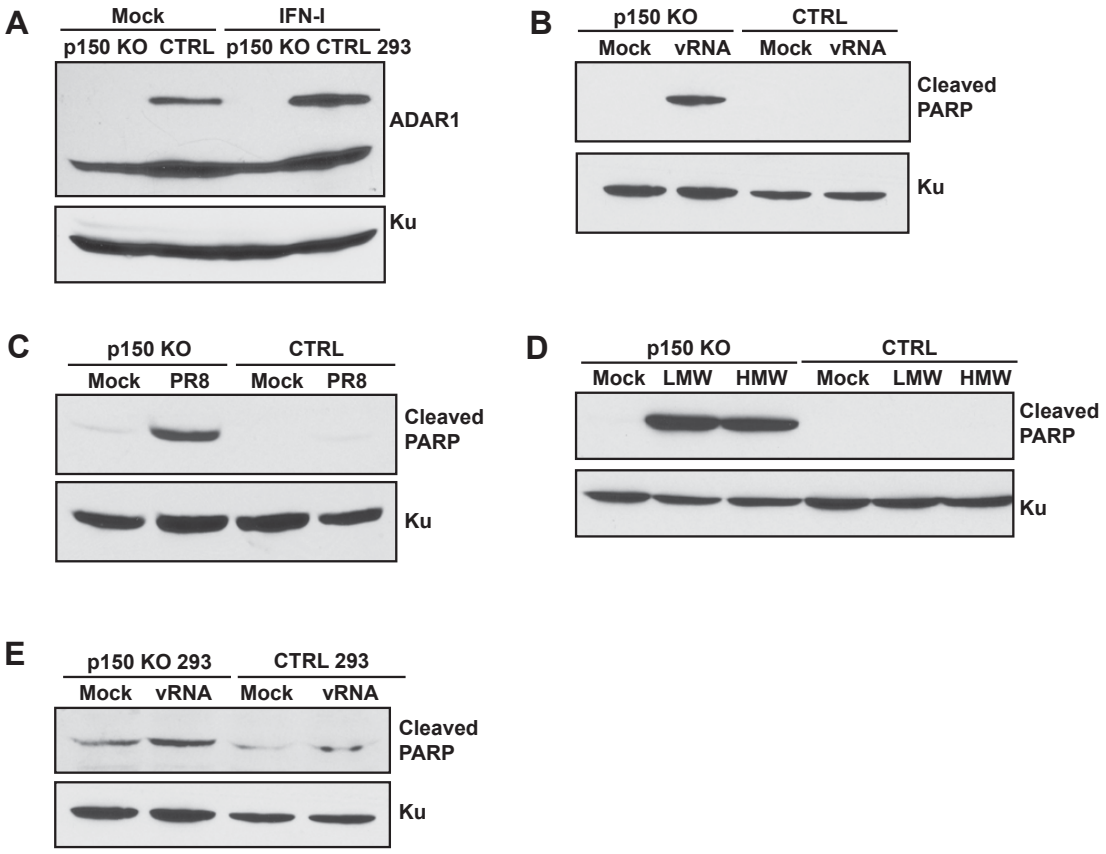

Figure III.8. p150 KOs show increased PARP cleavage following stimulation of RLRs

(A) Western blot analysis of ADAR1 expression in p150 KOs and CTRL 293s. p150 KOs, and CTRL 293s were mock treated or treated with IFN for 24 hours and expression of ADAR1 was examined by western blot. Expression of Ku is shown as a loading control. (B-D) Western blot analysis of PARP cleavage upon RLR stimulation. (B) PARP cleavage in p150 KOs following IAV vRNA transfection. p150 KOs and CTRL A549s were transfected with H1N1 vRNA. Lysates were collected at 24 hours post transfection. (C) PARP cleavage p150 KOs following H1N1 infection. p150 KOs and CTRL A549s were infected with H1N1 (MOI =1). Lysates were collected at 40 hours post infection. (D) PARP cleavage in p150 KO following poly I:C transfection. p150 KOs and CTRL A549s were transfected with LMW or HMW pI:C. Lysates were collected at 24 hours post transfection. (E) PARP cleavage in p150 KO 293s following IAV vRNA transfection. p150 KOs and CTRL 293s were transfected with H1N1 vRNA. Lysates were collected at 24 hours post transfection.

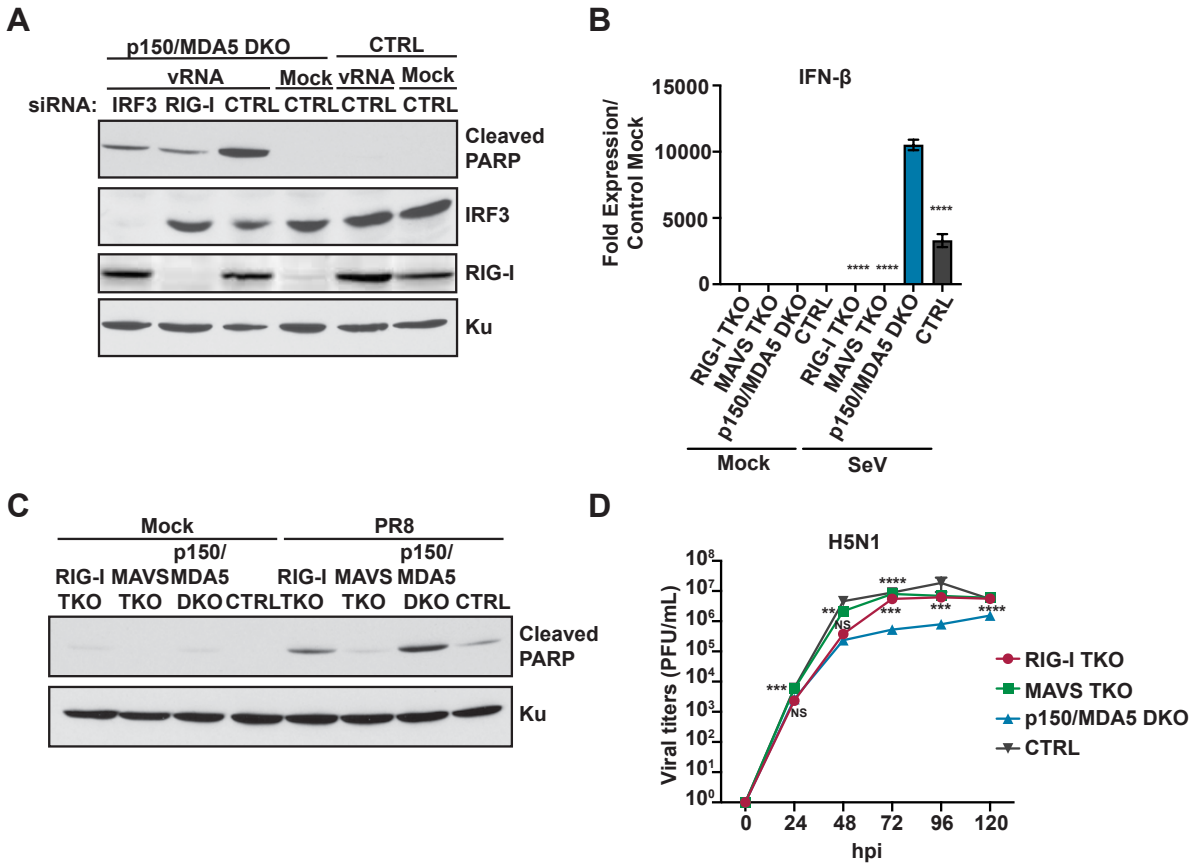

Figure IV.1. p150 suppresses RIG-I-signaling mediated induction of IFN-β and apoptosis

(A) Western blot analysis of PARP cleavage in p150/MDA5 DKOs following knockdown of RIG-I or IRF3 expression. RIG-I and IRF3 were knocked down in p150/MDA5 DKOs via siRNA transfection. Control siRNA were also transfected into p150/MDA5 DKOs and CTRL A549s. After 24h post siRNA transfection, cells were transfected with H1N1 vRNA for additional 24 hours. The cell lysates were analyzed for expression of RIG-I, IRF3, cleaved PARP, and Ku by western blot. (B) qRT-PCR analysis of IFN-β expression in p150/MDA5/RIG-I and p150/MDA5/MAVS TKOs after SeV infection. p150/MDA5/RIG-I TKOs, p150/MDA5/MAVS TKOs, p150/MDA5 DKOs, and CTRL A549s were infected with SeV and IFN-β mRNA levels were measured after 24 hours. Data are represented as fold expression relative to mock vector control A549s. (C) Western blot analysis of PARP cleavage TKOs following H1N1 infection. p150/MDA5/RIG-I TKOs, p150/MDA5/MAVS TKOs, p150/MDA5 DKOs, and CTRL A549s were infected with H1N1 (MO1 = 1) and lysates were collected after 40 hours. The levels of cleaved PARP and Ku were determined by western blot. (D) IAV replication in TKOs. p150/MDA5/RIG-I TKOs, p150/MDA5/MAVS TKOs, p150/MDA5 DKOs, and CTRL A549s were infected with H5N1 (MOI = 0.001) and viral titers were measured at the indicated time points post infection. Data are represented as mean titer of triplicate samples ± SD. * denotes p-value ≤ 0.5. ** denotes p-value ≤ 0.01. ***

Figure IV.1, continued. denotes p-value ≤ 0.001. NS denotes p-value ≥ 0.05. Data are representative of at least three independent experiments.

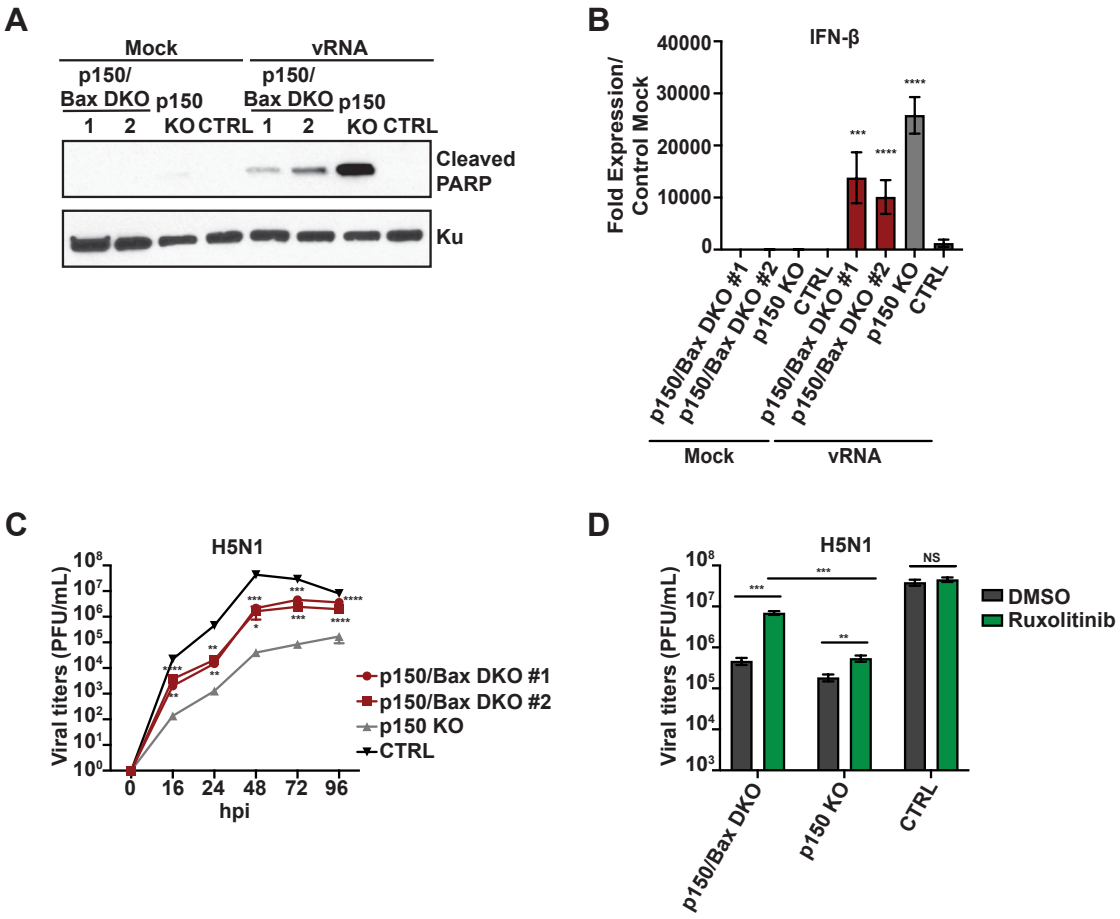

Figure IV.2. Increased type I IFN signaling and apoptosis reduce IAV replication in cells lacking p150.

(A) Western blot analysis of PARP Cleavage in p150/Bax DKOs following vRNA transfection. Two clones of p150/Bax DKOs, p150 KOs, and CTRL A549s were transfected with IAV vRNA for 24 hours. PARP cleavage and Ku expression were analyzed by western blot. (B) qRT-PCR analysis of IFN-β expression in p150/Bax DKOs following IAV vRNA transfection. Two clones of p150/Bax DKOs, p150 KOs, and CTRL A549s were transfected with H1N1 vRNA and IFN-β mRNA levels were determined 24 hours post transfection. Data are represented as fold expression relative to mock vector control. (C) IAV replication in p150/BAX DKOs. Two clones of p150/Bax DKOs, p150 KOs, and CTRL A549s were infected with H5N1 (MOI = 0.001) and viral titers were measured at the indicated time points post infection. Data are represented as mean titer of triplicate samples ± SD. (D) IAV replication in p150/Bax DKOs following inhibition of Janus kinases. p150/Bax DKOs, p150 KOs, and CTRL A549s were treated with 0.2 μM Ruxolitinib for 24 hours prior to infection. The following day cells were infected with H5N1(MOI = 0.001) in the presence of Ruxolitinib and viral titers were measured at 48 hours. Data are represented as mean titer of triplicate samples ± SD. * denotes p-value ≤ 0.5. ** denotes p-value ≤ 0.01. *** denotes p-value ≤ 0.001. NS denotes p-value ≥ 0.05. Data are representative of at least three independent experiments.

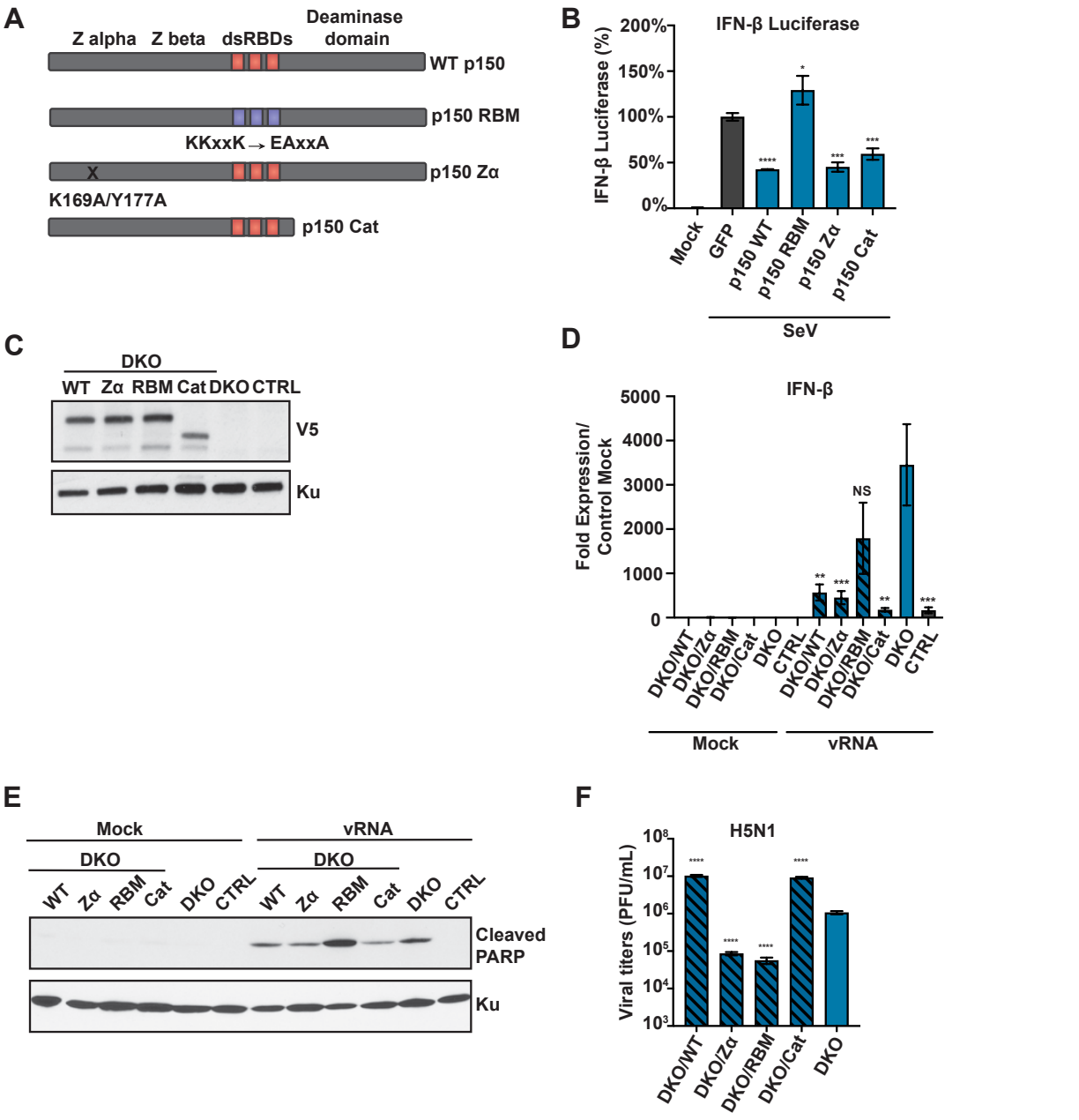

Figure IV.3. RNA binding activity of p150 is required for suppression of RIG-I signaling

(A) A schematic representation of different p150 mutants. (B) Analysis of IFN-β-Firefly reporter activity. A firefly luciferase reporter under the control of the IFN-β promoter was transfected along with wild-type and mutant p150 constructs into 293s. At 24h post-transfection, cells were infected with SeV and luciferase activity was measured 48 hours post-transfection. Data are represented as percent luciferase activity relative to GFP+SeV. (C) Western blot analysis of V5-tagged p150 expression in complemented cells. Lysates from p150/MDA5 DKOs stably expressing wild-type and mutant p150 constructs were analyzed by western blot using an anti-V5 antibody. (D) qRT-PCR analysis of IFN-β in V5-p150 complemented p150/MDA5 DKOs. p150/MDA5 DKOs

Figure IV.3, continued. complemented with different V5-p150 mutants were transfected with H1N1 vRNA and IFN-β mRNA levels were measured 24 hours post transfection. Data are represented as fold expression relative to mock CTRL A549s. (E) Western blot analysis of PARP cleavage in complemented p150/MDA5 DKOs. p150/MDA5 DKOs complemented with p150 mutants were infected with H1N1 (MOI = 1) and cell lysates were collected at 40 hours post infection for western blot analysis of cleaved PARP. (F) IAV replication in complemented p150/MDA5 DKOs. Complemented p150/MDA5 DKOs were infected with H5N1 (MOI = 0.001) and viral titers were measured at 48 hours. Data are represented as mean titer of triplicate samples ± SD. * denotes p-value ≤ 0.5. ** denotes p-value ≤ 0.01. *** denotes p-value ≤ 0.001. NS denotes p-value ≥ 0.05. Data are representative of at least three independent experiments.

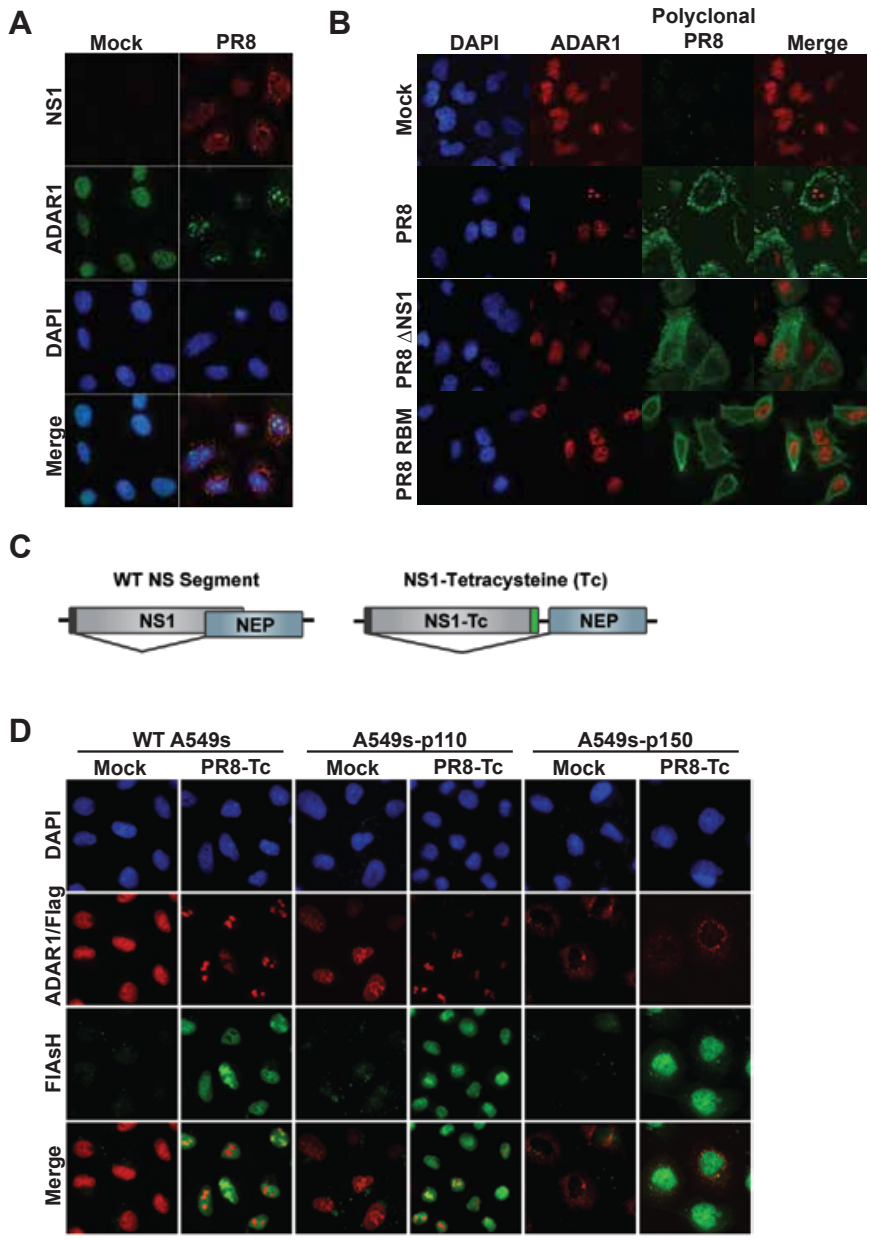

Figure V.1. The ADAR1 Isoforms differentially localize during IAV infection
A) Colocalization of ADAR1 and NS1 during IAV infection. WT A549s were infected with PR8 (MOI =5). At 16 hours post infection, cells were fixed and stained for ADAR1 and NS1. ADAR1 and NS1 localization was assessed via fluorescent microscopy. (B) ADAR1 and NS1 nucleolar localization is NS1 dependent. WT A549s were infected with PR8 (MOI=5), PR8 ΔNS1 (MO1=5), and PR8 RBM (MOI=5). At 16 hours post infection, cells were fixed and stained with anti-ADAR1 and anti-PR8 polyclonal antibodies and ADAR1 localization was assessed via fluorescent microscopy (C) Schematic illustrating the generation of the tetracysteine tagged NS1. The WT NS segment encodes the NS1 and NEP proteins through alternative splicing. To incorporate the tetracysteine tag, the NS splice acceptor site was mutated to allow for incorporation of the tetracysteine tag

Figure V.1, continued. on the N-terminus of NS1. The splice acceptor site was then duplicated to generate the NEP. (D) Differential ADAR1 isoform localization. WT A549s, Flag-p110 overexpressing A549s (A549-p110), and Flag-p150 overexpressing A549s (A549-p150) were infected with PR8-Tc (MOI = 5). At 16 hours post infection, cells were stained for FlAsH and ADAR1 or Flag. ADAR1 and NS1 localization were assessed via fluorescent microscopy. Images are representative of triplicate experiments.

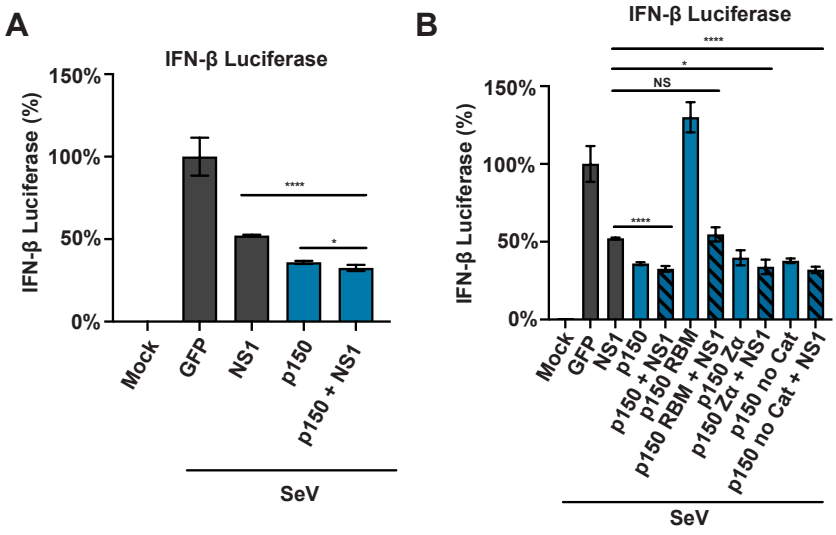

Figure V.2. The ADAR1 Isoforms differentially localize during IAV infection
(A) Analysis of IFN-β-Firefly reporter activity following transfection with p150 and NS1. The IFN-β-Firefly reporter was transfected along with a combination of p150 and NS1 or NS1 RNA binding mutant (RBM) into p150 KO 293s. Following transfection, cells were infected with SeV and luciferase activity in the lysates was measured 48 hours post transfection. Data are represented as percent luciferase activity relative to GFP+SeV. (B) Analysis of IFN-β-Firefly reporter activity following transfection of p150 mutants and NS1. The IFN-β-Firefly reporter was transfected along with mutant p150 and NS1 into WT 293s. Following transfection, cells were infected with SeV and luciferase activity was measured at 48 hours post transfection. Data are represented as percent luciferase activity relative to GFP+SeV. * denotes p-value $\leq$ 0.5. ** denotes p-value $\leq$ 0.01. *** denotes p-value $\leq$ 0.001. NS denotes p-value $\geq$ 0.05. Data are representative of at least three independent experiments

APPENDIX B

Tables

Table II.1. Oligonucleotide Sequences for Generating and Validating CRISPR KO Cells.

Oligonucleotide Sequences for sgRNAs to Generate CRISPR KO Cells		
Target	**Forward Primer**	**Reverse Primer**
ADAR1	caccgGACTCTGAGATCATACCTTC	aaacGAAGGTATGATCTCAGAGTCc
p110 promoter	caccgTATAACGTGGTTGGGCCGGA	aaacTCCGGCCCAACCACGTTATAc
p150 promoter	TTACTGGCTGGCATCTGCTTGCTTA	TGAGGTTGTAAACGAACCCAGACGG
MDA5	caccgCGAATTCCCGAGTCCAACCA	aaacTGGTTGGACTCGGGAATTCGc
RIG-I	CACCGGGGTCTTCCGGATATAATCC	AAACGGATTATATCCGGAAGACCCc
MAVS	caccgTCAGCCCTCTGACCTCCAGCG	aaacCGCTGGAGGTCAGAGGGCTGAc
Bax	CACCGTCGGAAAAAGACCTCTCGGG	AAACCCCGAGAGGTCTTTTTCCGA
Primer Sequences for PCR Amplification of sgRNA Target Site		
p110	GCCCCTACCAGCTGCGTCC	CGGGCCATTCAAAGACTACTGGTT
p150	GCCTGAGGTTTTGTGTGCCTTTGTT	GGAGACGATGTGTCTGCCTTGACAT
p150	TTACTGGCTGGCATCTGCTTGCTTA	TGAGGTTGTAAACGAACCCAGACGG
ADAR1	CAGGGCTGGACTTGTTTCCC	TTCTACGTGCTTCATCTCCTGTCA